THE EFFECTS OF OBESITY ON OCCUPANT INJURY RISK IN FRONTAL IMPACT: A COMPUTER MODELING APPROACH

by

Michael James Turkovich

Bachelor of Science, California Polytechnic State University, San Luis Obispo, 2004

Master of Science, California State University, Sacramento, 2007

Submitted to the Graduate Faculty of

the Swanson School of Engineering in partial fulfillment

of the requirements for the degree of

Doctor of Philosophy

University of Pittsburgh

2010

UNIVERSITY OF PITTSBURGH

SWANSON SCHOOL OF ENGINEERING

This dissertation was presented

by

Michael James Turkovich

It was defended on

November 2, 2010

and approved by

Jingwen Hu, PhD

Richard E. Debski, PhD, Associate Professor

Linda van Roosmalen, PhD, Assistant Professor

Dissertation Director: David Brienza, PhD, Associate Professor

THE EFFECTS OF OBESITY ON OCCUPANT INJURY RISK IN FRONTAL IMPACT: A COMPUTER MODELING APPROACH

Michael James Turkovich, PhD

University of Pittsburgh, 2010

Obesity is a condition that affects about 40% of US adults, and people with disabilities have a higher incidence of obesity than able-bodied individuals. Motor vehicle collisions (MVCs) are the number one cause of death in individuals under the age of 34 in the US, and people who ride in vehicles while seated in their wheelchairs are at increased risk of injury compared to people who ride in the automotive seat. Obese occupants appear to have a different risk of injury in MVCs than non-obese individuals. To reduce the risk of injury to obese occupants it is necessary to further understand the injury mechanisms to obese individuals in frontal MVCs. The purpose of this research was to investigate the mechanisms of injury and injury risk to obese occupants and obese wheelchair-seated occupants in frontal impact.

Three full body occupant models were created to investigate the effects of increased mass, changes in obese torso mechanical response and geometry, and a combination of mass and torso changes on occupant injury risk. To investigate the effects of obesity on wheelchair-seated occupants a wheelchair/occupant model was created and validated. Parametric studies were used on all the models to investigate injury risk in frontal impact.

The results show that increased mass is the most significant factor leading to injury for obese occupants. The differences in torso mechanical response and geometry as a result of increased adipose tissue in obese occupants, do not significantly affect the injury risk of obese

occupants. Changes in the obese torso coupled with increased mass cause increased pelvis and chest excursion which results in increased risk of lower extremity injury. As BMI increases in wheelchair-seated occupants the risk of lower extremity injury increases, and obese wheelchair-seated occupants have a higher risk of injury to the lower extremities than obese non wheelchair-seated occupants. This research suggests that the reduction in injuries to certain body regions reported in the literature are not due to a "cushion effect," but are more likely due to altered occupant kinematics that transfer load from the upper body to the lower extremities.

TABLE OF CONTENTS

LIST OF TABLES

LIST OF FIGURES

PREFACE

I am especially grateful to my family and friends who provided me with much needed support throughout the whole dissertation process. I know that this work would not have been completed without everything that they have done for me.

Finally I could not have completed this project without the support of the Rehabilitation Engineering Research Center on Wheelchair Transportation Safety funded by NIDRR through grant #H133E060064.

1.0   INTRODUCTION

1.1   BACKGROUND

Obesity is defined as abnormal or excessive fat (adipose tissue) accumulation that presents a risk

to health [1]. In 2005, 33% of US adults were overweight, 34% were obese, and 6% were

extremely obese. This translates to roughly 73% of US adults that are affected by this condition

[2]. In addition, people with disabilities have a 11.6% higher rate of obesity compared to able

bodied adults [3]. BMI is used by the World Health Organization to classify the degree of

obesity of an individual and is calculated using the equation:

$$BMI = \frac{w}{m^2}$$

Where w is body weight in kg, and m is height in meters.

Individuals are grouped into one of six categories depending on their BMI values.

Table 1-1 shows the World Health Organization's BMI classifications. Current obesity statistics

suggest that the majority of US adult males have a BMI greater than 25, which is considered the

cutoff between a normal classification and overweight classification.

Table 1-1. World Health Organization's BMI classifications

Classification	BMI
Underweight	< 18.50
Normal range	18.50 – 24.99
Overweight	25.00 – 29.99
Obese Class I	30.00 – 34.99
Obese Class II	35.00 -39.99
Obese Class III	> 40.00

Motor vehicle crashes (MVCs) are the number one cause of death for people ages 1-34 in the United States [4] even though implementation of automotive safety standards have been effective in reducing the overall number of fatalities in MVCs [5, 6]. The Federal Motor Vehicle Safety Standard 208 requires that all cars meet crash test standards based on a crash test of 30mph/20g frontal impact to a 50th percentile Hybrid III Anthropomorphic Test Device (ATD), which has a Body Mass Index (BMI) of approximately 25, in the driver seat of the vehicle [7]. Car interiors are designed to minimize the risk of injury to the theoretical occupant with a BMI of 25.

People who travel in motor vehicles while seated in their wheelchairs have an increased risk of injury in a MVC because the wheelchair is not designed to withstand MVC forces [8]. In addition, the wheelchair-seated occupant may be at a higher risk of injury due to poor wheelchair securement and/or occupant restraint [9]. Voluntary national and international standards have been developed to provide improved safety to wheelchairs and wheelchair-seated occupants

riding in motor vehicles [10-14]. These standards require that wheelchair tiedowns and occupant restraint systems (WTORS) be crash tested with a 30mph/20g frontal impact sled test, with a 50th percentile Hybrid III ATD seated in surrogate wheelchair.

With the increase in obesity in the United States, researchers have examined the relationships between obesity and occupant safety in motor vehicular accidents. Studies have revealed several trends in occupant injury and obesity. Boulanger et al. (1992) reported that obese individuals in MVCs were more likely to have rib fractures, pulmonary contusions, pelvis fractures, and extremity fractures, and less likely to injure the liver and head [15]. These findings were supported by those of Moran et al. (2002), who showed a decrease in head and abdominal injuries in obese individuals involved in MVCs [16]. Reiff et al., (2004) showed that there is a relationship between BMI and diaphragm injury in MVCs [17], and Cormier (2008) reported that obese individuals have an increased risk of thoracic injury in MVCs [18]. Viano et al. (2008) reported that obese individuals, because of their greater mass, have more kinetic energy and thus more force is required to prevent an obese individual from contacting the vehicle interior in a frontal MVC. Viano et al. (2008) also concluded that obese individuals are exposed to a higher risk for injury based on the Maximum Abbreviated Injury Scale (MAIS) system [19].

Arbabi et al. (2003) and Wang et al. (2003) analyzed the Crash Injury Research Engineering Network (CIREN) database to examine the effects of abdominal subcutaneous fat depth on injury patterns of adults in MVCs. Their results indicate that obese individuals have a decreased incidence of abdominal injury in MVCs, and the authors suggest that abdominal fat may provide a "cushion effect" on the abdomen which reduces the likelihood of an obese individual experiencing an abdominal injury in an MVC. Wang et al. (2003) also hypothesized that the mass of the occupant might play an important role in occupant dynamics and may

override the "cushion effect" for individuals with extreme obesity [20, 21]. Wang et al. (2003) suggests that numerical modeling of adipose tissue and obesity is necessary to fully understand the effects of obesity on occupant response in MVCs, and once this is achieved, vehicle interiors could potentially be modified to better accommodate obese individuals and reduce their risk of injury during MVCs.

However, several recent studies have suggested the opposite is true of obese abdominal injury. Zarzaur and Marshall (2008) examined seatbelt use, injury severity, and obesity using 7,459 cases from the National Accident Sampling System- Crashworthiness Data System (NASS-CDS) database. They reported that obese belted occupants are more likely to sustain an abdominal injury of any severity when compared to non-obese occupants, and belted non-obese individuals had lowest overall risk of injury [5]. Ryb and Dischinger (2008) examined 1,615 cases in the CIREN database and reported that overweight patients experienced more severe injuries, and obese patients had an increased risk of mortality. Their data also was in contrast to the abdominal injury findings of Arbabi et al., (2003) [22].

Finally, Zhu et al. (2010) analyzed real-world crash data from the NASS-CDS database and concluded that obese males have a higher risk of injury to the upper body. Zhu et al. (2010) also reported a U-shaped relationship between BMI and serious injury to the abdominal region and reported increased risk of abdominal injury but a decrease in serious abdominal injury, indicating that there might be some protective effect of adipose tissue [23].

Recent research has reported various findings for obese individuals with respect to mortality in MVCs. Choban et al. (1991) examined 351 hospital records of patients that were involved in a MVC and found that obese individuals experiencing blunt force trauma have an increased risk of mortality compared to non-obese individuals [24]. Zhu et al. (2006) analyzed

the effects of obesity on risk of fatality using the NASS-CDS database and reported that BMI and male risk of fatality were correlated but there was no relationship between BMI and female risk of fatality [25]. Sivak et al. (2010) found that an increasing BMI may lower the risk of fatality in properly restrained male occupants. They again suggest that the trends they reported are due to an interaction between increased occupants mass and increased "cushioning" of adipose tissue. They also reported a need for new numerical models that can accurately represent obese individuals to effectively evaluate new occupant restraint systems [26].

In an attempt to explain some of the differences on risk of injury to obese vehicle occupants that have been reported in the literature, Kent et al. (2010) compared the kinematics of 3 obese cadavers to 5 non-obese cadavers in frontal impact sled tests. These tests were conducted with a stock automotive seat, and a standard 3-point occupant restraint system with and without a pretensioner and load limiter. The results of the study showed that obese cadavers experience increased forward head, shoulder, hip, and knee excursion, and a decreased shoulder to hip excursion ratio. The obese cadavers experience increase hip displacement, as a result of the seatbelt penetrating the adipose tissue around the abdomen and pelvis (Figure 1-1). The increased pelvis motion creates increased load on the hips and chest as the head lags behind. They suggest that this decrease in shoulder to hip excursion may be a factor in the different injury patterns reported by real-world crash data studies. This study, however, was unable to explain the potential decrease in head and abdominal injury reported in previous studies [5, 15, 20, 21].
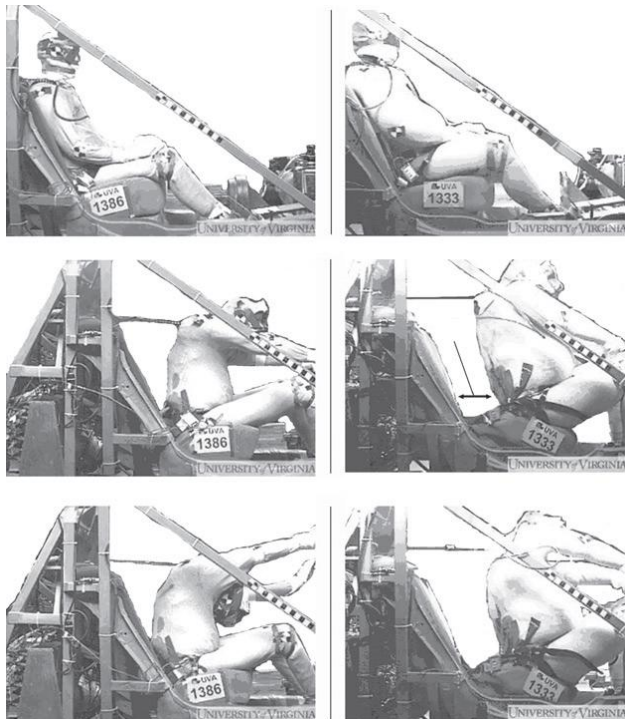
Figure 1-1. Kinematics of non-obese (Left) and obese (Right) cadavers in frontal impact sled tests (Figure from Kent et al., 2010).

The exact mechanism of injury to obese individuals in MVCs remains unknown. Based on the real-world crash injury research and the limited amount of cadaver studies there are several hypothesis that have been proposed as to why obese individuals experience different injuries in MVCs compared to non-obese individuals. Obese individuals are more likely to wear their seatbelts improperly by placing the lap belt over the abdomen instead of in contact with the pelvis [27, 28]. The improper use of seatbelts can lead to increased risk of injury to obese occupants. It has also been suggested that abdominal injury might be reduced due to a "cushioning effect" in which the abdominal adipose tissue actually provides a protective barrier to the internal organs during high speed abdominal loading in frontal impacts [20, 21, 26]. The increased mass of obese individuals may cause an obese individual to translate further forward in

a frontal impact thus increasing force by which the body contacts the restraint systems or the vehicle interior and causing an increased risk of injury to the occupant.

In order to provide improved safety to obese individuals in MVCs, improved understanding of the mechanisms of injury to obese individuals is needed. While cadaver testing is important, there is a lack of available obese cadaver data to accurately determine the mechanisms of injury to obese individuals. Computational modeling is a tool that can be used to examine the proposed mechanisms of injury to further contribute to the understanding of obesity and injury risk in frontal MVCs. Computer modeling can provide an alternative to expensive and time consuming cadaver testing. Computer modeling can also provide information on tissue stress/strain, and internal organ dynamics which cannot be readily obtained from cadaver testing.

1.2   LIMITATIONS OF PREVIOUS MODELS

Effective occupant protection in frontal impacts is achieved by a tight coupling of the occupant to the vehicle seat [29]. This coupling involves an interaction between the occupant, the lap belt, shoulder belt, and the seat. To provide tight coupling of the occupant, interaction between the pelvis and seatbelt is necessary. Therefore the lap belt-to-occupant interaction is critical in occupant safety [30]. To aid in the understanding of abdominal dynamics and injury due to high impact loading, two Finite Element (FE) models of the human abdomen have been developed [31, 32].

In 2001 Lee and Yang developed a finite element abdominal model called the Wayne State University Human Abdominal Model (WSUHAM). This model includes a human pelvis,

7

lumbar and thoracic spine, and part of the ribcage. The geometry of the solid structures were obtained from CT scans of an adult male cadaver and scaled to represent a 50th percentile male. Since the solid organs of the abdomen are the most likely to be injured in car accidents [33], this model used detailed representations of the liver, spleen, and kidneys. The less often injured hollow organs were modeled as three body bags with a constant atmospheric pressure. No studies have determined the properties of the skin, muscles, and adipose tissue during high impact loading, so the model assumed that the material properties of these superficial soft abdominal tissues had a Young's Modulus of 1 MPa and a uniaxial stress strain response (Yamada, 1970). The WSUHAM was validated against cadaver test data that included oblique pendulum tests, lateral drop tests, and frontal rigid bar tests to examine the effects of abdominal injury due to occupant contact with the vehicle interior [31].

In more recent attempts to understand abdominal impact injury, Ruan et al. (2005) developed an improved FE model of the abdomen [32]. This model was similar to the WSUHAM in that it focused on the solid organs, however the hollow organs were modeled with an entity called "abdomen" which was modeled with solid elements. The material properties of the "abdomen" were used to tune the mechanical response of the model. The Ruan model was validated against cadaver pendulum data, frontal rigid bar data, and seatbelt load data [32]. The Ruan model was able to accurately describe the force/deformation response of the human abdomen for both response corridors and individual tests. Further abdominal injury parameters including internal organ pressure, deformation, force, and viscous criterion (V*C) were analyzed from the model and compared to current pressure threshold data for human internal organs [34-37].

8

The previously developed abdomen FE models have been created based on the geometry of one average adult male. The models have all been validated against cadaver test data, and these cadaver data include 28 cadavers but only 4 were classified as obese. This indicates that the models provide an accurate representation of a 50th percentile adult male but a major limitation in using these models to examine obesity is that they lack the accurate shape and mechanical response of an obese individual's abdomen.

Several full body human models have been developed for use in automotive crash safety research [32, 38-45]. These models include finite element models with detailed representations of bones, internal organs, muscle and skin, and ellipsoid rigid body models. Due to the FE model's complexity they are computationally expensive. Mathematical Dynamic Models (MADYMO) has a library of several full body models including detailed FE human models and Hybrid III dummy models. These dummy models are rigid body ellipsoid models which simplify the model and thus reduce computational time while still providing a high degree of accuracy. The MADYMO whole body models have been used extensively for automotive safety and design research. The MADYMO Hybrid III ellipsoid models can also be scaled to different body dimensions using MADYMO Madyscale [46]. Madyscale allows model alterations to better represent occupants' different anthropometrics. However the scalability of the Madyscale model is based on data from Air Force personnel from the 1960s [47, 48]. The major limitation of this model is that while the mass of the scaled model is reasonable, the geometry of an individual with a certain BMI is very different from the US population today.

The use of MADYMO modeling software has also been used extensively to examine the wheelchair-seated individuals under impact loading conditions [49-52]. All of these studies have used the MADYMO Hybrid III family of dummy models to examine ATD and wheelchair

kinematics under frontal and rear impact loading conditions. None of these studies have

examined the effects of changes in obesity on occupant risk of injury to wheelchair-seated

occupants.

In a recent attempt to examine obesity using a full body computational model, Zhu et al.

(2010) used CT scans to create an accurate shape of obese individuals and modified the

MADYMO Hybrid III ATD with the geometry from the CT scans. They assumed a hyperelastic

material response of the new geometry. BMI, airbag inflation rate, steering wheel angle, seatbelt

pretensioners, and load limiters were varied and the risk of injury examined. The results of their

models support their real-world crash research findings, which indicated that obese males had a

higher risk of injury to all body regions. While this study is the first attempt to examine obesity

using computational methods, the limitations of the model include a lack of accurate mechanical

response of the obese abdomen. Furthermore, the shape of the modified torso is based on a

limited number of CT scans of individuals, and the model was not used to investigate the injury

mechanisms of obesity under frontal impact loading conditions.

1.3   PROBLEM STATEMENT AND THE NEED FOR OBESE MODELS

Approximately 70% of US adults are overweight or obese (BMI >25), and people with

disabilities tend to be at an even higher risk of obesity than able-body individuals [3]. Previous

research has shown that obese individuals are exposed to a different risk of injury than non-obese

individuals in MVCs. The exact mechanisms of injury to obese individuals remain unclear,

although several hypotheses have been proposed. In order to reduce risk of injury to obese

vehicle occupants and provide improved vehicle safety systems for the obese population, a clear understanding of the injury mechanism is necessary.

Understanding the response of obese individuals in MVCs requires computational models that accurately represent obese individuals. A model that can accurately simulate the mass of an obese individual, the interaction between lap belt and obese abdomen, as well as the kinematics of obese occupants during frontal impact will provide additional information of the injury mechanisms of obese individuals in MVCs. Once the injury mechanism for obese occupants is quantified, occupant safety systems can be improved and designed specifically for individuals based on their BMI.

1.4   OBJECTIVES

The objective of this research was to examine the injury mechanisms and injury risk for obese occupants and obese wheelchair-seated occupants when exposed to frontal impact loading using an Obese Abdomen FE model and an obese full body MADYMO model. It is hypothesized that the increase in occupant mass due to obesity will override any "cushion effect" due to increased adipose tissue and cause the occupant to contact the restraint system and/or vehicle interior with increased force, thus causing an increase in injury risk to the chest and lower extremities of obese occupants in motor vehicles. An overview of the research methodology is shown in Figure 1-2.

The research objective was investigated through the following specific aims:

1. Quantify the effect of adipose tissue on abdominal response

   a. Validate the Wayne St. Abdomen FE model [31] for frontal impact belt loading conditions

   b. Modify the Wayne St. Abdomen model (Obese Abdomen FE Model) to include adipose tissue representative of various BMI levels

   c. Use the Obese Abdomen FE model to determine the mechanical response of the abdomen for varying levels of BMI under different lap belt loading directions

2. Determine the mechanisms of injury and injury risk to obese occupants exposed to frontal impacts using an obese full body model

   a. Examine effects of occupant mass on occupant injury

   b. Examine the effects of obese torso/seat belt interaction on occupant injury

   c. Examine the combined effects of occupant mass and obese torso/seat belt interaction on occupant injury

3. Determine the effects of obesity on wheelchair-seated occupants in frontal impacts

   a. Create and validate a wheelchair occupant model

   b. Examine the combined effects of occupant mass and obese torso/seatbelt interaction on wheelchair-seated occupant injury
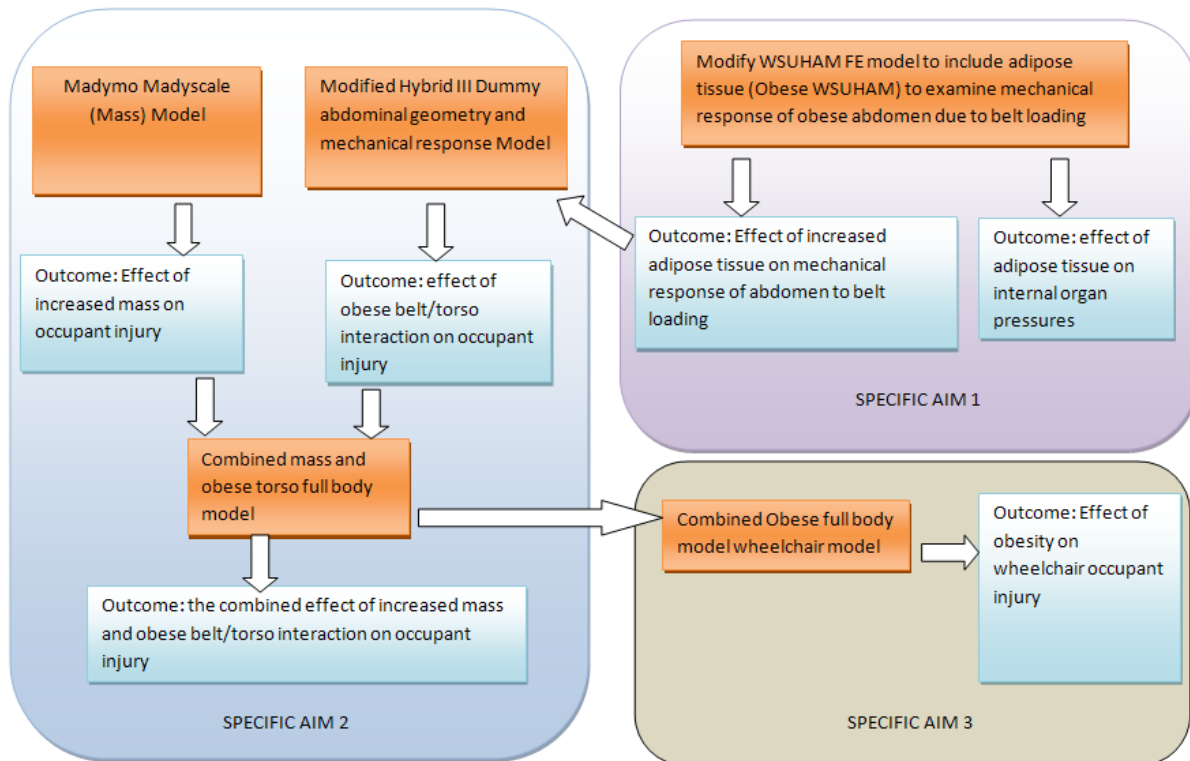
Figure 1-2. Overview of research methodology.

1.5   ORGANIZATION OF DISSERTATION

The development, validation, and mechanical response of the Obese Abdomen FE model are described in Chapter 2. Chapter 3 contains the development of the obese full body models and the simulations performed to examine the mechanism of injury due to obesity. The development and validation of the obese wheelchair occupant model and the investigation of the effects of obesity on wheelchair-seated occupants is described in Chapter 4. Chapter 5 discusses the research findings, gives a summary and study conclusions.

2.0 DEVELOPMENT OF AN OBESE ABDOMEN FINITE ELEMENT MODEL AND VALIDATION OF THE OBESE ABDOMEN MECHANICAL RESPONSE TO SEATBELT LOADING

2.1 OVERVIEW

This chapter describes the development, validation, and analysis of an Obese Abdomen FE Model. First the WSUHAM, which represents a 50th percentile male, was modified and validated for multiple seatbelt loading conditions available from the cadaver tests in the literature [53, 54]. The WSUHAM was then modified to represent obese abdomens of varying BMIs by adding elements representing adipose abdominal tissue to the model. The obese abdomen model was validated with a limited number of cadaver tests from the literature [53]. An analysis was performed on the Obese Abdomen FE Models to determine the effects of BMI on mechanical response due to seatbelt loading. Internal organ pressures were recorded to investigate the "cushion effect".

2.2   MODEL DEVELOPMENT

Abdomen/seatbelt interaction plays an important role in automotive safety. A properly worn seat belt consists of a lap belt placed securely against the occupant's pelvis, and a shoulder belt that crosses the midline of the sternum and contacts the shoulder [30]. Previous abdomen finite element models have been developed to examine abdominal response of a 50th percentile male with respect to rigid bar loading [31, 32], but there is a lack of abdomen models validated for multiple seatbelt loading conditions, and no obese abdomen models.

The WSUHAM previously developed by Lee and Yang (2001) was used as a base model in this study. The model was converted to LSDYNA version 971 (Livermore Software Technology Corporation, Ca) code from PAMCRASH and model modifications were performed using HYPERMESH version 9.0 (Altair Engineering Inc, Troy, MI). The skeletal geometry of the model is based on CT scans from one cadaver from the Visible Human Male Project (National Library of Medicine, Bethesda, MD) and was scaled to the geometry of a 50th percentile male based on data from Schneider et al. (1983). The skeletal geometry used in the model represents the human male torso from T7 vertebra to the sacrum. The hollow organs of the abdomen are modeled with 3 airbags that have zero inflow/outflow and the internal pressure is set to atmospheric pressure. The solid abdominal organs consisting of the kidneys, liver, and spleen are modeled with solid elements. The model has been validated for side impact pendulum tests, drop tests, and rigid frontal bar tests.

For the purpose of this study, several material property modifications were made to the WSUHAM. These material property parameter changes were calibrated through a series of model validations. The material properties of the lower airbags (hollow organs) were changed to linear viscoelastic, and the solid organs (liver, kidneys, spleen) were changed to linear

viscoelastic material properties used by Ruan et al. (2005). Finally the skin and muscle which

are combined into one component in the original model were modified to a hyperelastic material

using the LSDYNA card MAT_OGDEN_RUBBER. The hyperelastic material model has been

successfully used to model skin/adipose tissue in previous studies [55-57]. The components and

material properties of WSUHAM developed by Lee and Yang (2001), the Ruan et al. (2005)

model, and the Modified WSUHAM are displayed in Table 2-1.

Table 2-1. Comparison of the components and material properties of the WSUHAM, Ruan et al.

model, and the Modified WSUHAM.

Model	WSUHAM	Ruan et al. 2005	Modified WSUHAM
Elements	19,353 solid and 15,603 shell/membrane Solid organs-solid Skin-solid Muscle-solid Falciform ligament-solid Hollow organs-membrane Diaphragm-shell Blood vessels-shell	Liver – 4,439 brick Spleen – 792 brick Left kidney – 790 brick Right Kidney– 720 brick Abdomen – 8760 solid Diaphragm – 3024 shell	34,231 elements Solid organs-solid Skin-solid Muscle-solid Falciform ligament-solid Hollow organs-shell Diaphragm-shell Blood vessels-shell
Components	Bony skeleton t7-sacrum (Wang 1995) Liver, spleen, kidneys, inferior vena cava, abdominal aorta, hepatic vein/artery, renal vein/artery, spleenic vein/artery, diaphragm	Bony Skeleton (from Ruan et al. 2003) Liver, spleen, kidneys, abdominal aorta, inferior vena cava, diaphragm	Bony skeleton t7-sacrum (Wang 1995) Liver, spleen, kidneys, inferior vena cava, abdominal aorta, hepatic vein/artery, renal vein/artery, spleenic vein/artery, diaphragm
Bone	$\rho/E/\nu$ (ρ-kg.m^3, E-GPa) *Ribs, Sternum* – Elastic Plastic 2000/1.15e1/0.3 *Sacrum, Femur, Illiac Crest*-Elastic Plastic 2000/1.21e1/0.3 *Vertebrae*- Elastic Plastic 2000/2.65e-2/0.3	$\rho/K/G_0/G_\infty$ (ρ- kg/m3, K,G – GPa) *Ribs* – linear viscoelastic 2000/9.6/4.4/1.8 *Sternum* - Elastic plastic 2000/9.6/4.4/2.3 *Vertebrae* – Elastic plastic 2750/106.7/.0002	$\rho/E/\nu$ (ρ-kg/m^3, E-GPa) *Ribs, Sternum* – Elastic Plastic 2000/1.15e1/0.3 *Sacrum, Femur, Illiac Crest*- Elastic Plastic 2000/1.21e1/0.3 *Vertebrae*- Elastic Plastic 2000/2.65e-2/0.3

Table 2-1 (Continued)

Organs	E_1/E_2 (E-MPa)	$K/G_0/G_\infty/\beta$ (K-MPa, G-kPa)	$K/G_0/G_\infty/\beta$ (K-MPa, G-kPa)
	Liver – Nonlinear, viscoelastic (Type 22) 0.195/0.10 *Spleen* – Nonlinear, viscoelastic (Type 22) 0.488/.25 *Kidneys* – Nonlinear, viscoelastic (Type 22) 0.352/0.15 *Hollow organs* (Body bags) – membrane (Type 150)	*Liver* – linear viscoelastic 2.875/230/43.6/0.635 *Spleen* – linear viscoelastic 2.875/230/43.6/0.635 *Kidneys* – linear viscoelastic 2.875/230/43.6/0.635	*Liver* – linear viscoelastic 2.875/230/43.6/0.635 *Spleen* – linear viscoelastic 2.875/230/43.6/0.635 *Kidneys* – linear viscoelastic 2.875/230/43.6/0.635 *Hollow organs (airbag)*– *lower airbags* -linear viscoelastic 1.45/500/40/0.6 *Hollow organs (airbag)*- *upper airbags* $\rho/E/\nu$ (ρ- kg/m^3, E- GPa) 2700/4e-4/0.4
Other	$\rho/E/\nu$ (ρ- kg/m^3, E-GPa) *Major blood vessels* Elastic (Type 101) 1000/4e-4/0.4 *Diaphragm* Elastic (Type 101) 1000/3e-3/0.3 *Falciform ligament* Elastic plastic 1000/1.2e-2/0.4 *Costal Cartilages* Elastic plastic 1500/2.5e-2/0.4 *Intervertebral Discs* Elastic plastic (Type 1) 1000/1.03e-2/0.45 *Intercostal muscles* Elastic plastic 1000/1.03e-2/0.4 *Skin+superficial muscles* Elastic foam with hysteresis (Type 21) E=1MPa	$K/G_0/G_\infty$ (K- MPa, G-kPa) *Abdomen* – linear viscoelastic 0.145/15.03/5.01 *Intervertebral discs-* linear viscoelastic 1040/307/32/0 *Cartilage* – linear viscoelastic 1500/53/9/0.096 *Intercostal muscle* – linear viscoelastic 1100/2.1/.35/0 $\rho/E/\nu$ (ρ-kg/m^3, E- MPa) *Aorta*- linear elastic 1200/4/0.4 *Other vessels* – linear elastic 1200/20/0.4	$\rho/E/\nu$ (ρ- kg/m^3, E-GPa) *Major blood vessels* Elastic 1000/4e-4/0.4 *Diaphragm* Elastic 1000/3e-3/0.3 *Falciform ligament* Elastic plastic 1000/1.2e-2/0.4 *Costal Cartilages* Elastic plastic 1500/2.5e-2/0.4 *Intervertebral Discs* Elastic plastic 1000/1.03e-2/0.45 *Intercostal muscles* Elastic plastic 1000/1.03e-2/0.4 *Skin+superficial muscles* Hyper elastic (mat_77) $\rho/\alpha/\mu/\nu$ (ρ-kg/m3, μ- GPa) 1000/14/1.5e-6/.499

2.3   MODIFIED WSUHAM VALIDATION

Since the effect of seatbelt loading on abdominal response is the primary interest of this study, several cadaver seatbelt loading tests were used for model validation. The studies by Foster et al. (2006) and Lamielle et al. (2008) examined cadaver abdomen response to high speed seatbelt loading, and provide enough information to replicate the test conditions in the model. The model's ability to predict abdomen loading was first validated for the Foster et al. (2006) test setup. This test setup included a rigid seat and seatback, with a seatbelt wrapped around the anterior surface of the abdomen at the mid umbilicus and routed back behind the seatback. High speed pretensioners attached to the seatbelt ends were used to load the cadaver abdomens. Due to variations in the cadavers' anthropometry, average force-time, average abdomen penetration-time, and average belt displacement-time history curves were generated from the Foster et al. (2006) tests for the male non-obese cadavers with enough data available for model validation.

Lamielle et al. (2008) performed abdomen loading tests on cadavers using a similar test setup to that of Foster et al. (2006). The setup included a rigid seat and seatback, and cadavers were loaded using high speed pretensioners with the seatbelt wrapped around that anterior surface of the abdomen at the mid umbilicus and routed straight back behind the seatback. Four cadavers were tested with high penetration rates and low compression boundary conditions (PRT) to simulate out of position lap belts, and 4 were loaded with low penetration rates and high compression boundary conditions (MHA) simulating submarining. For model validation

purposes the average force-time, average abdomen penetration-time, and average belt displacement-time were used for each test condition. However for the PRT loading conditions one cadaver test had a belt displacement that was very different from the rest and was excluded most likely due to a very low BMI (BMI=20). For the MHA loading, two cadaver tests resulted in responses that skewed the whole average and thus were excluded.

Boundary conditions that represented the cadaver test conditions were incorporated into the Modified WSUHAM. These boundary conditions included a rigid seat and seatback, and a seatbelt. The LSDYNA BOUNDARY_PRESCRIBED_MOTION card was used to apply prescribed displacement to the belt ends. The CONTACT_AUTOMATIC_SURFACE_TO_SURFACE card was used to detect contacts between all anatomical structures, the belt and abdomen, abdomen and seat, and abdomen and seatback. Hourglassing control (LSDYNA Type 4) was also used to reduce excessive hourglassing energy due to high deformation of the soft tissues. All model output were filtered with a SAE CFC 300 Hz low pass filter. Figure 2-1 shows the initial boundary conditions of the model and the prescribed belt motion applied to the model for each test setup.

The skin and muscle elements in the model had the most influence on the model's response. A hyperelastic model was used to represent the skin and muscle. The hyperelastic material constants that provided a good fit for the MHA tests were $\mu = 4e\text{-}7$ GPa and $\alpha = 15$. The material constants that provide a good fit for the PRT and Foster tests were $\mu = 1.7e\text{-}6$ GPa and $\alpha = 15$. One material model was desired, so several simulations were performed while adjusting the material parameters to find a good fit to all loading conditions with one material model. The resulting material constants of $\mu = 1.5e\text{-}6$ GPa and $\alpha = 14$ were used for the model. The differences in material properties for various tests conditions are most likely due to the wide

19

range of cadavers used for testing. Once the material constants were determined they were not changed for any subsequent simulations.
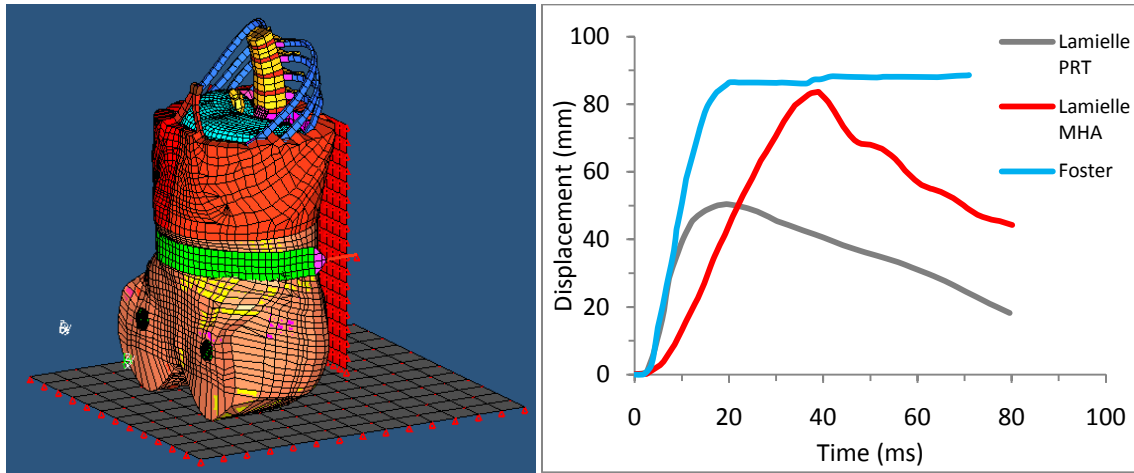
Figure 2-1. Boundary conditions applied to the model (Left) and prescribed seatbelt displacement based on data from Foster et al. (2006), and Lamielle et al., (2008) (Right).

To provide additional validation, several quantitative parameters were used to compare the model output to the test data. These parameters include Pearson's correlation coefficient, time of peak signal, and magnitude of the model's peak signal as a percent of the test signal's peak magnitude. Analysis was performed using these parameters on the model seatbelt force and abdomen penetration output for the three loading conditions.

2.4   MODIFIED WSUHAM VALIDATION RESULTS

Figure 2-2 shows the model predicted abdomen response for the MHA test condition at 10 ms intervals from 0-30ms. The model's deformation reflects the deformation reported in the cadaver testing.
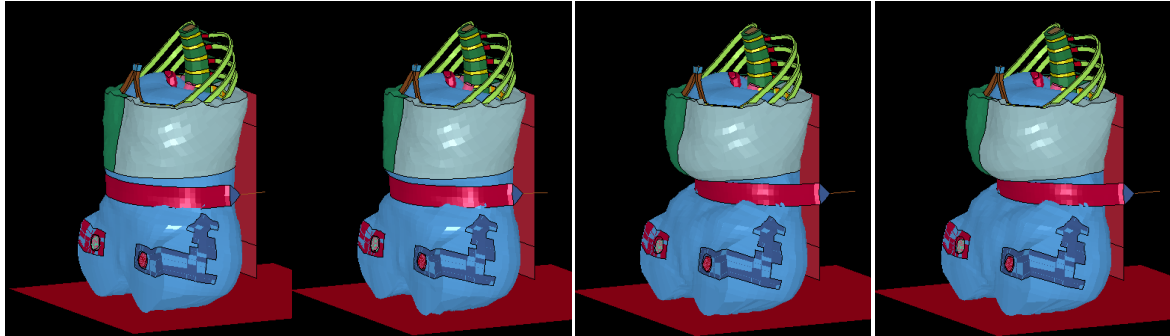
Figure 2-2. Model predicted abdominal deformation at 0, 10, 20, and 30 ms.

Figures 2-3, 2-4, and 2-5 show the model predicted force-time, and abdomen penetration-time curves for the test conditions of Foster et al. (2006) and Lamielle et al. (2008). Table 2-2 shows the quantitative validation of the Modified WSUHAM. The model predicted responses represent the test data well. Overall the model force peaks are within +- 1 ms, and the model displacement peaks are within 4 ms of the test data for all test conditions. The model's predicted peak force was 6397 N, 4789 N, and 3469 N for the Foster, PRT, and MHA tests respectively. These values are all within +-20% of the peak values of the test data. The model shows a high correlation with the test data for all loading conditions. The model predicts the MHA test conditions well, and the model slightly underestimates the displacement after 25 ms of the Foster and PRT tests. The model also tends to display a lack of energy in the force curves (i.e. area under the curve is less) in the MHA and PRT tests. This may be due to the assumptions that the

skin, muscle and fat are modeled as one set of elements and that the internal organs have been

greatly simplified, especially the hollow organs.
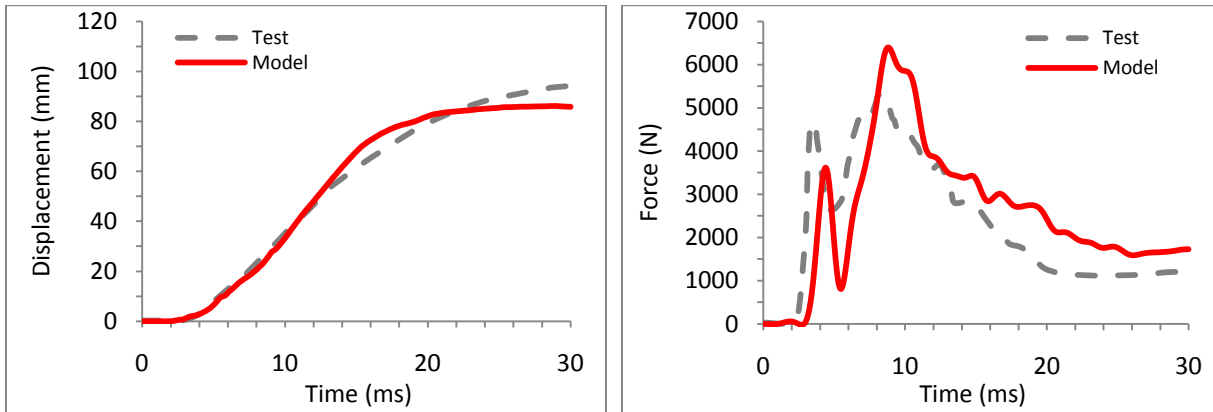
Figure 2-3. Model predicted abdomen penetration and seatbelt force for the Foster et al. tests.
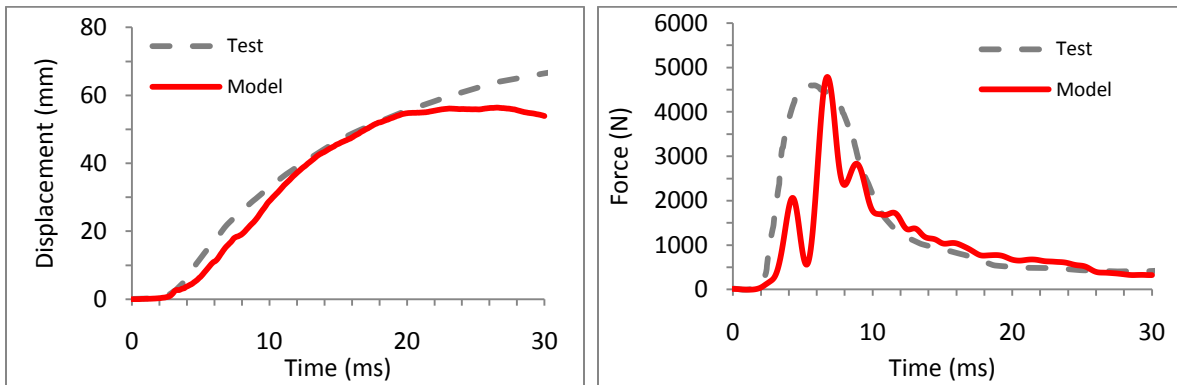
Figure 2-4. Model predicted abdomen penetration and seatbelt force for the Lamielle et al. PRT

tests.
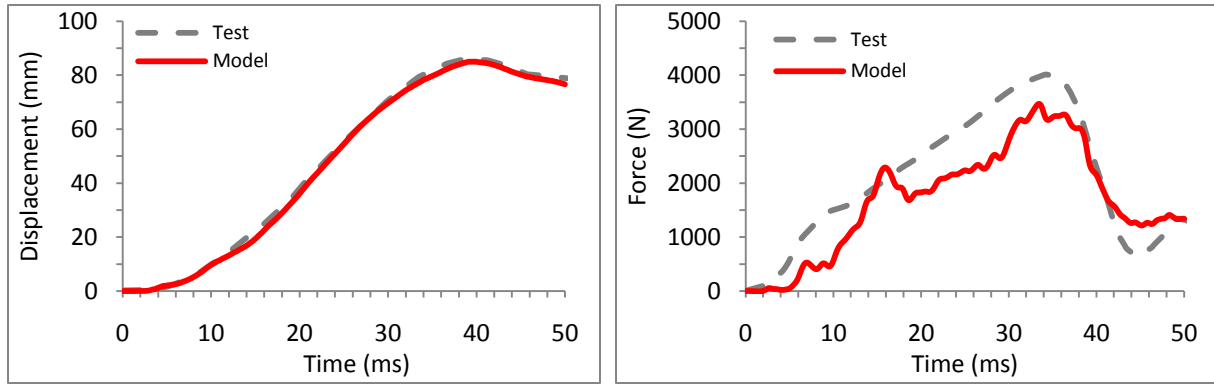
Figure 2-5. Model predicted abdomen penetration and seatbelt force for the Lamielle et al. MHA tests.

Table 2-2. Quantitative validation of the Modified WSUHAM

Signal	Pearson's Correlation Coefficient (r)	Difference in Peak Time (ms)	Difference in Peak Value as a % of the test data
Foster et al. Force	0.78	1	20
Foster et al. Penetration	0.99	4	10
Lamielle et al. MHA Force	0.93	1	13
Lamielle et al. MHA Penetration	.99	1	1
Lamielle et al. PRT Force	.77	1	4
Lamielle et al. PRT Penetration	0.98	4	15
Average	**0.91**	**2**	**10.5**

2.5   OBESE MODEL DEVELOPMENT

Once the Modified WSUHAM had been validated for multiple seatbelt loading conditions, obese abdomen models (Obese Abdomen FE model) were created. Three Obese Abdomen FE models were created with BMIs of 30, 35, and 40. To create the Obese Abdomen FE models, elements representing adipose tissue were added to the modified WSUHAM. In order to provide an accurate representation of an obese individual's torso geometry, virtual torso surfaces were generated for each BMI based on the statistical anthropometric model created by Reed et al. (2008). The torso surfaces are created from a sampling of 315 males and 449 females that were body scanned in a seated position. Principal Component Analysis (PCA) was used, along with regression to develop a statistical model that can generate an average shape torso based on input data such as height, weight, and gender. For this study average torso representations of a male, with a 50th percentile sitting height [58] and weight corresponding to BMIs of 30, 35, and 40 were used.

The torso surfaces in the form of IGES files were imported into HYPERMESH and aligned with the Modified WSUHAM using the H-points, L5/S1, and T12/L1 anatomical landmarks. Figure 2-6 shows the creation process of the Obese Abdomen FE models. First the torso surfaces were aligned with the FE model and shell elements were created from the skin solid elements (a). These elements were then projected and mapped normal to the torso surface (b). Eight node hexahedral solid elements were then used to fill the space between the model's original skin/muscle elements and the newly mapped shell elements (c). These new solid elements (light blue elements in Figure 2-6d) represent the added adipose tissue of the model and were assigned a new material property.
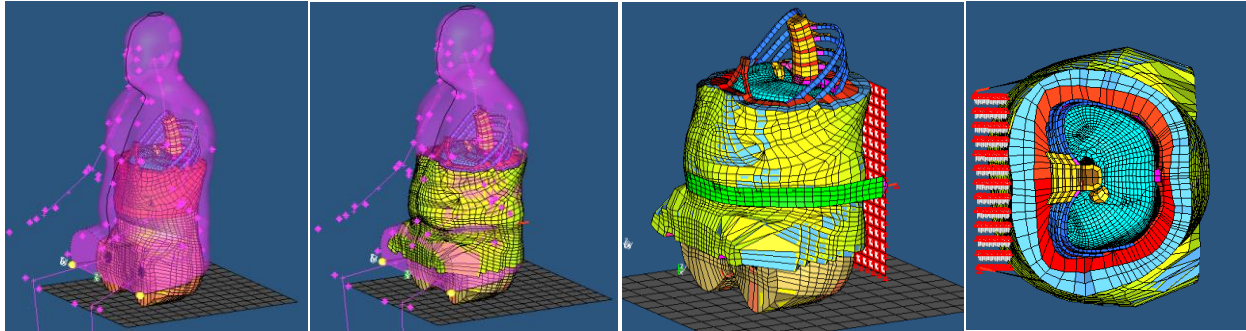
Figure 2-6. Process used to create the Obese Abdomen FE model with a BMI of 35.

Material properties for adipose tissue were taken from the literature [55, 56, 59]. A hyperelastic material model, which has been previously used to model adipose tissue [23, 56, 59] was used (LSDYNA card MAT_OGDEN_RUBBER) to represent the adipose tissue. A value of 900 kg/m^3 was assigned for the material density [23, 56], and hyperelastic material constants for strain rates of 20-260s^{-1} were used. The values assigned for the material constants were $\mu = 1.7$ kPa and $\alpha = 20$ [55, 59]. The minimum time step for the models was 3e-4 ms and run time was approximately 1 hour. Figure 2-7 shows the Obese Abdomen FE models that were created.
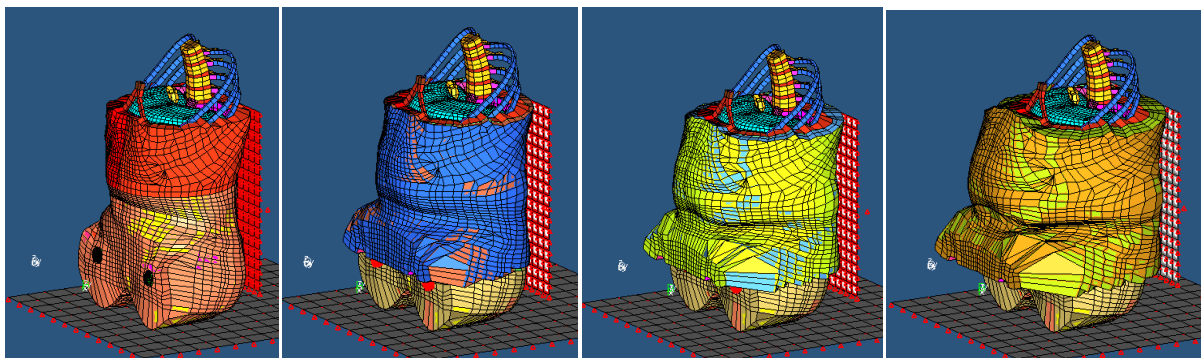
Figure 2-7. Obese Abdomen models: BMI 25 (Left), BMI 30 (Middle Left), BMI 35 (Middle Right) and BMI 40 (Right).

2.6   OBESE MODEL VALIDATION

Available cadaver test data only provides data for two obese cadavers (BMIs of 30 and 32) [53].

These test data were used to verify that the output of the Obese Abdomen FE models were

consistent with those reported in the literature. The output from the Obese Abdomen FE model

with a BMI of 30 was compared to test data for the two obese cadaver tests from Foster et al.

(2006). The same quantitative validation as was used for the Modified WSUHAM was also used

of the Obese Abdomen FE model. Figures 2-8 and 2-9 show the force-time and abdomen

penetration-time history curves for the model predicted response and the test data, and Table 2-3

shows the quantitative validation results for the Obese Abdomen FE model. For the Foster A1

test there was an instrument malfunction and abdomen penetration data was not completely

collected (Figure 2-8). Overall the model predicts the force and penetration of the obese cadaver

tests well. The model predicted peak abdominal force was 11861 N, and 8013 N for the A1 and

A2 tests respectively. The models predicted response is within +- 3ms of the test data and the

peak force is approximately +-25% of the peak test force for both cadaver tests. The model

predicts the abdominal penetration well, but slightly under estimates the penetration of the A2

test after about 22 ms. The correlation coefficient for the A2 force output is 0.53 which is low.

This may be due to the fact that the A2 test cadaver has a BMI of approximately 32 and the FE

model represents a BMI of 30 further indicating a need for abdomen models with accurate BMIs.

26
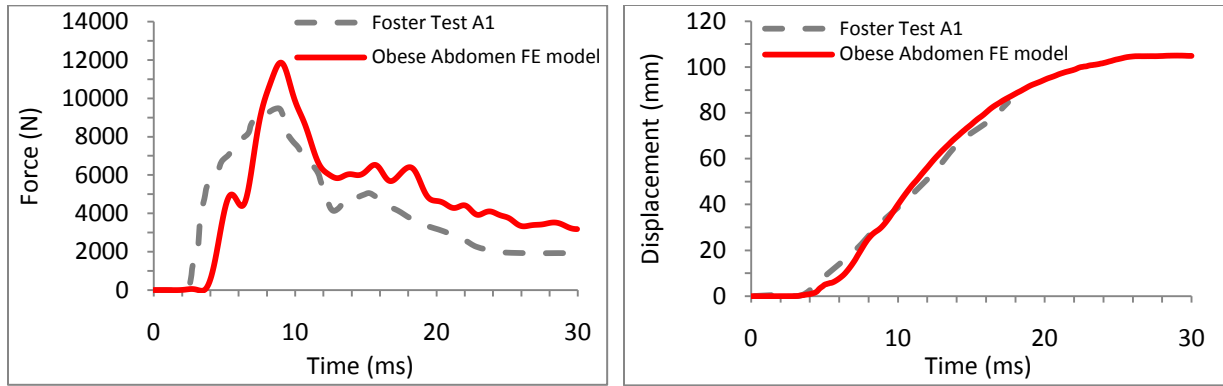
Figure 2-8. Model predicted seatbelt force and abdomen penetration compared to the A1 Foster et al. (2006) cadaver test.
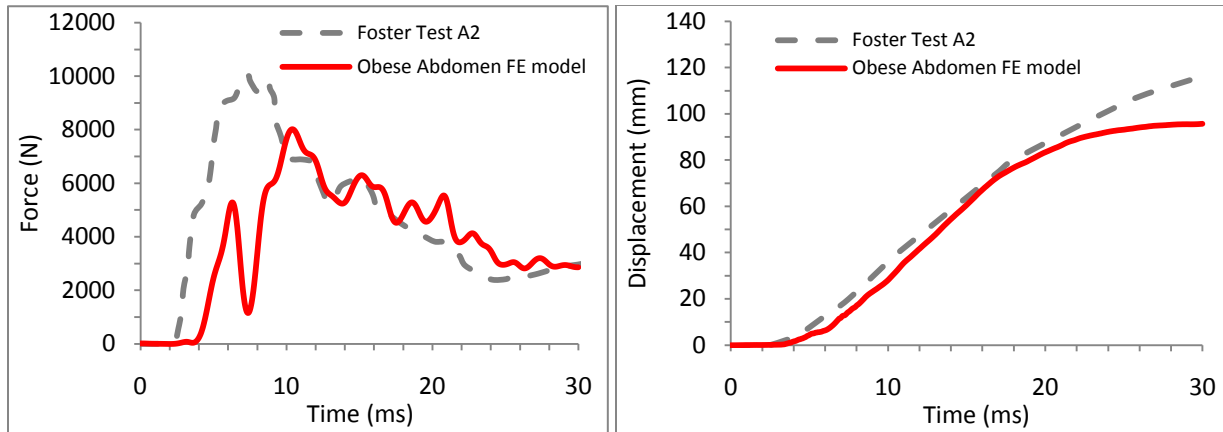
Figure 2-9. Model predicted seatbelt force and abdomen penetration compared to the A2 Foster et al. (2006) cadaver test.

Table 2-3. Quantitative Validation of the Obese Abdomen FE model

Signal	Pearson's Correlation Coefficient (r)	Difference in Peak Time (ms)	Difference in Peak Value as a % of the test data
Foster et al. A1 Force	0.77	0	25
Foster et al. A1 Penetration	0.99	0	2
Foster et al. A2 Force	0.53	3	20
Foster et al. A2 Penetration	.99	0	18
Average	**0.82**	**0.75**	**16.25**

2.7   ANGLED BELT LOADING

In order to further understand the effects of obesity on occupant injury, the Obese Abdomen FE

models were used to simulate real world abdominal lap belt loading conditions to examine obese

abdominal response to lap belt loading. Three lap belt positions were used representing a low,

middle, and high lap belt fit (Figure 2-10). Low lap belt position represents "proper" belt fit,

which consists of the lap belt fitting low and snug against the pelvis, and near the thigh-

abdominal junction [60].   The middle and high belt positions were chosen based on field data

collected in the Rehabilitation Engineering Research Center on Wheelchair Transportation

Safety (Project 3) which show that both obese and wheelchair-seated occupants can miss use the

occupant restraint system. Figure 2-11 shows examples of good and poor belt fit representative

of low, middle and high belt positions.
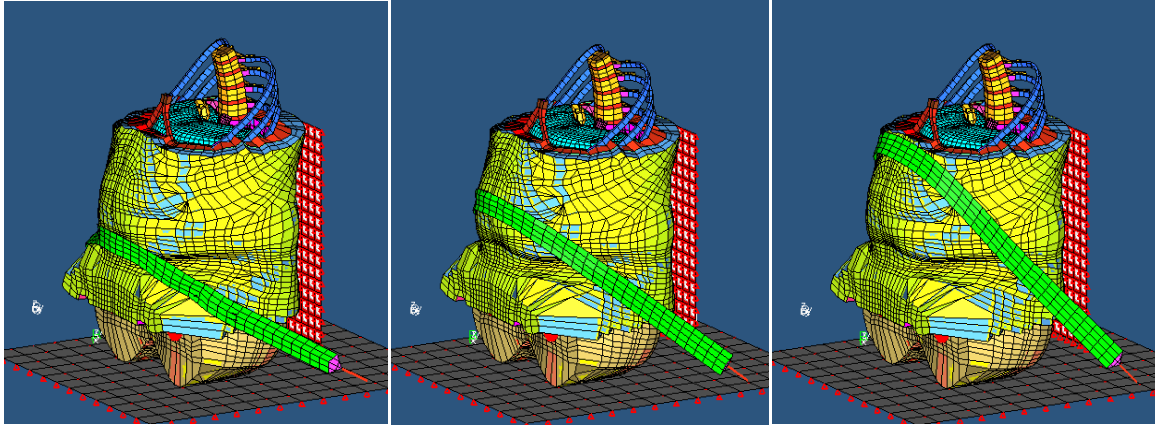
Figure 2-10. Lap belt positions of low (Left), middle (middle), and high (Right) for the Obese

Abdomen FE model with a BMI of 35.

Figure 2-11. Example of good and poor lap belt fit, classified as low (Left), middle belt fit

(middle), and high belt fit (Right).

The motion assigned to the belt was the same prescribed motion as used in the previous

Foster validation of the Modified WSUHAM.   The skeleton components of the models were

fixed so that the resulting abdominal response would be a material response and the effects of

mass inertia of the model would be minimized. The 3 belt positions were run for BMI levels of 25, 30, 35, and 40 and abdomen force/deformation plots were generated.

2.7.1   Results

Figure 2-12 shows the abdominal force-deformation plots for each BMI level for low, middle, and high belt fit. For a BMI of 25 the force is very high because as the seatbelt penetrates the abdomen and the belt interacts with the rigid skeleton. The low force recorded for a BMI of 25 with a high belt position is due to a combination of the belt angle and abdomen geometry which causes the belt to slide down the abdomen before penetrating the skin. This belt sliding does not occur in higher BMIs because the geometry of the obese abdomen (i.e. a more round belly) prevents this from happening. As BMI increases the force deformation curves for the varying angles tend to become similar in shape and magnitude. At a BMI of 35 and 40 the force deformation curves have the same shape and same peak magnitude between about 6000 -9000 N regardless of belt angle. This is because as the adipose tissue increases the seatbelt-skeleton interaction becomes less important as the amount of adipose tissue starts to dominate the abdomen response. The slight increase in peak force seen from a BMI of 35 to 40 is likely due to the increase in the amount of adipose tissue the seatbelt has to penetrate into.
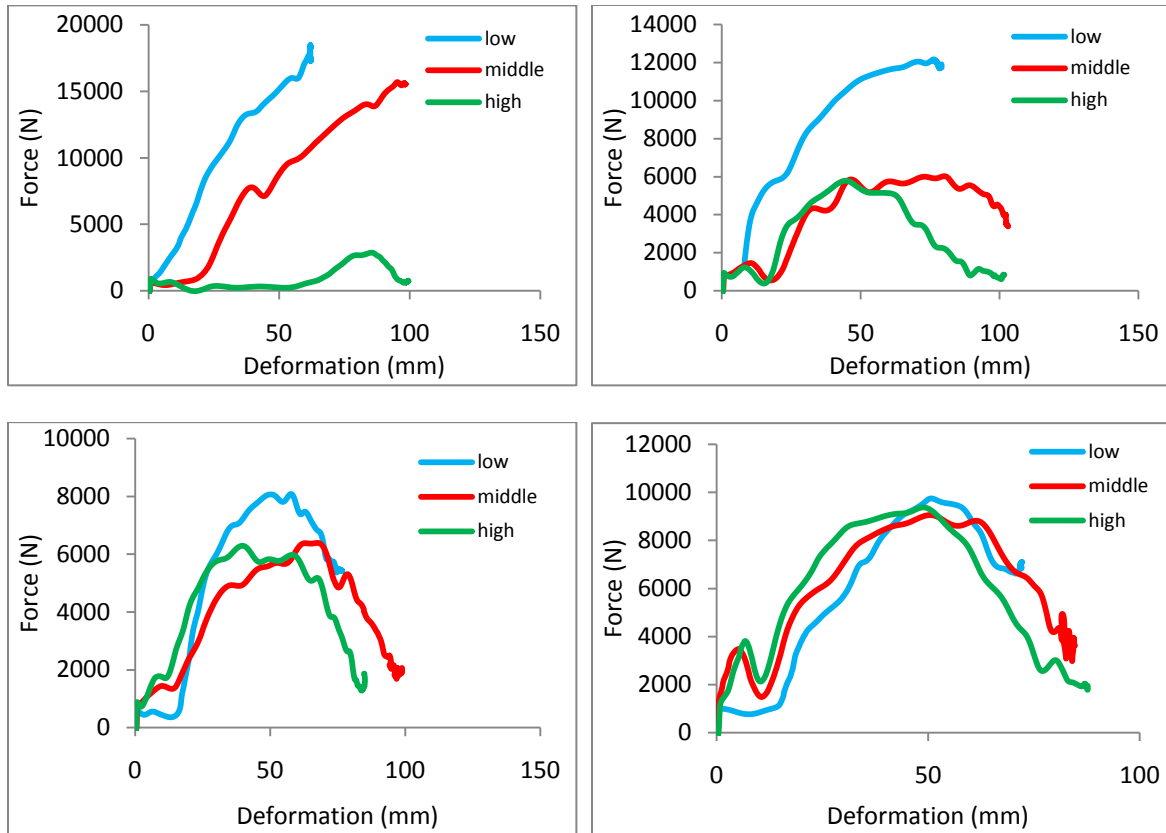
Figure 2-12. Model predicted abdomen force-deformation curves for BMI of 25 (Upper Left), BMI of 30 (Upper Right), BMI of 35 (Lower Left), and BMI 40 (Lower Right) as lap belt position was varied.

2.7.2 Organ Pressure

One of the main points of discussion in the literature is that the increased adipose tissue on the abdomen of obese individuals may provide a cushion effect to the internal organs of the abdomen thus reducing the chance of injury as reported by some studies [20, 21]. To investigate this hypothesis the peak pressures experienced by the liver, spleen, and kidneys due to seatbelt loading were recorded during the angled loading tests. In addition to the 3 belt positions

previously described an additional position of an angle of "0 degrees" similar to the validation loading conditions in which the belt is placed flat against the anterior of the mid umbilicus and routed straight back were also performed for all BMI cases while the skeleton was fixed. Peak pressures were recorded and compared. Correlation and one way ANOVA were performed between peak pressure of the spleen, liver, and kidneys, and BMI. Significance level was set at alpha =0.05.

Results of the ANOVA indicate no significant differences in peak pressure for any of the solid organs (liver ($p=0.328$), spleen ($p=0.883$), left kidney ($p=0.688$), and right kidney ($p=0.280$)) as BMI increased. Table 2-2 shows the peak pressure values and correlations for the spleen, liver and kidneys. The model predicted a slight negative relationship between BMI and kidney peak pressures and a positive correlation between BMI and liver and almost no relationship between BMI and spleen pressure. No pressure was recorded for a BMI of 25 with high belt position due to the seatbelt sliding down the abdomen before applying load to the abdomen. Results should be interpreted cautiously as the FE model has not been validated with organ pressure data.

Table 2-4. Maximum pressures for the liver, spleen and kidneys for varying levels of BMI. Pressure values reported in units of kPa.

BMI	Position	Spleen max pressure	Liver max pressure	Left kidney max pressure	Right Kidney max pressure
25	0	77.83	86.34	194.75	242.60
25	low	1.84	4.17	7.91	9.23
25	middle	5.87	24.52	15.88	35.43
25	high	N/A	N/A	N/A	N/A
30	0	82.01	100.10	148.83	210.40
30	low	5.73	33.85	20.63	54.18
30	middle	42.17	96.17	47.32	60.15
30	high	18.54	216.86	51.77	509.47
35	0	53.72	80.27	64.77	100.23
35	low	5.11	22.16	9.11	12.39
35	middle	12.89	55.75	27.16	38.15
35	high	12.95	100.86	24.30	43.25
40	0	61.46	103.20	75.70	59.90
40	low	5.45	26.21	8.58	16.00
40	middle	33.76	114.28	25.76	56.30
40	high	36.50	134.65	33.50	53.30
Correlation Coefficient		**0.09**	**0.31**	**-0.20**	**-0.21**

2.8   SUMMARY

An Obese Abdomen FE Model was created and validated to study the effects of obesity on abdomen force deformation response. First the WSUHAM was modified with a hyperelastic material for the skin and muscle and validated for multiple seatbelt loading conditions. The Modified WSUHAM is able to predict abdomen force and penetration response over 3 different seatbelt loading conditions reported in the literature [53, 54]. The Modified WSUHAM was then

used to create 3 Obese Abdomen FE Models with BMIs of 30, 35, and 40 based on the geometry used by Reed et al. The Obese Abdomen FE Model with a BMI of 30 was validated with data from two obese cadaver abdomen tests in the literature [53].

The effects of obesity on mechanical response of the abdomen were studied through a series of simulations with realistic lap belt loading conditions. Simulations were run with low, middle, and high belt fit on the abdomen for BMI levels of 25, 30, 35, and 40. Results indicate that the force deformation response of the abdomen changes as BMI increases. Initially the abdomen force is very high (>10000 N) for BMIs of 25 and 30 because the seatbelt is loading the pelvis. At higher BMIs (35 and 40) the adipose tissue becomes more significant, and lap belt contact with the pelvis is reduced. This results in the abdomen force deformation response converging in magnitude and shape regardless of seatbelt angle at higher levels of BMI (35 and 40). The resulting force deformation response for high BMIs is approximately haversine in shape with a peak force between 6000-9000 N.

Finally to examine the cushion effect hypothesis, organ pressures for the spleen, liver, and kidneys were recorded for all seatbelt angle simulations. There was no significant difference in pressures as BMI increases, indicating that there is no statistically significant cushion effect. Correlations indicate that there might be a slight cushion effect for the kidneys, whereas the liver experiences higher pressures with increased BMI. This could be due to the fact that the increased mass of the adipose tissue moving into the liver, which is located in the anterior portion of the abdominal cavity, causes higher pressures, however since the kidneys and spleen are located on the lateral aspects of the abdomen, the adipose tissue may buffer these organs. This could explain the conflicting reports in the literature on obese abdominal injury in MVCs [5, 15, 20-23]. It also suggests that direct contact from the deforming adipose tissue may actually increase

the likelihood of injury. This may be significant in other types of abdomen loading such as abdomen contact with the vehicle interior and or steering wheel. However it is important to note that this model has not been validated for internal organ pressures so more research on the effects of BMI on internal organ pressures is needed.

3.0 THE EFFECTS OF OBESITY ON OCCUPANT INJURY RISK IN FRONTAL IMPACTS

3.1 OVERVIEW

Literature suggests that obese occupants have a different risk of injury in MVCs than non-obese occupants [5, 15, 16, 18-26, 61-63]. The current hypotheses suggest that:

1. The increased mass of the obese occupant causes increased force, and thus increased risk of injury on the occupant when contacting the vehicle interior and or safety system [15, 19, 21, 26, 62].

2. The obese occupant may be predisposed to poor belt fit due to geometry of the torso causing increased risk of injury [5].

3. There may be a cushion effect that absorbs some of the force on the body thus reducing the risk of injury to certain body regions [20, 21, 26].

However the exact mechanism of injury to obese occupants is still unknown. This chapter describes the development of three MADYMO whole body models, and the subsequent simulations run to investigate the mechanisms of injury and injury risk to obese occupants. Figure 3-1 describes the approach used to investigate these hypotheses.

36
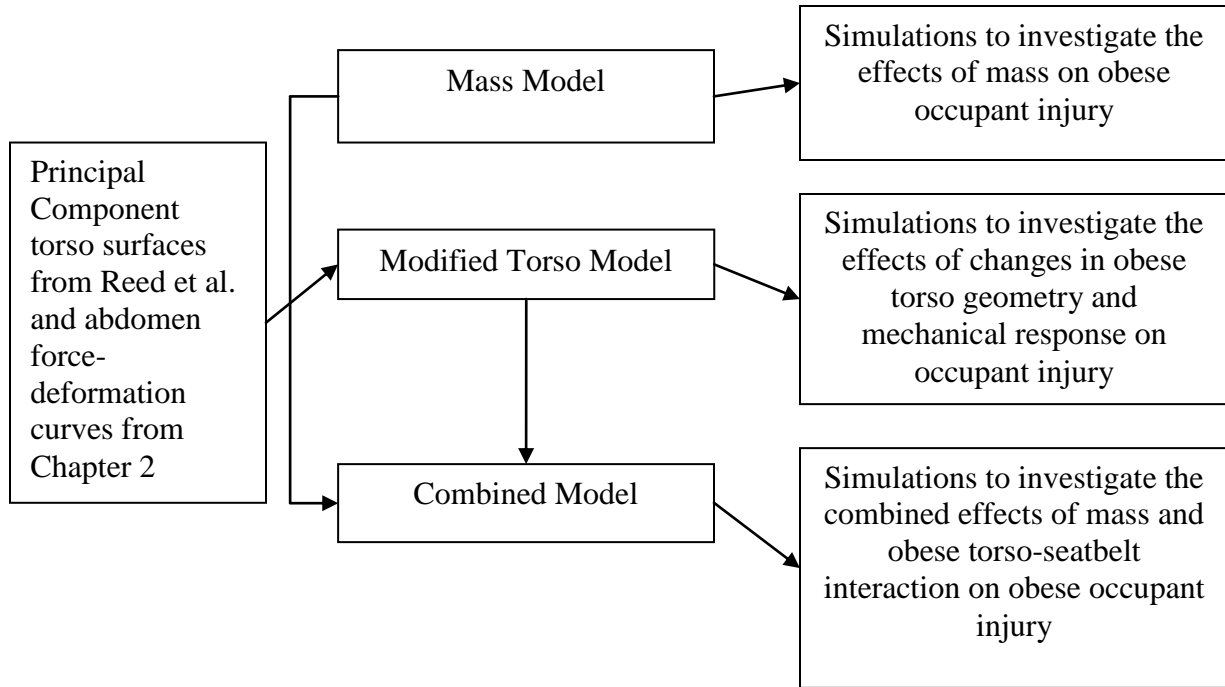
Figure 3-1. Flow chart describing the research setup.

3.2   DEVELOPMENT OF OBESE WHOLE BODY MODELS

3.2.1   Mass Model

A model (Mass Model) was created using MADYMO Madyscale (TNO, Delft, Netherlands) to

investigate the effects of increased mass due to increased BMI on occupant injury in MVCs.

MADYMO Madyscale is a computer program that scales the mass and inertial characteristics of

the rigid body ellipsoid MADYMO Hybrid III ATD according to anthropometric data taken from adult humans [47, 48]. The resulting model does a good job representing the mass of an occupant but does a poor job representing the geometry of the individual, and does not scale the contact characteristics of the ATD ellipsoids. The input variables used for the Madyscale program for this study were gender, height, and weight. Three male ATDs were created with BMIs of 25, 30, and 39. The program has a range of heights and weights that it can scale, and as a result a BMI of 39 is the maximum allowable BMI given a male 50th percentile stature. Figure 3-2 shows the three Mass Models created.

Figure 3-2. Mass Models with a BMI 25 (Left), BMI 30 (Middle), and BMI 39 (Right) in a MADYMO vehicle environment.

3.2.2   Modified Torso Model

A second model (Modified Torso Model) was created to examine the effects of obese torso geometry, obese torso mechanical response, and seatbelt interaction on obese occupant injury without considering the mass effects. The 50th percentile MADYMO Hybrid III ATD was used

as a base model. PCA torso surfaces used in chapter 2 were meshed, imported into MADYMO, and fit to the MADYMO Hybrid III ATD creating three ATDs with torso geometry of 25, 30, and 39 BMI respectively while the mass of the model remained representative of a BMI 25. Force-deformation contact properties were assigned between the meshed torsos and the seatbelt based on the various belt position force-deformation curves obtained from the Obese Abdomen FEM developed in Chapter 2. The force-deformation curves for a BMI of 40 from Chapter 2 were assigned to the Modified Torso Model with a BMI of 39 since the two surfaces were compared and there were minimal differences. For the high belt angle for a BMI of 25 the force-deformation curve was low due to belt sliding, so the force deformation curve for the BMI 25 with a middle belt angle was used. Figure 3-3 shows the Modified Torso Model.

Figure 3-3. Modified Torso Model with BMIs of 25 (Left), 30 (Middle) and 39 (Right).

3.2.3 Combined Model

Finally, in order to examine the interaction of increased mass and changes in torso geometry and mechanical response due to obesity on occupant injury, the Mass Model and the Modified Torso Model were combined to create a more realistic model (Combined Model) shown in Figure 3-4.

Figure 3-4. Combined Model with BMIs of 25 (Left), 30 (Middle), and 39 (Right).

3.3   VALIDATION

A limited amount of kinematic data for obese cadavers is available in the literature [62]. Kent et al. (2010) reported kinematics of obese and non-obese cadavers in sled tests with 3-point restraint systems with and without load limiters and pretensioners. However detailed descriptions of the test setup were not provided and only peak excursions of the head, shoulders, hips, and knees were reported. The main trends reported by Kent et al. (2010) were increased forward excursion in the obese cadaver group, and a decrease in the shoulder to hip excursion

ratio for the obese group compared to the non-obese group. For model validation purposes the test setup was replicated as best as possible using the Combined Model with a BMI of 25 to represent the non-obese group, and a BMI of 39 to represent the obese group. Model predicted excursion values were compared to the data provided by Kent el al. Figure 3-5 shows the forward excursion values predicted by the model and the average forward excursion values for the test data reported by Kent et al. (2010).
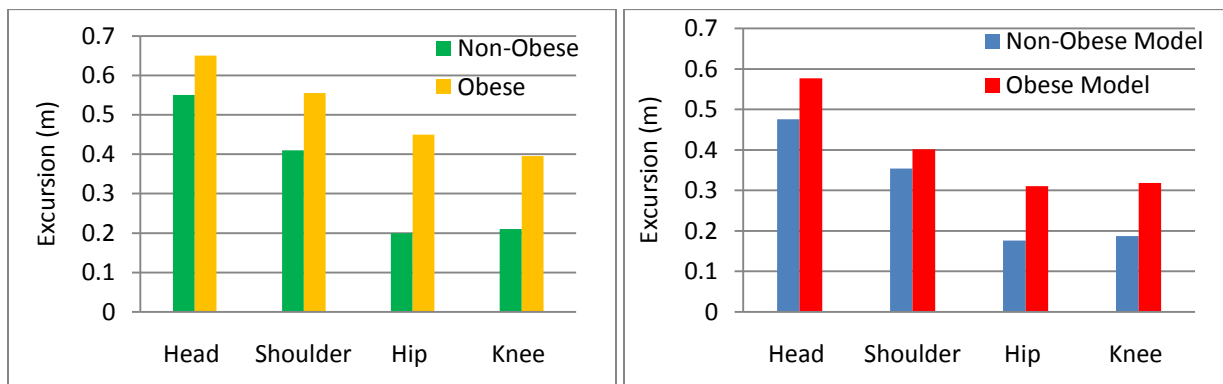
Figure 3-5. Average peak forward excursions reported by Kent et al. for obese and non-obese cadavers (Left) and model predicited peak forward excursions (Right).

The model predicts the trends seen in the test data well. There is an increase in all excursion values for the obese model compared to the non-obese model. The magnitude of the excursion values are lower for the model compared to the cadaver data of Kent et al. (2010), but this is likely due to a lack of detailed information on the test setup conditions used by Kent et al. More detailed information about the test conditions would likely yield more accurate model excursion data. The key data from Kent et al. (2010), important for model validation, suggests a reduced shoulder to hip ratio excursion ratio in the obese cadaver group compared to the non-

obese group. The model accurately predicts this phenomenon as shown in Figure 3-6 providing

further justification that the model is sufficiently validated.
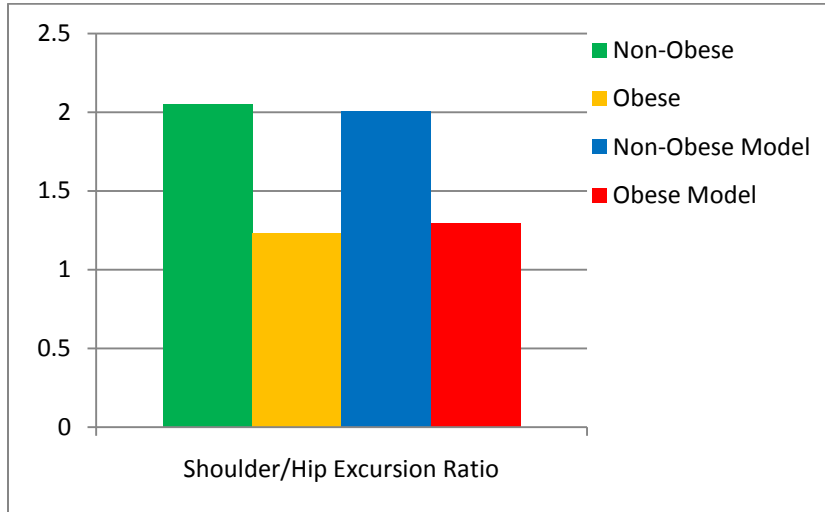
Figure 3-6. Average shoulder-hip excursion ratio from Kent et al. cadaver data and Combined

Model predicted shoulder-hip excursion ratio.

3.4   PARAMETRIC ANALYSIS

A parametric analysis was performed using the obese whole body models to investigate the

effects of obesity on occupant injury while controlling for several vehicle design parameters.

The Design of Experiments (DOE) method using Taguchi's orthogonal arrays was utilized

because it allows for a reduced number of simulations to be run, yet can still predict significant

trends in the data [64, 65]. The obese models were placed in a vehicle interior, available in

MADYMO, representing an average sedan interior, containing a standard automotive airbag and

FE lap and shoulder belts (Figures 3-2-4). Eight variables with two or three levels each were controlled for in this study. A full factorial design with 8 factors and 3 levels each would require 6561 runs, however by using an orthogonal array and a fractional factorial design, significant trends in the data can be predicted with only 18 runs. A parametric analysis was performed on each model (Mass Model, Modified Torso Model, and Combined Model) for a total 3 separate analyses and an overall total of 54 simulations.

The factors included in the DOE were BMI, crash severity, load limiter force, pretensioner force, airbag inflation rate, seatbelt angle, knee-knee bolster distance, and knee bolster stiffness. These variables have been shown to influence occupant safety in MVCs [65-68]. Frontal impact crash severities, measured as change in velocity (delta v), of 25, 30, and 35 mph were used based on federal crash regulations and previous studies [7, 65, 69]. The 25 mph delta v is based on the FMVSS 208 unbelted occupant safety test, the 30 mph delta v is used in the original FMVSS 208 occupant safety tests, and the New Car Assessment Program uses a 35 mph delta v crash severity. The load limiter force used two levels of 4 and 6 kN based on the findings of Foret et al. (2001). Pretensioner force has been varied to investigate its effect on occupant safety [65, 70] and for this study it was varied between 0, 1, and 2 kN based on data from the NHTSA occupant restraint testing database. Airbag inflation rate can protect the upper body and head in an MVC and its inflation rate was scaled +- 20% from the baseline inflation rate used in the original MADYMO vehicle setup. Knee bolster stiffness levels were 30, 70, and 120 N/mm based on previous research [65, 67, 71], and knee bolster distance was set at 50, 70, and 120 mm based on the research reported by Atkinson et al. (1999), Kim et al. (2005) and data from the Rehabilitation Engineering Research Center on Wheelchair Transportation Safety (Project 3). Finally lap belt angles corresponding to the belt angles used in Chapter 2 (low,

middle and high) were used to control for the possible poor belt fit due to increasing BMI. For each belt angle and BMI, the corresponding force-deformation response obtained in Chapter 2 was assigned as the contact characteristic between the abdomen mesh and the lap belt. Figure 3-7 shows the design variables used in this DOE, and Table 3-1 shows the Taguchi array test matrix with the eight variables and associated levels.
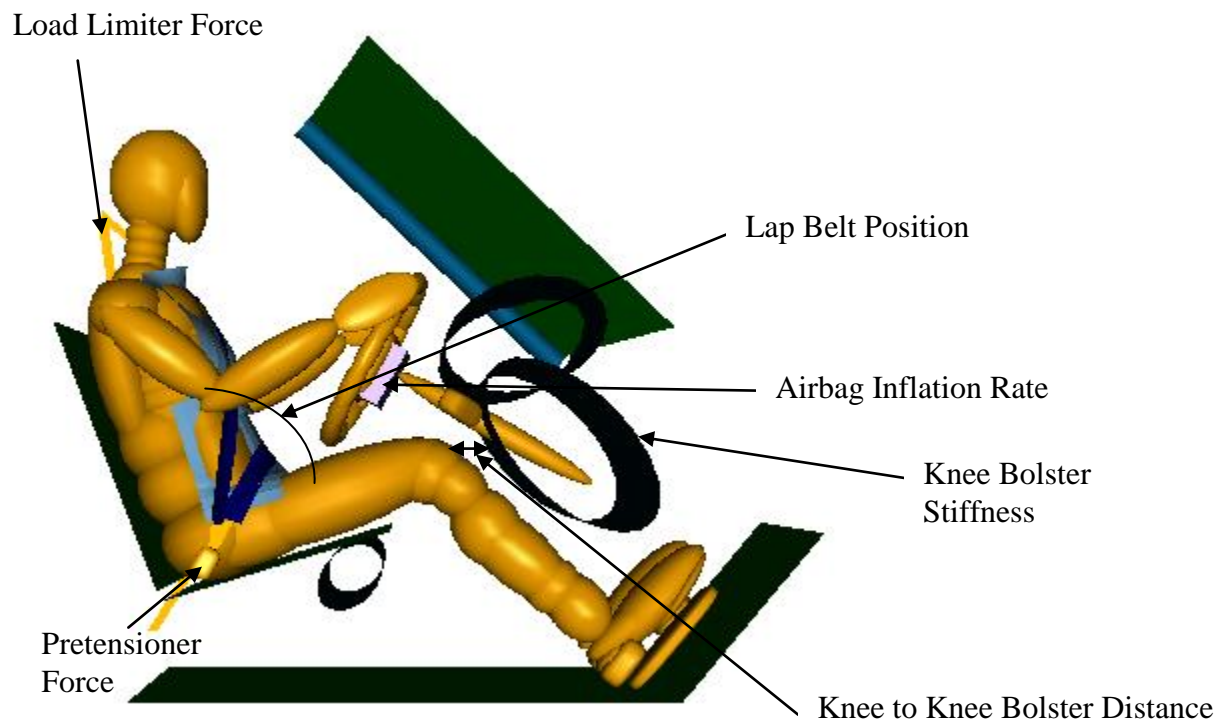
Figure 3-7. Description of the DOE factors.

Table 3-1. DOE Taguchi Array test matrix.

Simulation #	Load Limiter (kN)	BMI (kg/m^2)	Crash Severity (mph)	Belt Position	Knee-knee bolster distance (mm)	Knee bolster stiffness (N/mm)	Airbag Inflation Rate (%)	Pretensioner force (kN)
1	4	25	25	low	50	30	80	0
2	4	25	30	middle	70	70	100	1
3	4	25	35	high	120	120	120	2
4	4	30	25	low	70	70	120	2
5	4	30	30	middle	120	120	80	0
6	4	30	35	high	50	30	100	1
7	4	39	25	middle	50	120	100	2
8	4	39	30	high	70	30	120	0
9	4	39	35	low	120	70	80	1
10	6	25	25	high	120	70	100	0
11	6	25	30	low	50	120	120	1
12	6	25	35	middle	70	30	80	2
13	6	30	25	middle	120	30	120	1
14	6	30	30	high	50	70	80	2
15	6	30	35	low	70	120	100	0
16	6	39	25	high	70	120	80	1
17	6	39	30	low	120	30	100	2
18	6	39	35	middle	50	70	120	0

3.4.1 Output/Statistics

Output values used to assess the effect of BMI on occupant injury were injury criteria used in

FMVSS 208 testing. These parameters include Head Injury Criteria (HIC), Chest 3ms Injury

Criteria, Chest Deformation, and Femur Force Criteria (FFC). HIC is defined as

$$HIC = \left[\frac{1}{(t_2 - t_1)} \int_{t_1}^{t_2} a \; dt \right]^{2.5} (t_2 - t_1)$$

where a is the head acceleration in units of g and t is time.

The HIC value should not exceed 700 and is associated with a 5% risk of severe, AIS 4+, head

injury [72]. Figure 3-8 shows the risk of severe head injury as a function of HIC based on the

data of Mertz et al., 1997.
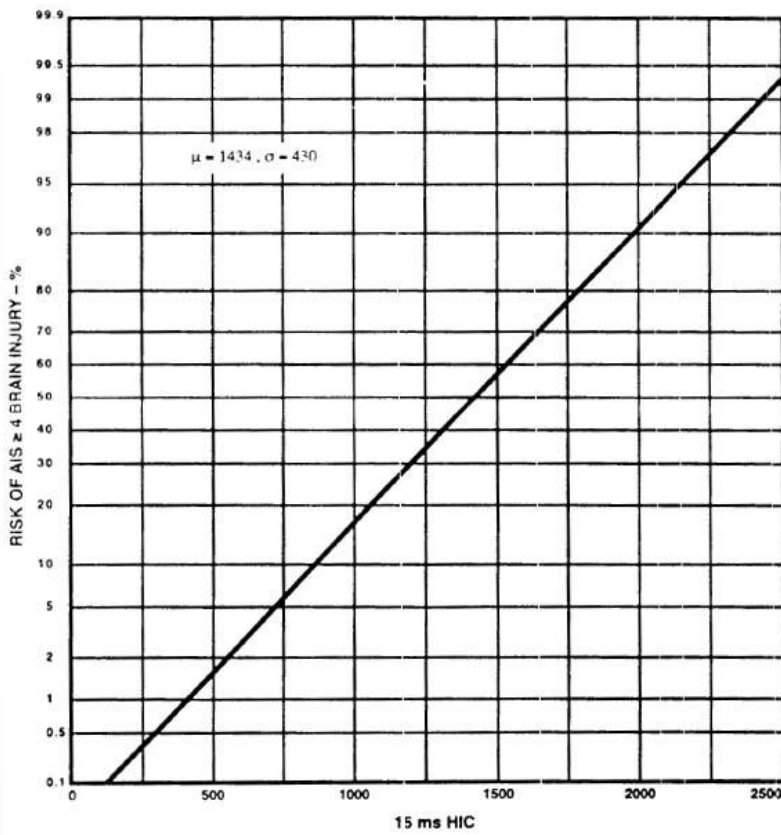
Figure 3-8. Probability of Severe Head injury based on HIC. (Figure adopted from Mertz et al. 1997.)

Chest 3ms Criteria is defined as the resultant chest acceleration for a duration of more than 3 ms and it shall not exceed 60 g. This value is based on cases of humans falling from heights of up to 100 feet and estimated whole body accelerations [73]. Based on the cases analyzed, a value of 60 g was recommended as representation of a 20% risk of an AIS 4+ chest injury. This measure of chest injury has been very controversial because of the data that it is based on.

Chest deflection is defined as the compressive displacement of the sternum relative to the thoracic spine and cannot be greater than 63 mm. Depending on the mode of chest loading,

airbag or seatbelt, a deflection of 60 mm represents a 45-70% risk of an AIS 3+ chest injury [72] (Figure 3-9).
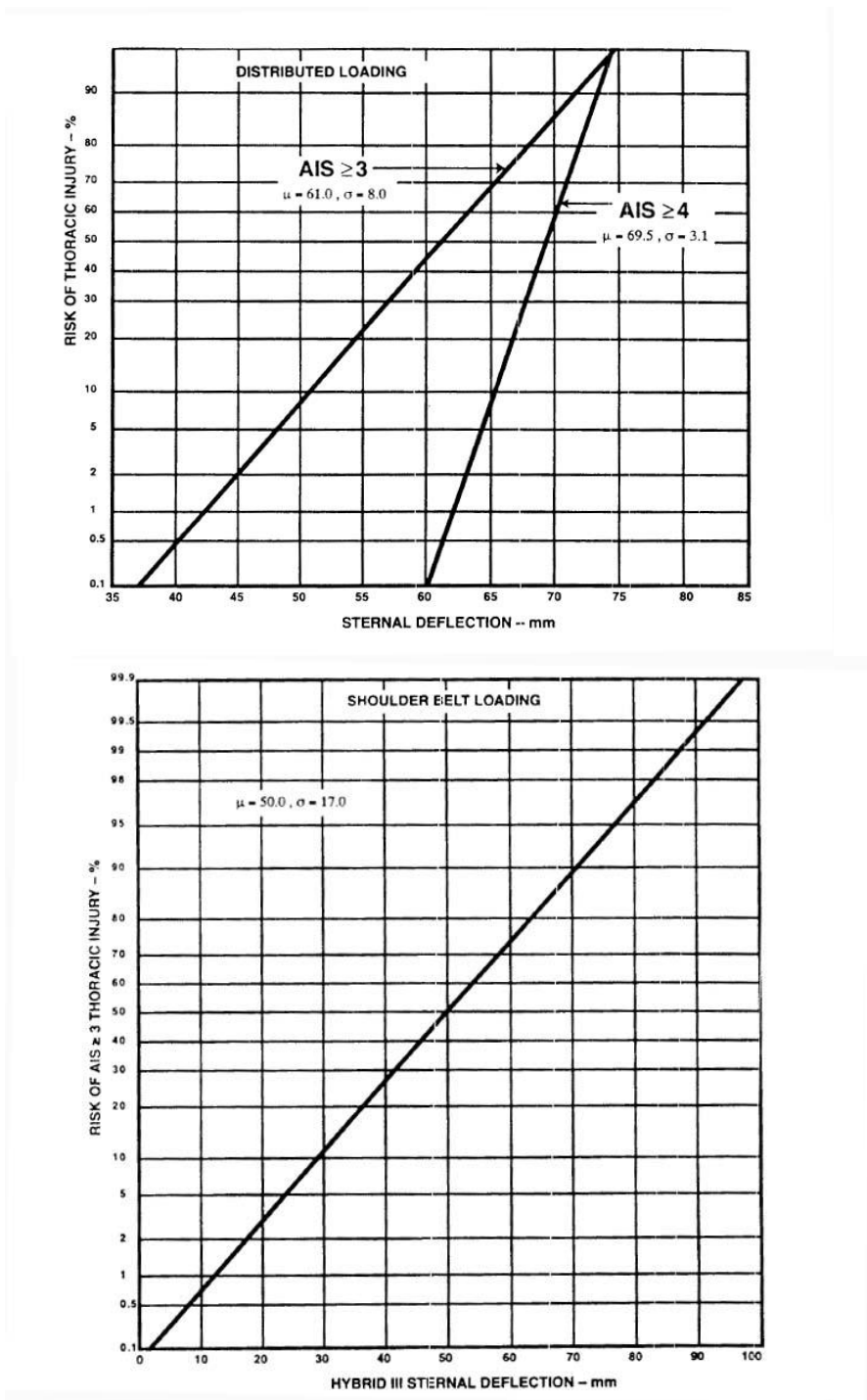
Figure 3-9. Risk of chest injury for distributed loading (Top) and seatbelt loading (Bottom) as a function of chest deformation. (Figures adopted from Mertz et al. 1997)

The Femur Force Criteria is defined as the axial force in the femur and must not exceed 2250 pounds (10,000 N), and this value is correlated with a 35% risk of AIS 2+ injury [74, 75] (Figure 3-10). For the purposes of this study the femur force for the right and left femurs were averaged.
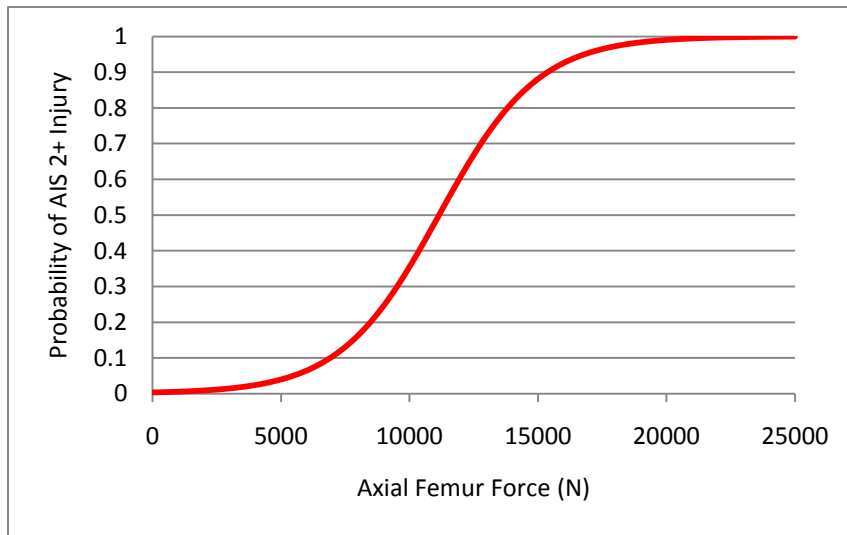
Figure 3-10. Probability of AIS 2+ knee-thigh-hip injury

An Analysis of Covariance (ANCOVA) was used to test the significance level of the main effects of the factors for each injury parameter. In the ANCOVA the injury parameter was defined as the dependent variable, and the factors in the Taguchi array were assigned as independent variables or covariates. To examine the main effects of BMI on injury risk while controlling for covariates, the BMI variable was treated as a fixed effect in the model and the other variables (Crash Severity, Load Limiter, Belt Position, Knee Bolster Distance, Knee Bolster Stiffness, Airbag Inflation Rate, Pretensioner Force) were treated as covariates. The DOE using a Taguchi array allows for examination of the main effects of several factors while

49

performing a limited number of simulations. However the Taguchi array used in this study does not allow for the examination of interactions between variables. Using the Taguchi method assumes that any interactions that do exist are relatively insignificant. As a result an effort was made to select variables that were independent of each other and it was assumed that all factor interactions were insignificant. SPSS (PASW Statistics 18) was used to perform all statistical calculations and a significance level of alpha = 0.05 was used.

3.5   RESULTS

3.5.1   Mass Model

Figures 3-11, 3-12, 3-13, and 3-14 show the average values, due to the main effects of the controlling factors, for HIC, Chest 3ms, Chest Deformation, and FFC for the Mass Model. Figure 3-11 shows the significant factors for HIC as an injury criteria. Crash Severity (p=0.000) and Airbag Inflation Rate (p=0.037) were significant, however BMI (p=0.930) was not a significant factor for HIC after controlling for other factors in the Taguchi array.
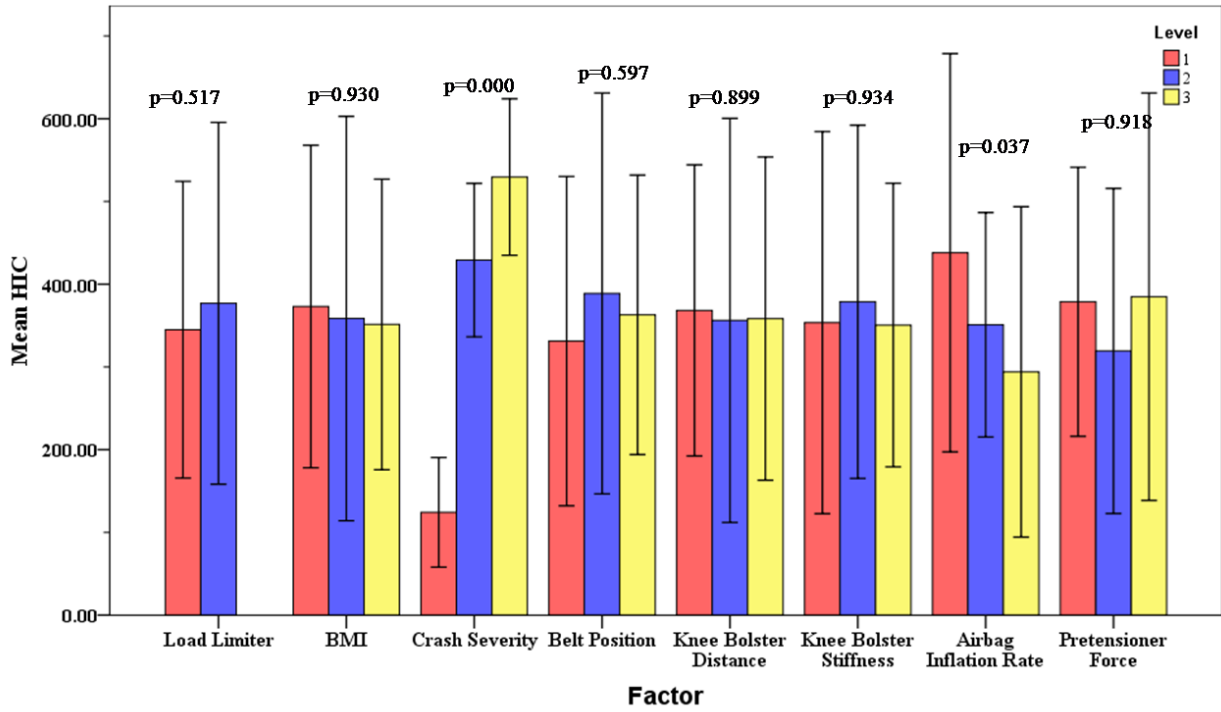
Figure 3-11. Mean HIC values for all factors for the Mass Model.

The only siginifcant factor for Chest 3ms injury criteria was Crash Severity (p=0.000) (Figure 3-12).
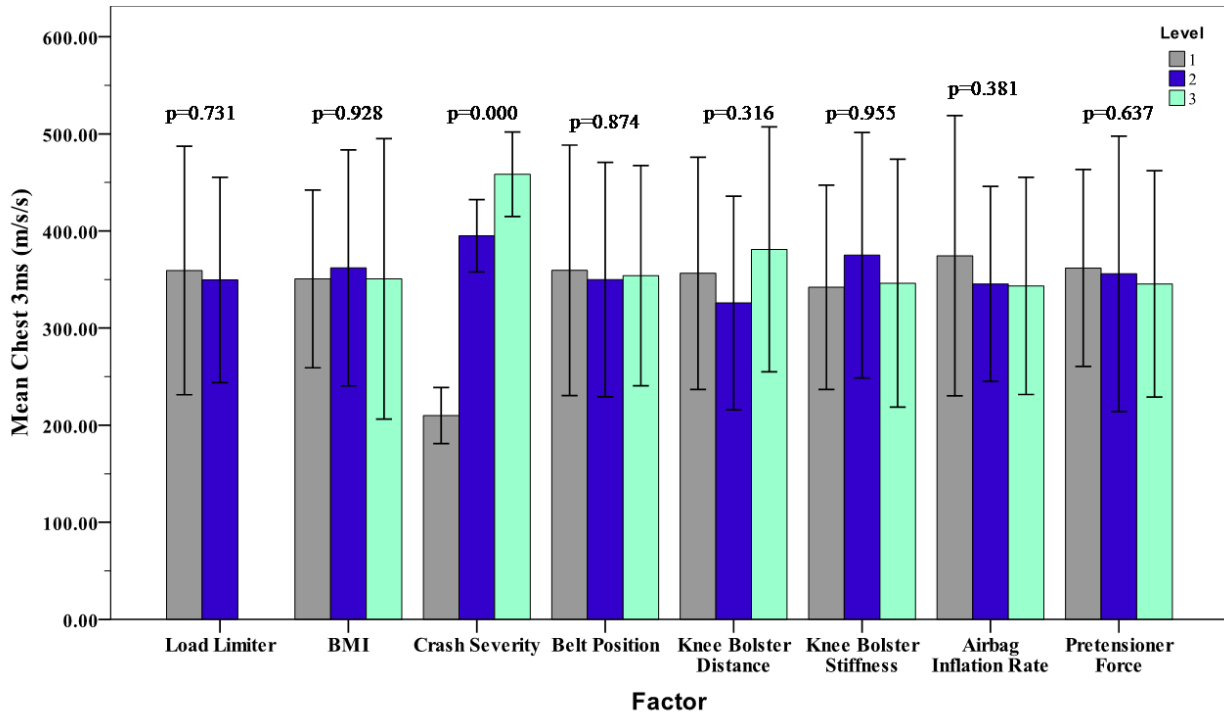
Figure 3-12. Mean Chest 3ms values for all factors for the Mass Model.

BMI was siginificant (p=0.004) for Chest Deformation along with Crash Severity (p=0.000) and BMI accounts for approximately 75.70% ($\eta^2_{partial} = 0.757$) of the variation in the Chest Deformation and Chest Deformation increases as BMI increases (Figure 3-13).
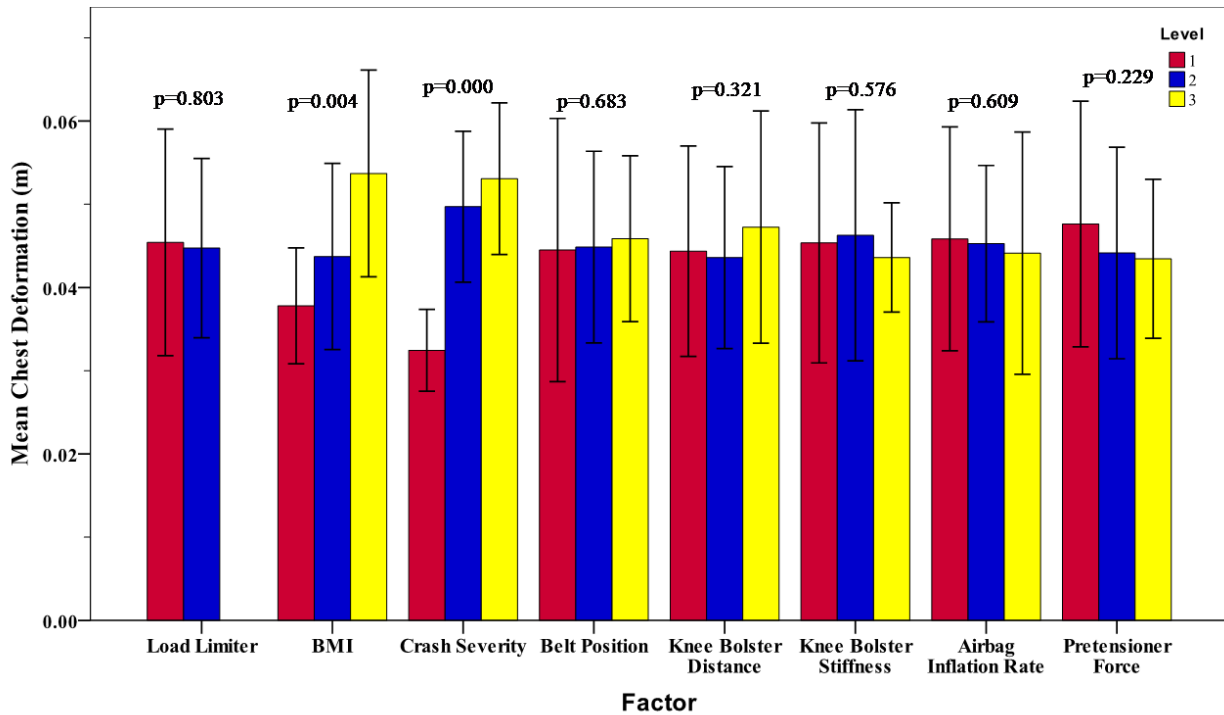
Figure 3-13. Mean Chest deformation values for all factors for the Mass Model.

Significant factors for FFC were Belt Postion (p=.037), Knee Bolster Distance (p=.006), Pretensioner force (p=0.006), and BMI (p=0.001). BMI accounts for approxiametly 85.00% of the variation ($\eta^2_{partial}$ = 0.850) and FFC increases as BMI increases (Figure 3-14).
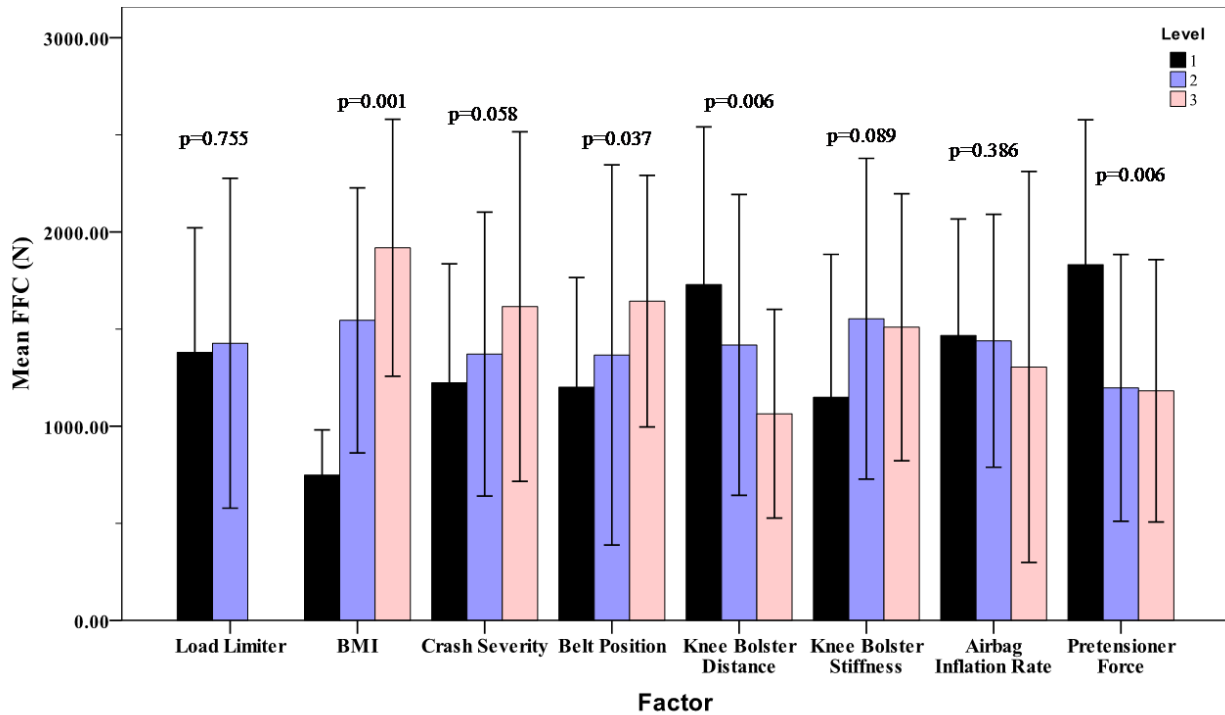
Figure 3-14. Mean FFC values for all factors for the Mass Model.

3.5.2   Modified Torso Model

Figures 3-15, 3-16, 3-17, and 3-18 show the average values due to the main effects of the

controlling factors for HIC, Chest 3ms, Chest Deformation, and FFC for the Modified Torso

Model. BMI was not a significant factor in the Modified Torso Model for any of the injury

criteria examined. For HIC, Crash Severity (p=0.000), and Airbag Inflation Rate (p=0.025) were

signifcant (Figure 3-15).
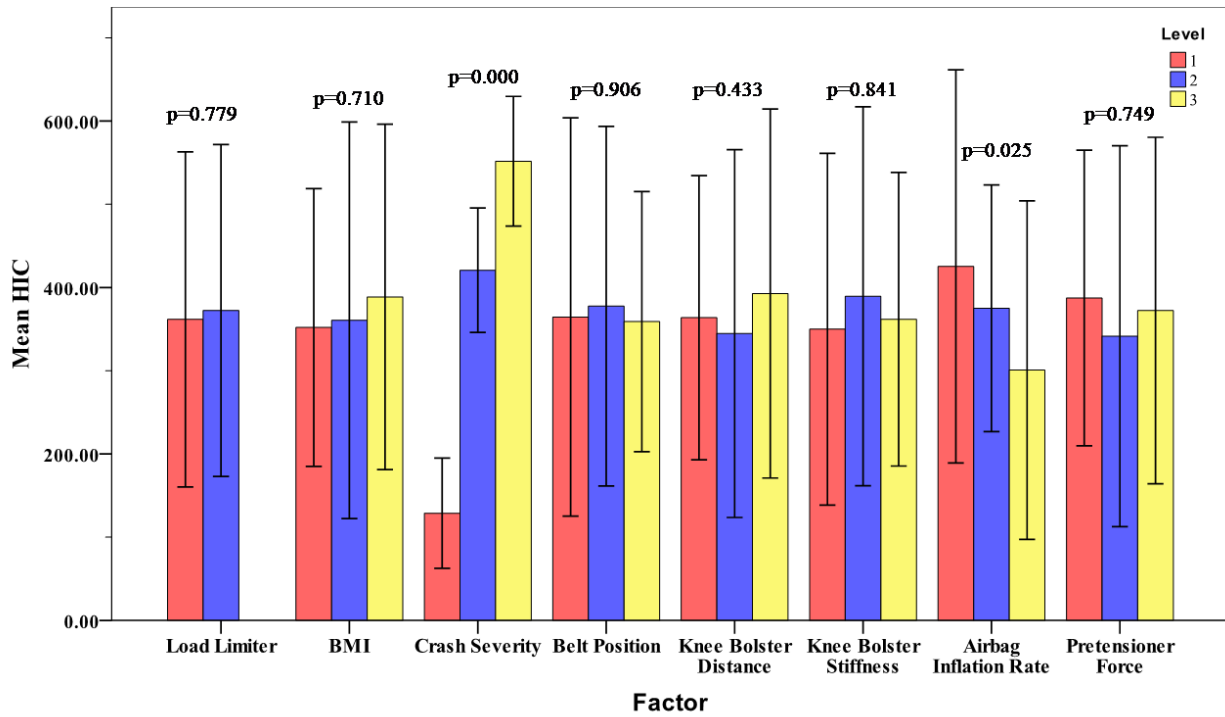
Figure 3-15. Mean HIC values for all factors for the Modified Torso Model.

Crash Severity (p=0.000) was the only siginifcant factor for Chest 3ms injury criteria(Figure 3-16).
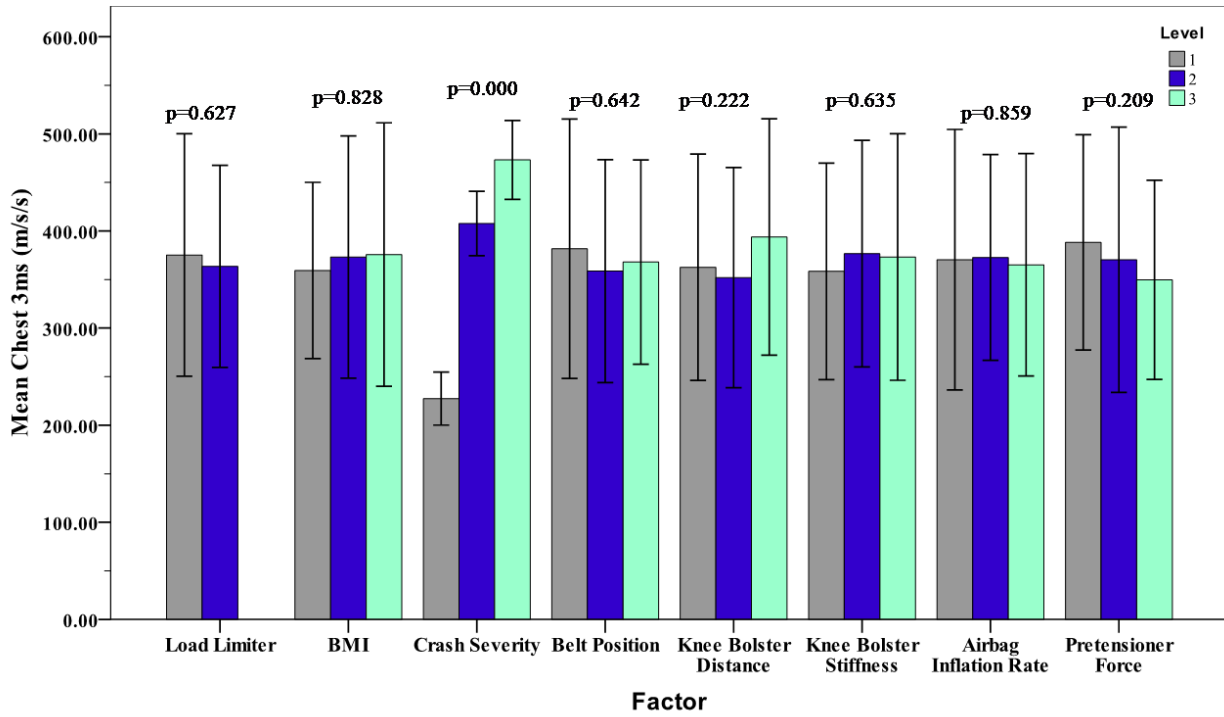
Figure 3-16. Mean Chest 3ms values for all factors for the Modified Torso Model.

Figure 3-17 shows that Crash severity (p=0.000), and Knee Bolster Distance (p=0.038) were significant for Chest Deformation.
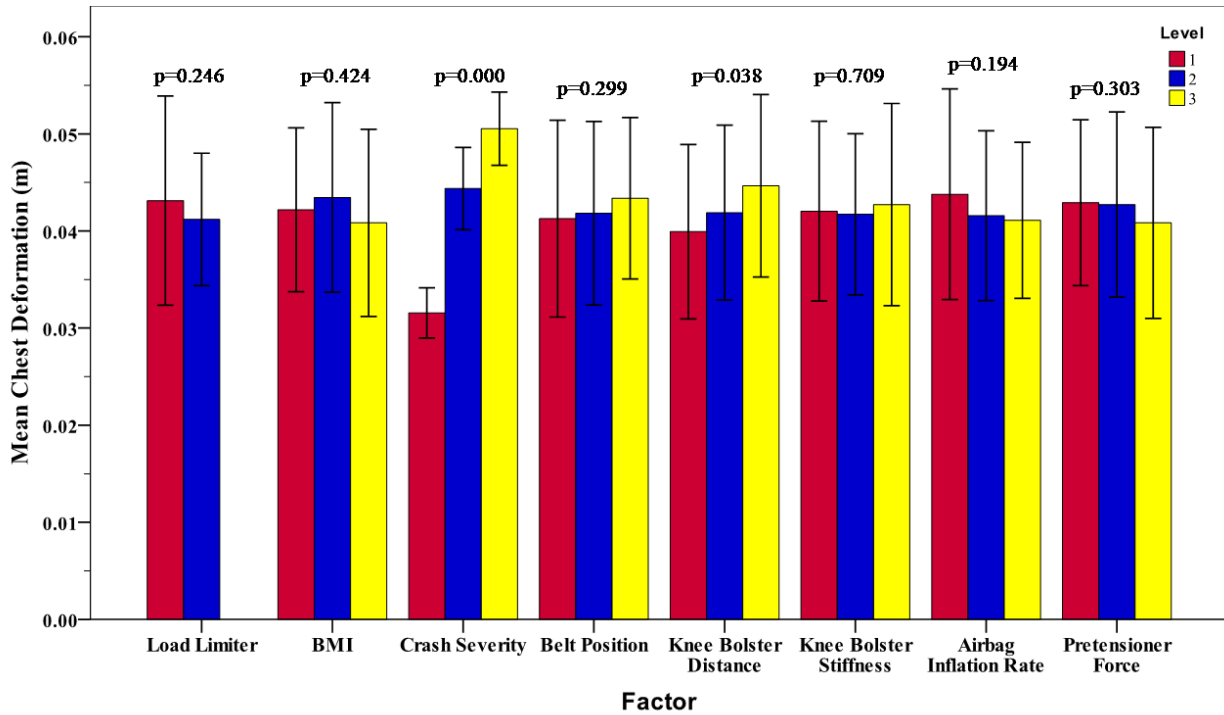
Figure 3-17. Mean Chest deformation values for all factors for the Modified Torso Model.

Figure 3-18 shows that for FFC, Crash Severiy (p=0.001), Belt Position (p=0.021), Knee Bolster Stiffness (p=0.000), and Pretensioner Force (p=0.008) were significant factors.
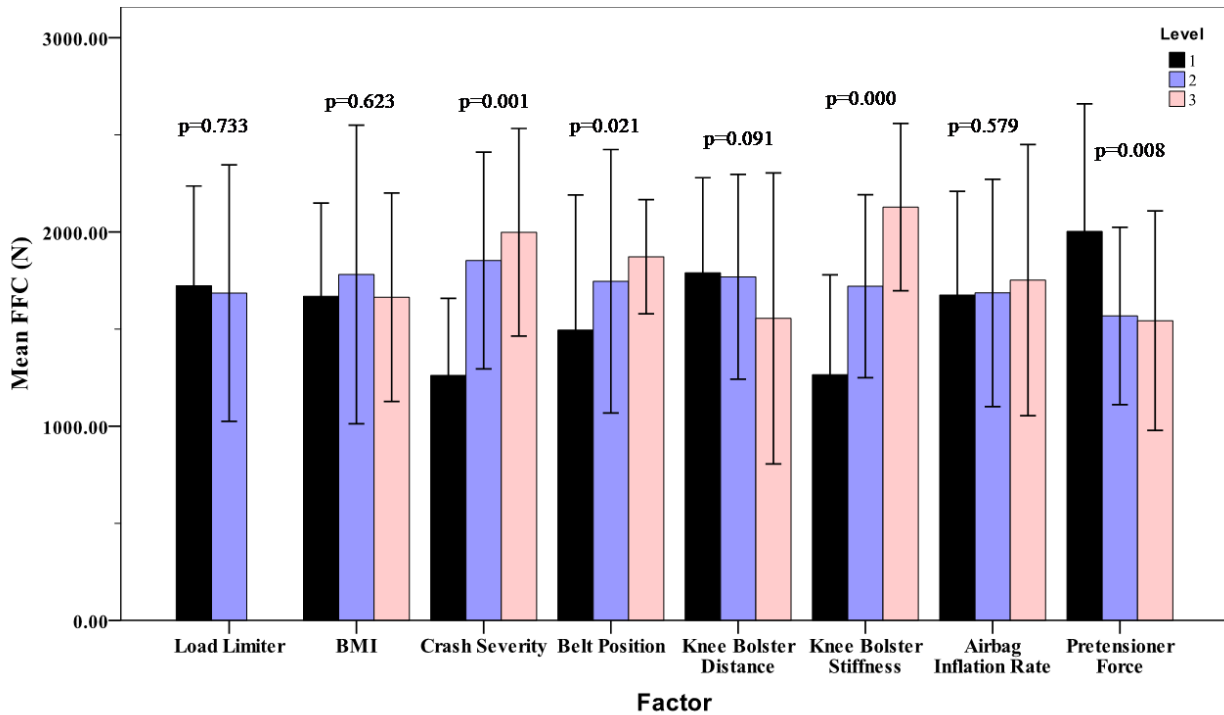
Figure 3-18. Mean FFC values for all factors for the Modified Torso Model.

3.5.3   Combined Model

Figures 3-19, 3-20, 3-21, and 3-22 show the average values due to the main effects of the controlling factors for HIC, Chest 3ms, Chest Deformation, and FFC for the Combined Model. Figure 3-18 shows that for HIC, Crash Severity (p=0.000) was significant factor and Airbag Inflation Rate was approaching significnace (p=0.103).
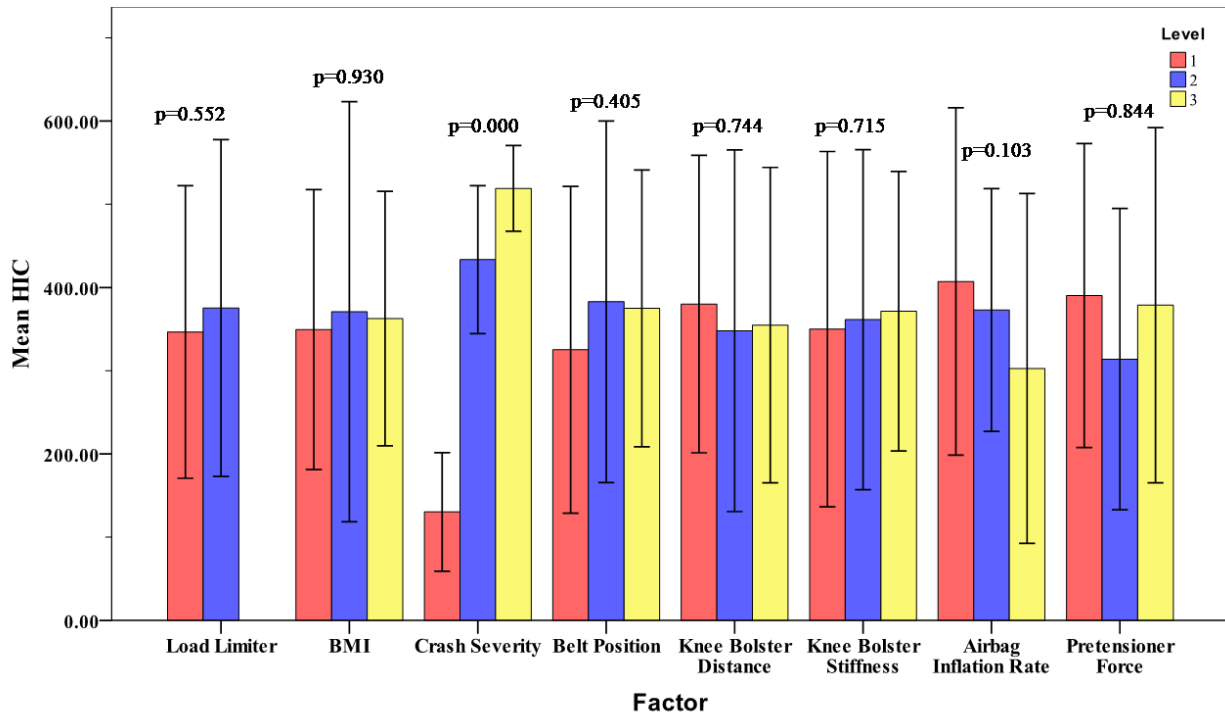
Figure 3-19. Mean HIC values for all factors for the Combined Model.

Crash Severity (p=0.000) was the only significnat factor for Chest 3ms (Figure 3-20).
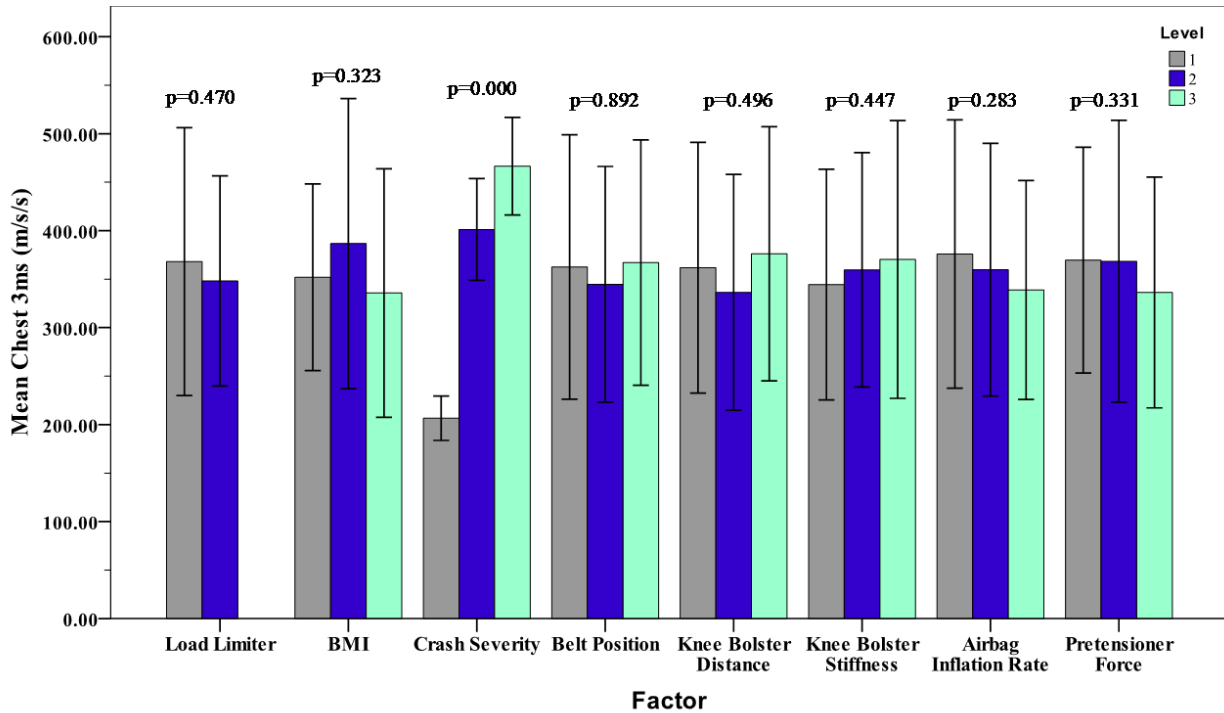
Figure 3-20. Mean Chest 3ms values for all factors for the Combined Model.

For Chest Deformation, Crash Severity (p=0.000), Knee Bolster Distance (p=0.038), Airbag Inflation Rate (p=0.049), were significant. BMI was approaching significance (p=0.056) and could account for 51.40% ($\eta^2_{partial} = 0.514$) of the Chest Deforamtion variation in the Combined Model. Chest deformation increases as BMI increases (Figure 3-21).
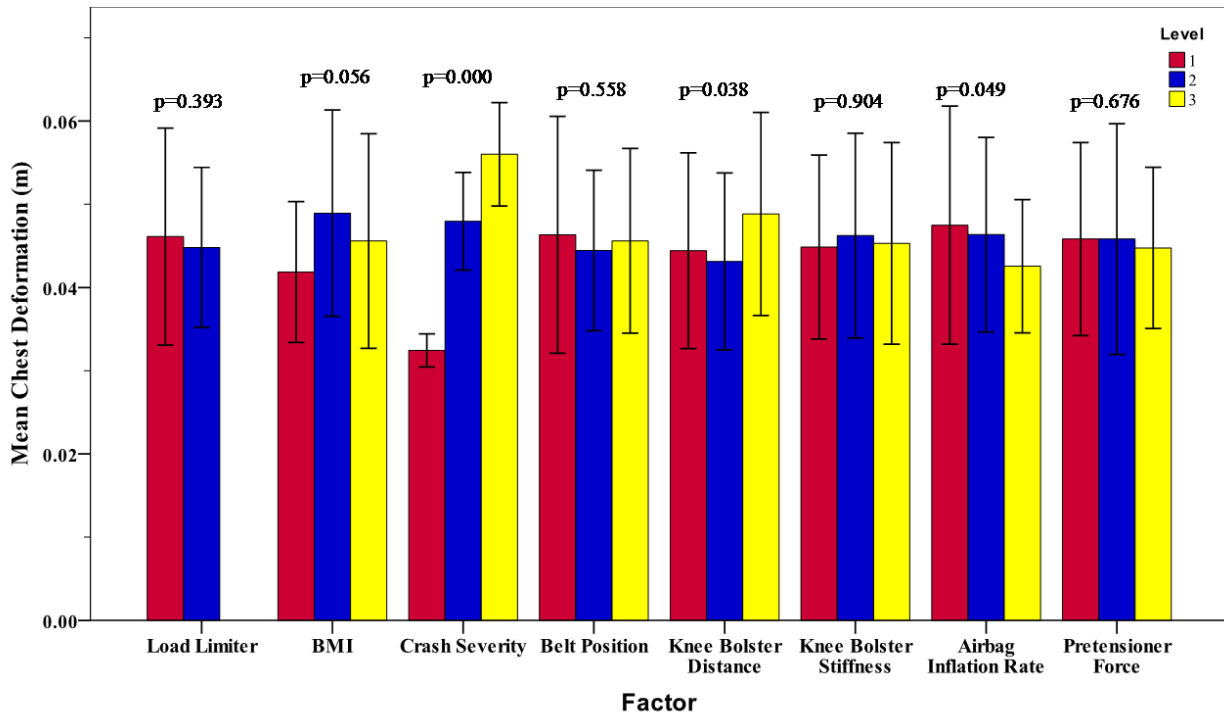
Figure 3-21. Mean Chest deformation values for all factors for the Combined Model.

Figure 3-22 shows the average values of the main effects of the controlling factors for FFC. Crash severity (p=0.000), Knee Bolster Stiffness (p=0.001), Pretensioner Force (p=0.007), and BMI (p=0.015) were significant factors. BMI accounts for 65.00% of the variation ($\eta^2_{partial}$ =0.650) in FFC, and FFC increases as BMI increases.
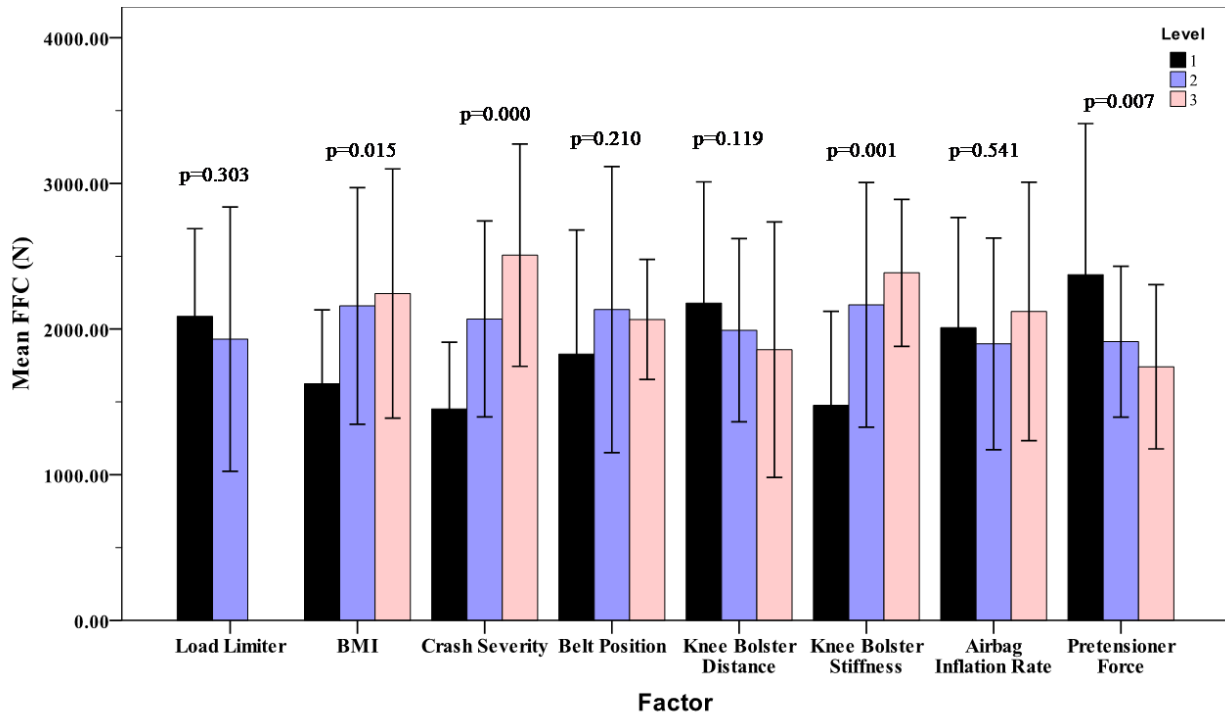
Figure 3-22. Mean FFC values for all factors for the Combined Model.

Table 3-2 shows a summary of all p-values for all the models and each injury parameter. As discussed above Crash Severity was a significant factor for almost all injury levels regardless of the model. BMI was significant for FFC for both the Mass Model and Combined Model. BMI was also significant for Chest deformation in the Mass Model.

Table 3-2. Summary of p-values for all models. Bold indicates marginal significance, and red indicates significance at alpha=0.05.

Model	Injury parameter	Load Limiter	BMI	Crash Severity	Belt Position	Knee Bolster Distance	Knee Bolster Stiffness	Airbag Inflation Rate	Pretensioner Force
Mass Model	HIC	0.517	0.930	0.000	0.597	0.899	0.934	0.037	0.918
	Chest 3ms	0.731	0.928	0.000	0.874	0.316	0.955	0.381	0.637
	Chest Deformation	0.803	0.004	0.000	0.683	0.321	0.576	0.609	0.229
	FFC	0.755	0.001	**0.058**	0.037	0.006	**0.089**	0.386	0.006
Modified Torso Model	HIC	0.799	0.710	0.000	0.906	0.433	0.841	0.025	0.749
	Chest 3ms	0.627	0.828	0.000	0.642	0.222	0.635	0.859	0.209
	Chest Deformation	0.246	0.424	0.000	0.299	0.038	0.709	0.194	0.303
	FFC	0.733	0.623	0.001	0.021	**0.091**	0.000	0.579	0.008
Combined Model	HIC	0.552	0.930	0.000	0.405	0.744	0.715	0.103	0.844
	Chest 3ms	0.470	0.323	0.000	0.892	0.496	0.447	0.283	0.331
	Chest Deformation	0.393	**0.056**	0.000	0.558	0.038	0.904	0.049	0.676
	FFC	0.303	0.015	0.000	0.210	0.119	0.001	0.541	0.007

3.6   SUMMARY

Three obese whole body models were used to examine the mechanisms of injury to obese occupants in frontal MVCs. Factors that have been shown to influence occupant injury in MVCs were controlled for in a DOE. Simulations were run to examine the effects of mass (Mass Model), torso shape and mechanical response changes due to obesity (Modified Torso Model), and the interaction between mass and changes in the obese torso (Combined Model), on occupant injury.

The results of the DOE indicate that the average injury risk levels for all injury criteria were below injury limits specified by FMVSS 208. The injury levels obtained in this study are

similar to those of a previous study using MADYMO to examine the effects of obesity [23]. The result of the DOE also indicate that the mass of the obese occupant is the most important factor affecting injury risk to obese occupants. The Mass Model predicts an average increase in chest injury risk due to the main effects of BMI of about 9.5% from approximately 0.5% to a 10% probability an AIS 3+ chest injury, based on the injury risk curve for distributed loading of Mertz et al.[72]. The probability of an AIS 3+ chest injury based on the seatbelt loading curve of Mertz et al. [72] increased from approximately 20% for a BMI of 25 to approximately 60% for a BMI of 39. The probability of injury to the lower extremity was extremely low (<1%); however there was 46% increase in the risk of an AIS 2+ injury to the lower extremities as BMI increased from 25 to 39. These trends in injury are consistent with previous research showing increased lower extremity and chest injuries in obese occupants in MVCs [15, 17-19, 23, 25, 62]. The increase in chest and lower extremity injury due to mass is because with greater mass the occupant translates further forward, with greater force, causing more severe contact with the vehicle interior and occupant restraint systems.

The effects of the changes in torso geometry and abdominal mechanical response due to obesity alone, do not significantly affect the injury risk based on results the Modified Torso Model. This is likely due to the fact that there needs to be significant changes in mass in order for the differences in the obese torso to influence the risk of injury. In addition, the use of a pretensioner probably offsets the changes in belt fit as a result of increasing obesity. The Combined Model predicts an increase in risk of injury to the lower extremities which is consistent with previous research [15, 16, 19, 23, 62]. The probability of an AIS 2+ lower extremity injury was extremely low (<1%) however the probability increased approximately 27% from a BMI of 25 to 39. Chest deformation was marginally significant in the Combined

model (p=0.056). The trend in chest injury is associated with an increase in the probability of an

AIS 3+ chest injury from approximately 1% to approximately 9% based on the distributed

loading chest injury risk curve [72] , and an increase in chest injury risk from 30% to

approximately 45% based on the seat belt loading chest injury risk curve [72]. This is different

from the Mass Model which predicts a significant increase risk of injury due to chest

deformation (p=0.004). This suggests that the addition of changes to the obese torso, along with

increased mass have a significant effect on obese occupant kinematics and obese occupant injury

risk.

To further explain the changes in occupant injury risk based on the interaction between

occupant mass and obese torso changes, 6 additional simulations were performed. The Mass

Model, and the Combined Model with BMIs of 25, 30, and 39 were used and the vehicle

environment was removed so that the resulting model consisted of the ATD in a standard sedan

bucket seat, a standard 3-point restraint system with a load limiter set to 4 kN and pretensioner

with the pretensioner force set at 1 kN, and a 30 mph delta v crash severity. The vehicle

environment was removed so that the differences in the two models could be examined without

the confounding effects of the vehicle environment. Forward excursions of the ATD chest and

pelvis were analyzed to provide additional information on the kinematics of obese occupants in

frontal impacts. Figure 3-23 shows the excursion of the ATD pelvis for the Mass Model and

Combined Model as BMI increases. There is more forward excursion for the Combined Model

for all levels of BMI and an average increase of 44% in forward pelvic excursion from the Mass

Model to the Combined Model. This suggests that the change in torso geometry and mechanical

response due to increasing BMI along with increased mass allows the pelvis to translate further

forward in a frontal impact than increased mass alone. This increase in forward translation of the

pelvis is most likely the result of the additional pelvis displacement before the lap belt begins to interact with the pelvis.
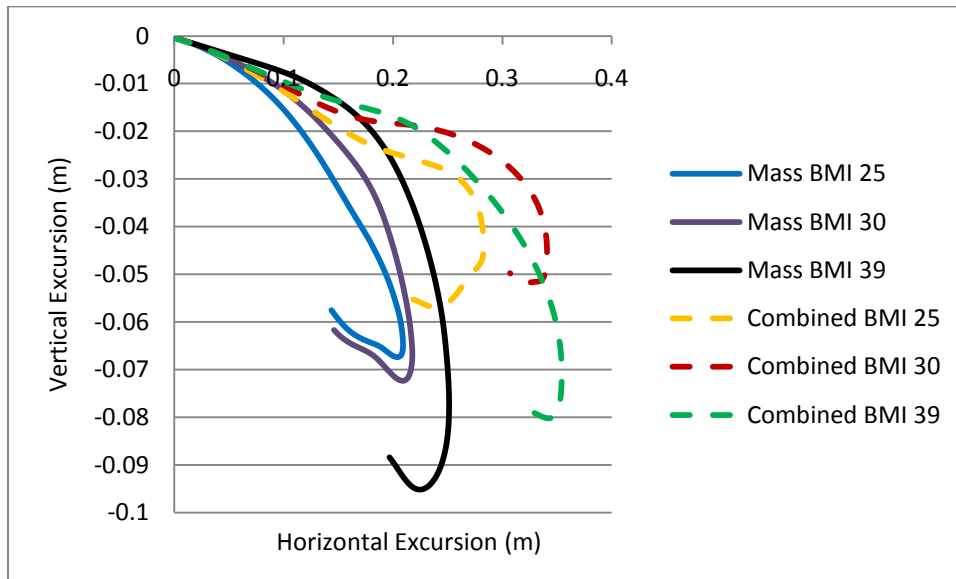
Figure 3-23. Pelvis forward excursion for the Mass Model and Combined Model.

The forward chest excursion for both models is shown in Figure 3-24. There is an average increase of 12% in forward chest excursion for the Combined Model compared to the Mass Model. Compared to the pelvis excursion the affects of the changes in an obese torso combined with the increased mass have much less influence on chest kinematics compared to increased mass alone.
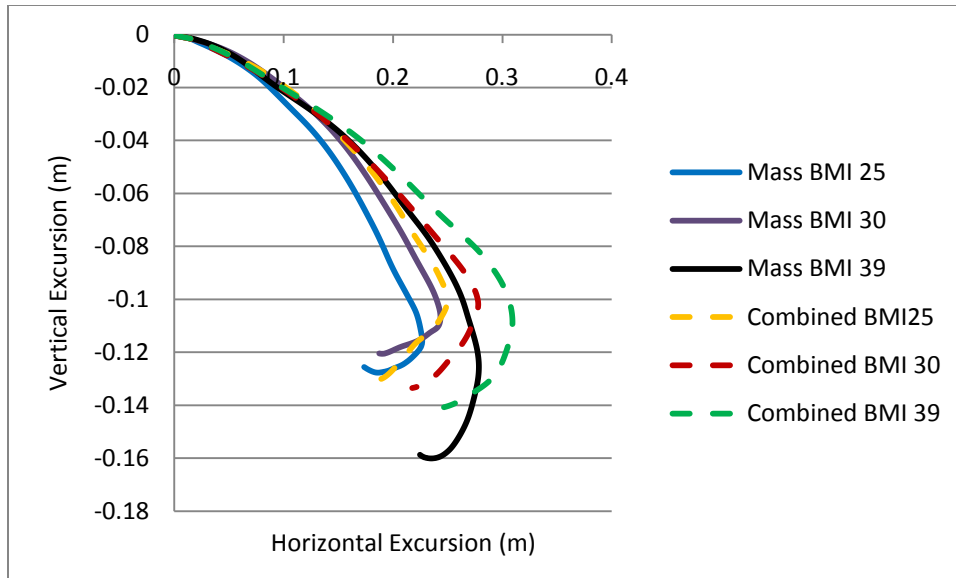
Figure 3-24. Chest forward excursion for the Mass Model and Combined Model.

The Combined Model predicts kinematics similar to those reported by Kent et al. (2010). The kinematics can explain the results in the injury criteria predicted by the Combined Model. Overall, as BMI increases the occupant tends to translate further forward. The addition of poor belt fit due to the obese abdomen causes the occupant to lead with their pelvis and lower extremities in a frontal impact as the adipose tissue prevents lap belt contact with the bony pelvis. Therefore with the increased mass and additional displacement provided by changes in the obese torso, the lower extremities tend to bear more load in a frontal impact. The chest experiences increased forward translation as BMI increases as a result of increased occupant mass. The increased forward translation results in a potential increase in chest injury risk, however the change in the obese torsos also causes the chest and head to lag behind the pelvis and lower extremities, thus transferring some of the load to the lower extremities, which could cause the slight decrease in significance of chest deformation predicted by the Combined Model.

The changes in kinematics could also help explain why studies have reported a reduction in mortality to obese occupants [19, 25, 26]. The upper torso and head are "protected" as they lag behind the lower extremities. This transfer of load from the shoulder, chest, and pelvis to the lower extremities, and abdomen could reduce upper torso loading and injury risk. The findings also suggest that the differences in occupant injury risk are not due to a cushion effect from padding due to increased adipose tissue, but rather a change in occupant kinematics that transfer the main load of the impact from the bony shoulder/chest and pelvis to the lower extremities as a result of the increased mass and the increased torso adipose tissue causing poor belt fit. This would also suggest that at some point, at a BMI greater than 40, the increase in mass will override this slight protection of the upper body as the whole body will translate further forward with increased momentum resulting in more force applied to the occupant when contacting the vehicle interior or occupant restraint system.

4.0 THE EFFECTS OF OBESITY ON WHEELCHAIR-SEATED OCCUPANT INJURY IN FRONTAL IMPACTS

4.1 OVERVIEW

People with disabilities are more likely to be obese than able-bodied individuals and are at an increased risk of injury when seated in their wheelchair in an MVC [3, 8]. Therefore understanding obese wheelchair-seated occupant injury risk is important for providing improved safety to these individuals. This chapter describes the development, and validation of an obese wheelchair occupant model, and subsequent analysis of obese wheelchair-seated occupant injury risk. First a surrogate wheelchair model occupied by a 50th percentile Hybrid III ATD, subjected to a frontal impact is developed. This model is validated with sled test data. Finally the Combined Model developed in Chapter 3 is incorporated into the surrogate wheelchair model and a parametric analysis is performed to determine the effects of obesity on injury risk to wheelchair-seated occupants.

4.2   SURROGATE WHEELCHAIR MODEL DEVELOPMENT

4.2.1   Model Validation Data

Two sled tests were performed in accordance with ISO 10542-3 to provide kinematic and kinetic

data for use in the validation of the computer model. A surrogate wheelchair was occupied by a

50th percentile Hybrid III ATD. The ATD was restrained by a vehicle anchored, three point

(lap/shoulder belt) occupant restraint system. The wheelchair was secured to the sled via a single

point docking system (QLK100, Q'Straint, Fort Lauderdale, FL) (Figure 4-1).

Figure 4-1. Sled test setup (Left) and the single point docking system (Right).

The docking system was bolted to a metal plate that was attached to the sled. Four load

cells were placed under the four corners of the metal plate. The occupant restraint system was

also fitted with 3 load cells (2 on the lap belt, 1 on the shoulder belt), and accelerometers were

fitted to the approximate wheelchair center of gravity (CG), ATD pelvis, ATD chest, and ATD

head CG. Three high speed digital cameras (1000 fps) were used to record the tests. The

occupied wheelchair was subjected to a 20g/30mph frontal impact pulse. Data collected included the force on the lap and shoulder belts, the force acting on the bolt/docking system, wheelchair CG acceleration, and accelerations of the ATD head, chest, and pelvis. The force acting on the bolt/docking system was calculated as the sum of the resultant force of the four load cells under the docking system, All data were filtered per SAE J211 [76]. The data from the tests were used in the validation of the computer simulation model.

4.2.2   Model Development

A system representing the 20g/30mph frontal impact sled tests (Figure 4-2) was created with MADYMO. A surrogate wheelchair was created using ellipsoids, cylinders, and joints, based on the geometry and inertial characteristics of the surrogate wheelchair used in the sled tests described in ISO 10542-3. The docking system, which consisted of ellipsoids that were of relevant dimensions and material properties, was rigidly fixed to the sled platform. The docking system hardware attached to the wheelchair was also modeled using ellipsoids, connected by fixed and translational joints to account for dynamic material bending and permanent deformation seen in the sled tests. The bolt, modeled as an ellipsoid was attached to the hardware via two rotational joints. These joints allowed for the deformation experienced by the wheelchair docking hardware during the sled tests to be captured in the model. A nut was placed at the bottom of the bolt to effectively anchor the bolt into the docking system. This was also modeled with an ellipsoid attached to the docking bolt ellipsoid. The MADYMO rigid body ellipsoid Hybrid III ATD was positioned in surrogate wheelchair according to ISO 10542-3. The three-point occupant restraint was simulated using finite element belt segments in locations

71

where the belts contacted the ATD, to accurately simulate occupant/belt interaction, and non

finite element belt segments, available in MADYMO, for belt/anchor point connections.
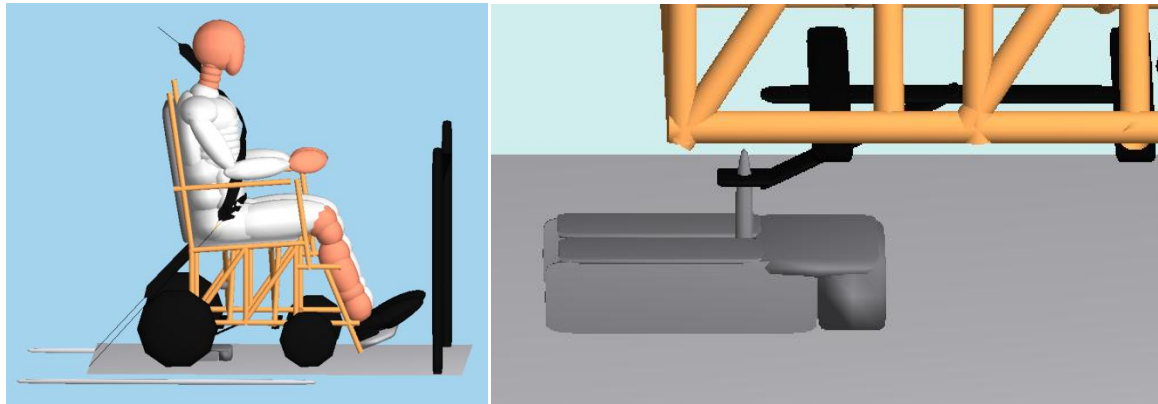
Figure 4-2. The computer model consisting of the surrogate wheelchair, ATD, and docking

system (Left) and the single point docking system and wheelchair docking hardware recreated in

MADYMO^{TM} (Right).

4.3   VALIDATION

Overall model response was adjusted by changing parameters such as friction, stiffness, and

damping characteristics of the wheelchair wheels, seat pan, seatback, the docking system,

docking bolt assembly, and seat belts. The overall kinematics of the model and sled tests were

compared. In addition head, chest, pelvis, and wheelchair cg accelerations, and docking bolt

force, and seatbelt force parameters were used to validate the model. The output from the two

sled tests were averaged and compared to the model predicted response. To provide additional

validation several quantitative parameters were used to provide a quantitative validation similar

to that of previous MADYMO wheelchair models [49, 51, 52, 77, 78]. The parameters used for quantitative validation include Pearson's correlation coefficient (r), time of peak output, and magnitude of peak output. The model predicted output was compared to the average output of the two sled tests.

Figure 4-3 shows high speed images, taken at 25 ms intervals from 0-175ms, of the two sled tests compared to those of the model. Figures 4-4, 4-5, and 4-6 show the model predicted response for head, chest, pelvis, wheelchair cg accelerations, docking bolt force, and seatbelt force compared to the average of the sled test data.
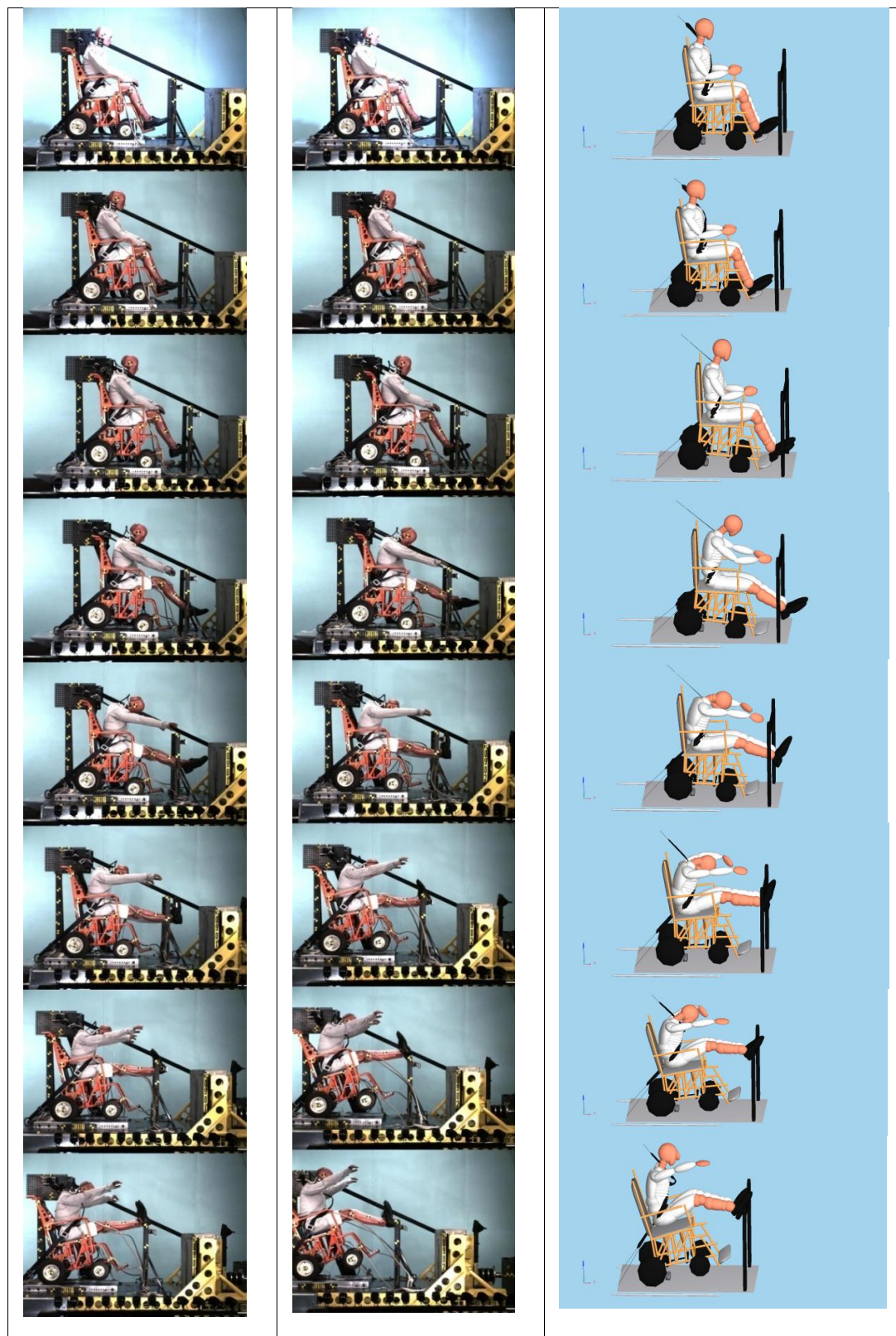
Figure 4-3. Overall wheelchair response for the two sled tests (Left) and model predicted response (Right).
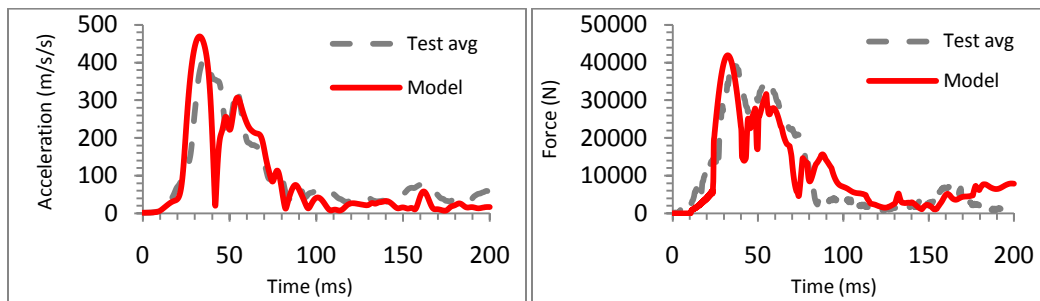
Figure 4-4. Model predicted wheelchair CG acceleration (Left) and model predicted docking bolt force (Right) compared to sled test data.
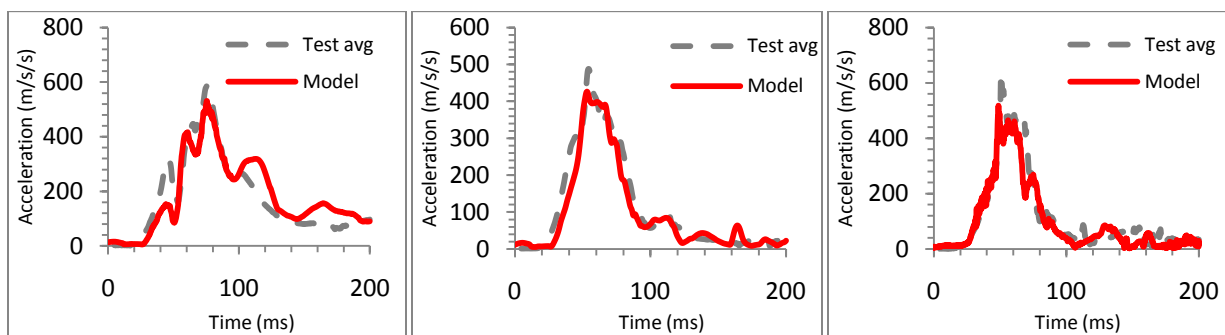
Figure 4-5. Model predicted ATD head (Left), chest (Middle), and pelvis (Right) acceleration compared to sled test data.
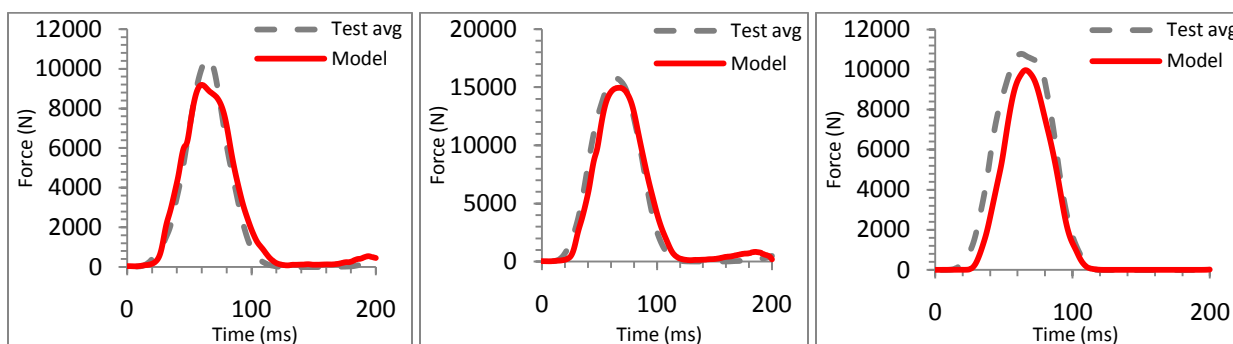
Figure 4-6. Model predicted left lap belt force (Left), right lap force (Middle), and shoulder belt force (Right) compared to the sled test data.

75

The images in Figure 4-3 show that the general wheelchair and ATD motion of the model is similar to the kinematics of the sled tests. The model displays the forward rotation, and translation of the wheelchair and ATD at the initial onset of the acceleration pulse, the model also captures the rearward rotation of the wheelchair after about 100 ms. Overall the model predicts the test response very well. The validation variables shown in Figures 4-4, 4-5, and 4-6 show that the model accurately predicts the time history kinematics of the sled tests.

Table 4-1 shows the quantitative values of the model predicted output compared to the average of the two sled tests. The predicted model response is highly correlated with the test data with an average value of r =0.95 across all output variables. The model predicted peak values are all within +-19% of the peak average test values and the model predicted peaks are within +- 5 ms of the average test values. The average difference in time of peak signal is 2 ms across all variables and an average difference of 11% in the magnitude of peak signal across all variables between the model and sled test data.

Table 4-1. Quantitative validation of the Wheelchair Model.

Signal	Pearson's Correlation Coefficient (r)	Difference in Peak Time (ms)	Difference in Peak Value as a % of the sled test data
Left lap belt force	0.99	5	13
Right lap belt force	0.99	3	5
Shoulder belt force	0.98	3	7
Wheelchair CG acceleration	0.87	2	15
Pelvis acceleration	0.95	2	19
Chest acceleration	0.97	1	13
Head acceleration	0.91	0	9
Bolt force	0.87	3	5
Average	**0.94**	**2**	**11**

4.4   PARAMETRIC ANALYSIS

To investigate the effects of BMI on wheelchair occupant injury, a DOE study was used. The

DOE was the same as the one used in Chapter 3, except the vehicle environment was modified to

represent a generic mini-van based on the data available from the Rehabilitation Engineering

Research Center (Project P3). The Taguchi Array used in Chapter 3 was used again for this study

to reduce the number of simulations from 6561 to 18. The Combined Model ATDs, with BMIs

of 25, 30, and 39, were placed in the previously validated surrogate wheelchair model (Obese

Wheelchair-seated Occupant Model). Figure 4-7 shows the Obese Wheelchair-seated Occupant

Model and Table 4-2 shows the DOE test matrix.

Figure 4-7. The Obese Wheelchair-seated Occupant Model with BMIs of 25 (Left), 30 (Middle),

and 39 (Right).

Table 4-2. DOE Taguchi Array test matrix

Simulation #	Load Limiter (kN)	BMI (kg/m^2)	Crash Severity (mph)	Belt Position	Knee-knee bolster distance (mm)	Knee bolster stiffness (N/mm)	Airbag Inflation Rate (%)	Pretensioner force (kN)
1	4	25	25	low	50	30	80	0
2	4	25	30	middle	70	70	100	1
3	4	25	35	high	120	120	120	2
4	4	30	25	low	70	70	120	2
5	4	30	30	middle	120	120	80	0
6	4	30	35	high	50	30	100	1
7	4	39	25	middle	50	120	100	2
8	4	39	30	high	70	30	120	0
9	4	39	35	low	120	70	80	1
10	6	25	25	high	120	70	100	0
11	6	25	30	low	50	120	120	1
12	6	25	35	middle	70	30	80	2
13	6	30	25	middle	120	30	120	1
14	6	30	30	high	50	70	80	2
15	6	30	35	low	70	120	100	0
16	6	39	25	high	70	120	80	1
17	6	39	30	low	120	30	100	2
18	6	39	35	middle	50	70	120	0

4.4.1   Output/Statistics

The output values used to assess the main effects of BMI on occupant injury were Head Injury Criteria (HIC), Chest 3ms Injury Criteria, Chest Deformation, and Femur Force Criteria (FFC), and for the purposes of this study the femur force for the right and left femurs were averaged. The same statistical procedure as in Chapter 3 was used to evaluate the significance of BMI, and SPSS was used for all statistics and a significance level was alpha = 0.05.

4.5   RESULTS

Figures 4-8, 4-9, 4-10, and 4-11 show the average values of the main effects for the controlling factors for HIC, Chest 3ms, Chest Deformation, and FFC for the ObeseWheelchair-seated Occupant Model. The only significant factors for HIC and Chest 3ms were Crash severity (p=0.000). For Chest Deformation, Crash severity (p=0.000) was significant and Knee Bolster Distance was approaching significance (0.096). BMI was not significant (p=0.140), however as indicated by Figure 4-12, Chest Deformation increases as BMI increases. Crash severity (p=0.000), Belt Position (p=0.042), Knee Bolster stiffness (p=0.008), Pretensioner Force (p=0.020), and BMI (p=0.004) were all significant for FFC. BMI could account for 74.70% of the variation in FFC ($\eta^2_{partial}$ =0.747), and FFC increased as BMI increased (Figure 4-11).
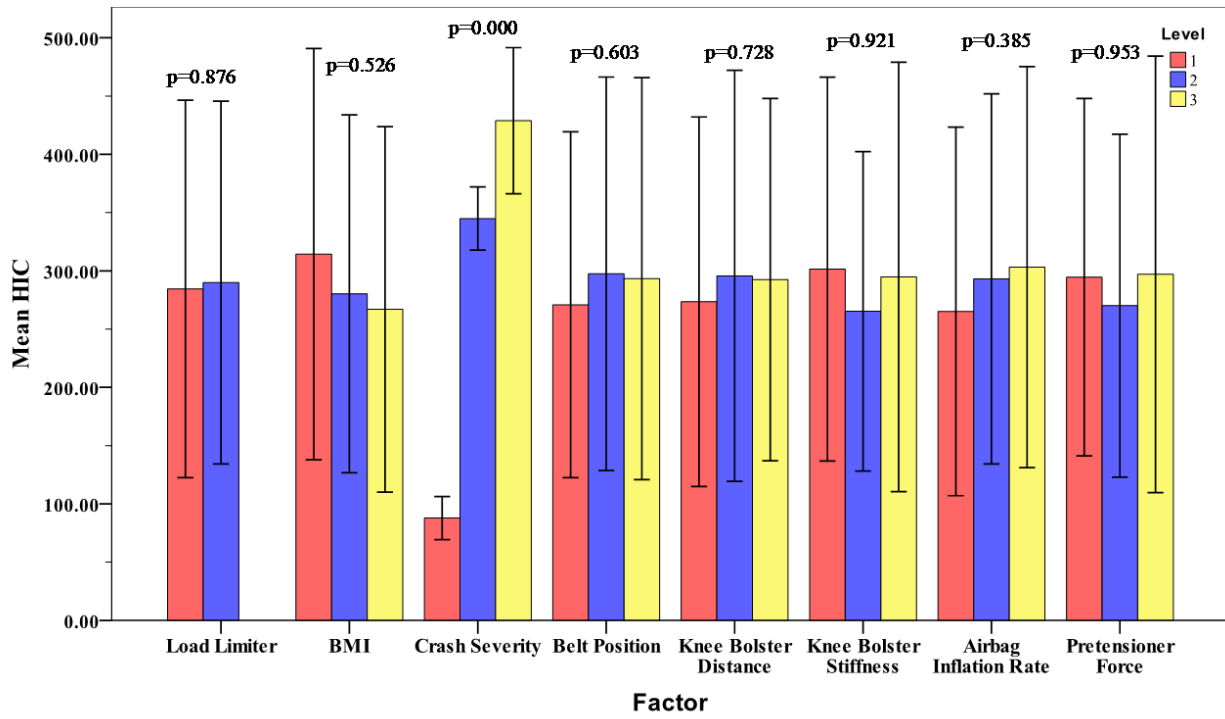
Figure 4-8. Mean HIC values for all factors for the Obese Wheelchair-seated Occupant Model.
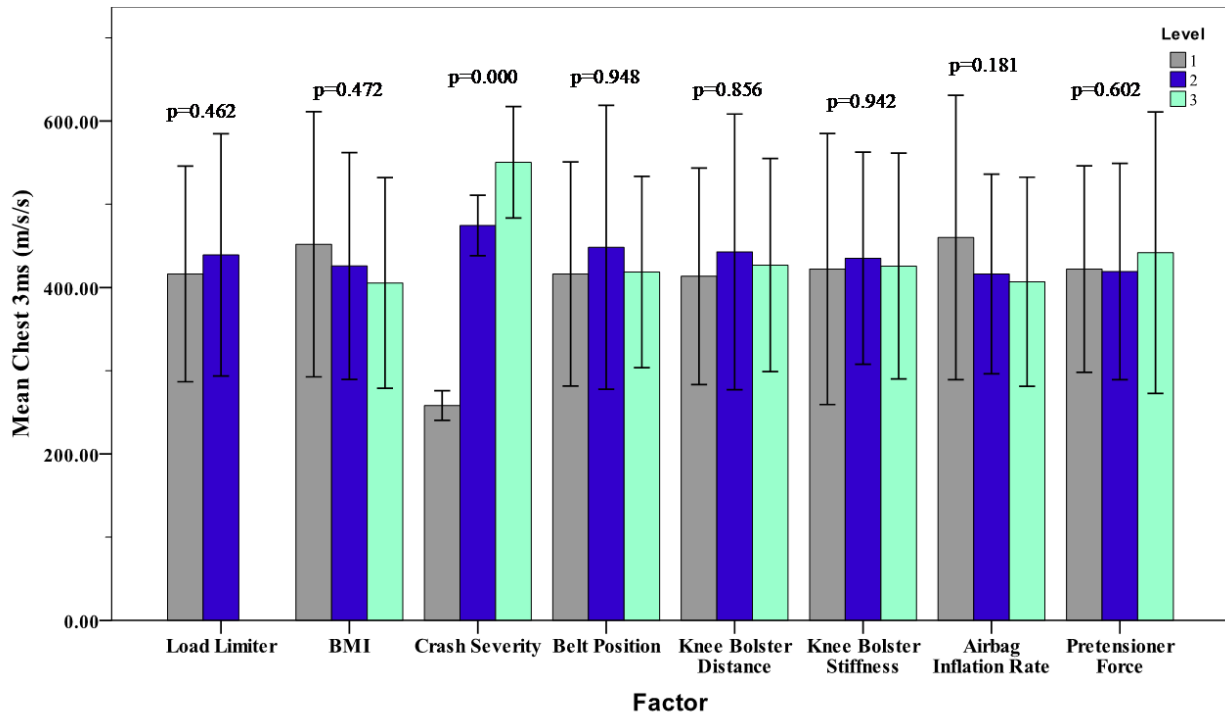
Figure 4-9. Mean Chest 3ms values for all factors for the Obese Wheelchair-seated Occupant
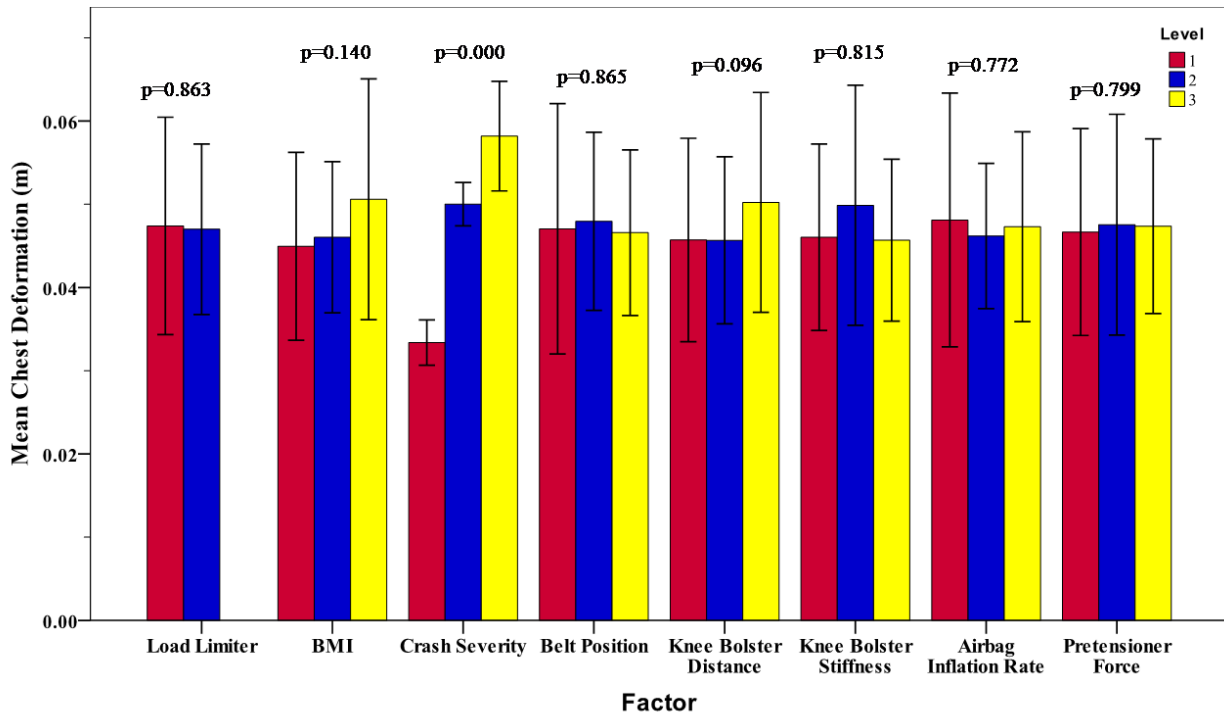
Model.

Figure 4-10. Mean Chest deformation values for all factors for the Obese Wheelchair-seated Occupant Model.
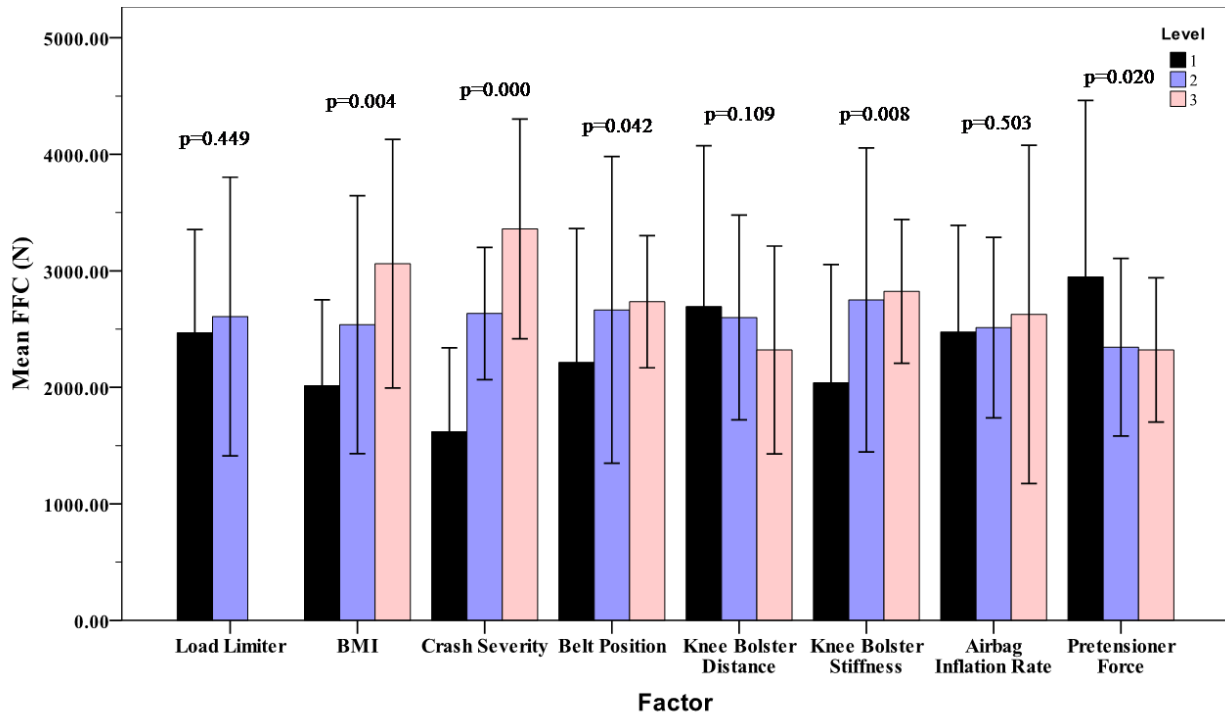
Figure 4-11. Mean FFC values for all factors for the Obese Wheelchair-seated Occupant Model.

Table 4-3 provides a summary of p-values for all injury parameters for the Obese Wheelchair-seated Occupant Model. As can be seen Crash Severity was significant for all injury parameters and FFC was the only injury parameter that was significantly affected by BMI.

Table 4-3. Summary of p-values for the Obese Wheelchair-seated Occupant Model. Bold indicates values that are marginally significant and red indicates significant values at alpha=0.05

Model	Injury parameter	Load Limiter	BMI	Crash Severity	Belt Position	Knee Bolster Distance	Knee Bolster Stiffness	Airbag Inflation Rate	Pretensioner Force
Obese Wheelchair-seated Occupant Model	HIC	0.876	0.526	0.000	0.603	0.728	0.921	0.385	0.953
	Chest 3ms	0.462	0.472	0.000	0.948	0.856	0.942	0.181	0.602
	Chest Deformation	0.863	0.104	0.000	0.865	**0.096**	0.815	0.772	0.779
	FFC	0.449	0.004	0.000	0.042	0.109	0.008	0.503	0.020

4.6   SUMMARY

A surrogate wheelchair model occupied by a 50th percentile male ATD was created in MADYMO. The model was validated with sled test data. The general kinematics compare well with the model predicted kinematics (Figures 4-3-6). In addition a quantitative validation was also conducted. The model was highly correlated with the test data ($r > 0.87$), and peak values, and timing of peak values were all within 5ms and 20% of the peak value of the test data. These values are also in the range of values reported by previous research that have validated wheelchair models using the same parameters [49, 51, 52, 77, 78].

As expected Crash Severity is a significant factor in all injury criteria. After controlling for covariate factors, BMI was significant for FFC and approaching significance for Chest Deformation. The average risk of an AIS 2+ lower extremity injury increased by approximately 70% as BMI increased from25 t0 39 for wheelchair seated occupants. The injury trends are

similar to the findings in Chapter 3 for non-wheelchair-seated occupants. However the

wheelchair occupant average femur force across all BMI levels was also 49% higher than the

average femur force of the non-wheelchair seated occupant in the Combined Model. To

compare the effect of obesity on wheelchair seated occupants and non-wheelchair seated

occupants 6 additional simulations were performed. The Obese Wheelchair-seated Occupant

Model and the Combined Model with BMIs of 25, 30, and 39 were used for these simulations.

The resulting models consisted of the ATD in a standard sedan bucket seat or surrogate

wheelchair, a standard 3-point restraint system with a load limiter set to 4 kN and pretensioner

with the pretensioner force set at 1 kN, and a 30 mph delta v crash severity. The vehicle

environment was removed so that the differences in the two models could be examined without

the confounding effects of the vehicle environment. Excursions of the ATD chest and pelvis

were analyzed. Figures 4-12 and 4-13 show the ATD pelvis and chest excursions for the Obese

Wheelchair-seated Occupant Model and the Combined Model as BMI was varied.
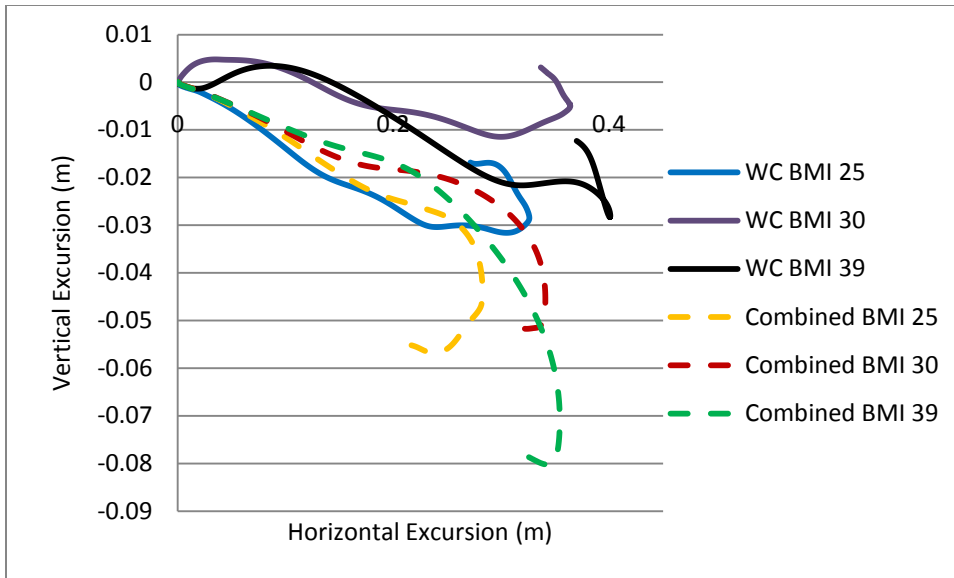
Figure 4-12. Pelvis excursion for the Obese Wheelchair-seated Occupant Model and Combined
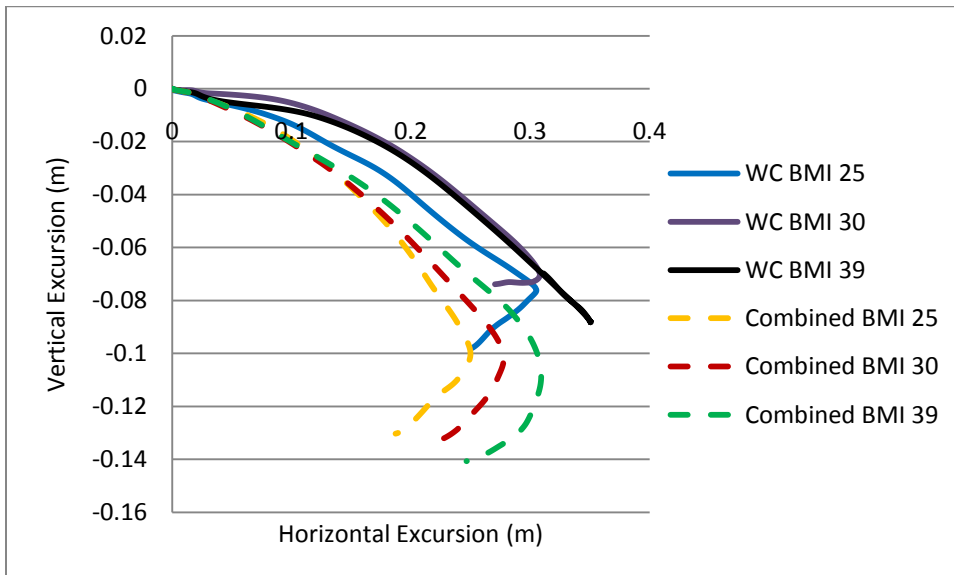
Model

Figure 4-13. Chest excursion for the Obese Wheelchair-seated Occupant Model and Combined

Model

The Obese Wheelchair-seated Occupant Model suggests that obese wheelchair seated occupants have different kinematics compared to non-wheelchair seated occupants. The wheelchair-seated occupant tends to translate further forward than non-wheelchair seated occupants. The chest excursion was greater for each level of BMI for the Obese Wheelchair-seated Occupant Model compared to the Combined Model. There was also more pelvis excursion in the Obese Wheelchair-seated Occupant model. This would explain why the Obese Wheelchair-seated Occupant Model predicted a greater risk of injury to the lower extremities.

Overall the simulations suggest that the wheelchair occupant tends to lead with their hips more than the non-wheelchair seated occupant as BMI increases. The increased pelvis excursion results in increased force transmitted through the lower extremities while the head and chest lag behind the lower body and experience less of the load. The fact that a surrogate wheelchair is used in these simulations could influence the results. A surrogate wheelchair seating system is designed to be the "worst case scenario" which means that the seat pan is a smooth rigid surface and the seat pan angle is very small. A simulation was performed using the Obese Wheelchair-seated Occupant Model with a BMI of 39 and no vehicle environment, and the friction between the ATD and the seat was doubled. The resulting forward translation of the pelvis was reduced 14% from 401 cm to 343 cm. indicating that wheelchair seat position and seat material are important considerations for wheelchair-seated occupants.

5.0   DISCUSSION AND CONCLUSION

This study used a FE abdomen model and full body models to examine the effects of obesity on occupant and wheelchair-seated occupant injury. Model simulations suggest that the mass of the obese occupant influences occupant injury risk the most, however the interaction of mass and changes in obese torso due to increased adipose tissue, alter the kinematics of the obese occupants. The lower extremities have a significantly increased risk of injury due to obesity and the model predicts that the chest is approaching significance for increased risk of injury. These changes in the injury risk are due to the mass and the increased abdominal adipose tissue which causes increased pelvis excursion relative to the increase in chest excursion. In addition obese wheelchair-seated occupants experience similar injury trends to non-wheelchair seated obese occupants, however they experience more forward excursion for each level of BMI compared to non-wheelchair seated occupants. The findings of this study should be considered with limitations of the study.

5.1   LIMITATIONS

5.1.1   FE Abdomen Model Limitations

There are several major assumptions of the Abdomen FE model. First, the model is validated for

force deformation response of the whole abdomen, and while this is valid for overall abdomen

response, the dynamics of the inside of the abdomen have not been validated. This study

examined the cushion effect using the maximum pressure experienced by the kidneys, spleen,

and liver as indicators of injury. The model has not been validated for internal organ pressures.

Caution must be used when interpreting these values as there is no data available on abdomen

belt loading and the resulting pressures experienced by the abdominal organs. The maximum

prescribed motion of the seatbelt in the model was less than 100 mm. The prescribed motion may

need to be greater in order to replicate loading conditions that might cause injury. At higher

deformation levels there could be a greater cushion effect than was seen in the model.

This model also assumes that the skin and muscle can be combined in to one component

with one material property. This assumption was made because there is limited data available on

the skin, abdominal muscle, and adipose tissue under high loading conditions seen in MVCs.

Under loading conditions that have lower deformation (i.e. Lamielle et al. PRT) the model

consistently underestimates the force both in magnitude and shape, suggesting lower energy in

the model compared to cadavers. This indicates that the model's assumption of combining the

skin and muscle components may need to be modeled in greater detail to accurately describe the

abdominal response. In addition a more detailed modeling of internal organs including the

hollow organs will provide a more accurate model with an improved overall response.

When creating the Obese Abdomen FE model, a modification in abdomen geometry was

performed, and the additional elements that were created were assigned adipose tissue material

properties. The creation of the Obese Abdomen FE model assumed that as BMI increases it is

solely due to increases in subcutaneous adipose tissue. This limitation does not account for

changes in visceral adipose tissue as BMI increases. People carry different amounts of

subcutaneous and visceral adipose tissue and the model does not account for this. By including a

separation of subcutaneous and visceral adipose tissue and their respective distributions into the

abdomen model it would improve the response. This would also provide a more detailed internal

organ structure, which will provide an improved abdominal force deformation response,

particularly in the later stages of loading when the greater deformations indicate more interaction

with the internal part of the abdomen.

5.1.2   Model Boundary Conditions Limitations

The model was validated for seatbelt loading at the mid umbilicus with the seatbelt routed

straight back. This configuration is not representative of real world seatbelt position on the

abdomen. While it may represent a "worst case" abdomen loading, it is not a realistic

automotive loading condition. In this study the model was validated for this loading condition,

but then used to investigate abdomen loading under more realistic seatbelt positions. The model

has not been validated for these conditions so it was assumed that the validated model was able to capture the abdomen response to various other belt loading conditions.

5.1.3   Limitations of the MADYMO Models

Using the rigid body MADYMO Hybrid III ATD is beneficial in that it allows for fast computational time which means that numerous simulations can be run in a timely manner. However, the use of a rigid body model also means that one has to sacrifice some level of accuracy as material deformation is not accounted for in the rigid body computations. Transferring the force deformation response of the FE abdomen to the rigid body model and modeling the deformation as the characteristic contact results in some loss of accuracy. Due to the large differences in individuals and in the force deformation response seen in cadavers, this loss of accuracy was deemed acceptable.

Another limitation of the rigid body model is that it represents an ATD, and not a human. ATDs have been validated against numerous cadaver tests, but there is still some variation and differences in ATD response compared to cadavers. In addition cadavers do not fully represent live humans. However since no injury testing can be performed on live humans, the cadaver and subsequent ATDs developed are the best alternatives that the automotive industry can use.

The results of the full body model Design of Experiments must be interpreted within the context of the variable ranges used in the study. While the factor levels were chosen within realistic ranges, the vehicle model represented a standard sedan configuration. So caution should be used when trying to extrapolate the results to drastically different vehicle environmental

conditions. The findings of this study are limited to the frontal impact MVC. There are large differences in injury to occupants depending on the direction of the crash. For example relatively minor rear impacts tend to cause neck injuries to occupants were as high impact frontal impacts often do not cause any neck injury.

5.1.4   Model Validation Quality

Currently there is no universal approach to model validation, but validation consists of both quantitatively and qualitatively accessing the model output. The abdomen FE model was validated using a qualitative comparison, and using several quantitative parameters. These included correlation coefficient, and measures of model's ability to predict peak signal values. These parameters have been used in previous studies as validation factors because the peak signal and overall trend of the data are often factors of interest to the researcher [49, 52, 79-81]. Previous human FE models used for automotive safety tend to use qualitative validation [31, 32, 45, 65]. When comparing the current model to previous human FE models, the time history curves suggest that the abdomen FE models are sufficiently valid. For example in a lower extremity injury study by Kim et al. (2005) a lower extremity finite element model was validated and peak values reported ranged from 0-36% of the test data. In the current model the peak values are within +/-25% of the test data. In addition the use of quantitative parameters provides additional information, and the resulting values are within the ranges of previously validated full body MADYMO models [49, 52, 79-81]. The MADYMO full body model was validated against cadaver data [62]. There is little information on the cadaver test setup making a detailed accurate model difficult, but the model approximates the cadaver tests well, slightly under predicting the peak excursions and accurately predicting the shoulder to hip ratio. Compared to a

previously developed obese full body model which was validated against the same cadaver data, the current model's validation is similar, and it predicts the cadaver shoulder to hip ratio response better than the previous model [23].

5.1.5   Limitations due BMI

This study examined the effects of BMI from 25 to 40. There is a limited amount of data available for individuals with BMIs greater than 40. There is some evidence that the extreme cases of BMI (>40) may respond differently than less obese individuals [23]. Therefore the findings of this study are limited to BMIs in the 25-40 range. It was also assumed that the injury thresholds were the same regardless of BMI. The findings of this study suggest trends in risk of injury but it is not precisely known if these trends continue for extreme cases of BMI, so care must be taken when drawing conclusions about injury risk to individuals with BMIs greater than 40. In addition this study only examined obese male occupants. Research has shown that there are differences in injury risk to both obese males and females [23, 25], therefore the conclusions of this study are limited to obese adult males in frontal impacts.

5.1.6   Wheelchair Occupant Study Limitations

A surrogate wheelchair was used in this study. The surrogate wheelchair is designed to represent average manual and powered wheelchair dimensions that can be repeatedly crash tested without damaging the wheelchair. The seating system of a surrogate wheelchair represents a "worst case

scenario" seating system consisting of a rigid smooth seat. The surrogate wheelchair does not exactly replicate the response of a real wheelchair in an MVC. Wheelchairs can be damaged and or come apart in an MVC causing much different injury risk that this study does not replicate. Further, a computer model of a powered wheelchair should be created and used to examine the effect of BMI on occupant injury with seating systems that are more representative of a powered wheelchair.

5.2   FUTURE WORK

This research provides new insight into the mechanisms of injury to obese occupants. Obesity in both wheelchair-seated occupants and non-wheelchair-seated occupants is examined. This research provides some answers but creates many more questions, and there is much more research needed before the effects of obesity on occupant injury are fully understood.

5.2.1   Anthropometric Research

This research only analyzed adult male occupants. Further research is needed to address the differences in occupant injury risk due to obesity based on gender. Obese models of females that account for differences in geometry and mass of males and females could provide new insight into reasons behind injury patterns. In addition further data is needed to investigate extreme obesity. In order to do this, anthropometric data of extreme obesity (BMI>40) is needed, which

will need to include mass distribution and inertial characteristics as well as data on changes in body shape.

Further a large scale anthropometric study is needed to reclassify the 50th percentile individual in America. Current standards and research is outdated and with the epidemic of obesity effecting almost 70% of the US population, safety systems that protect the 50th percentile male are becoming designed for a smaller and smaller percentage of the population as the population becomes more obese. A reclassification of the 50th percentile male occupant would provide optimal safety to a much larger percentage of the current population.

5.2.2   Improvement of the Abdomen FE Model

In order to investigate the effects of adipose tissue on abdominal response the addition of the contributions of visceral adipose tissue is necessary. CT scans of the abdomen of obese individuals could allow of digitization and segmentation of the visceral fat and subcutaneous fat which then could be incorporated into the Obese Abdomen FE model providing a more accurate representation of the obese abdomen. In addition to the distribution of the adipose tissue, mechanical testing of human adipose tissue, both subcutaneous and visceral, at high loading rates will provide more accurate material models and thus improve the abdomen FE model.

Studies on pressures of internal abdominal organs due to high loading rates will provide data for further validation of the abdomen FE model and allow for more rigorous investigation of internal interactions of the abdomen in high speed loading. Additional model simulations with the Obese Abdomen FE model with boundary conditions representative of impacts with rigid parts of the vehicle interior (car door, steering wheel) could provide more insight into the

possible cushion effect or lack thereof. The FE abdomen models the rest of the human body as lumped masses rigidly attached to the FE model. In reality the abdomen is part of a complex system. To provide accurate results for whole body occupant injury an Obese Full body FE model could provide more data on occupant injury due to increased adipose tissue.

5.2.3 Wheelchair Related Research

Kinematics of the surrogate wheelchair need to be compared to the kinematics of a wide range of wheelchairs, both manual and powered. This research need to be performed to investigate if the ATD kinematic seen in the surrogate wheelchair are in fact representative of real occupant kinematics in real wheelchairs. The effects of BMI on wheelchair-seated occupants in various crash directions (rear, side impacts) should also be investigated to better understand the interaction between occupant BMI and the wheelchair. Wheelchair users have additional issues with seatbelts as sometimes the wheelchair cannot accommodate proper seatbelt usage (i.e. armrest can prevent proper belt fit). Further simulations with belt fit scenarios specific to wheelchair users need to be performed to examine the effects of BMI and belt fit issues, commonly seen with wheelchair users, on occupant injury. As suggested by this research, the seating configuration of the wheelchair can have a significant effect on occupant kinematics and occupant injury. Therefore future research should investigate various wheelchair seating configurations including seating surfaces to find an optimal seating configuration that reduces injury risk for obese wheelchair-seated occupants.

5.2.4   Occupant Safety Systems

The next step in this research should include using the obese models developed in this study and an optimization algorithm to try and develop design guidelines for occupant restraint systems based on an individual's BMI.   By identifying important design variables of the occupant restraint system and the optimizing them through computer modeling, occupant restraint systems that are optimized for a person's BMI could be developed, thus improving safety of restraint system based on BMI.   The study examined the effects of obesity on occupant injury in frontal impacts.   Further research is needed to examine the effects of obesity on occupant injury for rear, side, and rollover MVCs.   Different crash directions cause different mechanisms of injury and the addition of increased adipose tissue may provide a "cushion effect" in some cases such as side impacts.   Also different types of restraint systems, such as 4-point restraint systems, might improve obese occupant safety and need to be examined.

5.3   CONCLUSIONS

A computer modeling approach was used to examine the injury mechanisms and risk of injury due to obesity on male occupants in frontal MVCs. An Obese Abdomen FE model was created and validated. This model was then used to determine the mechanical response of the human abdomen as BMI increases. In addition, the cushion effect was examined by recording peak pressures of the abdominal organs as a result of seatbelt loading. The mechanical response of the

human abdomen was then imported into a whole body MADYMO model that was modified with FE torso surfaces representing varying levels of BMI. A DOE parametric analysis was used to examine the effects of BMI on occupant injury risk while controlling several vehicle environment variables. Finally a wheelchair-seated occupant model was created and validated in MADYMO. This model was used to examine the effects of obesity on wheelchair-seated occupants. The main conclusions of this study are:

1. Increased mass is the most significant injury mechanism to obese occupants, causing a 9% increase in injury risk to the chest based on the distributed chest loading injury risk curve, and a 40% increase in chest injury risk based on the seatbelt loading injury risk curve. Lower extremity injury risk was small but increased 46% from a BMI of 25 to 39.

2. The changes in torso mechanical response and geometry as a result of increased adipose tissue alone, do not significantly affect the injury risk of obese occupants.

3. The addition of changes in obese torso coupled with increased mass caused increased pelvis and chest excursion compared to the mass model, which results in a 27% increase risk of lower extremity injury from a BMI of 25 to 39. Chest injury risk was approaching significance.

a. The addition of torso changes slightly reduces the significance of chest injury as BMI increases, most likely due to the pelvis leading and chest lagging behind resulting in more force applied to the lower extremities.

b. The model simulations suggest that the reduction in injuries to certain body regions reported by the literature are not due to a "cushion effect" but are more likely due to altered occupant kinematics which transfer the load from the upper body to the lower extremities.

4. Obese Wheelchair-seated occupants are at an increased risk of injury to the lower extremities in frontal MVCs.

a. The increased risk of injury to the lower extremities is partially due to the use of a surrogate wheelchair seating system which causes more forward translation of the wheelchair-seated occupant as BMI increases.

5. The force-deformation response of the human abdomen under seatbelt loading conditions changes as BMI increases. The pelvis/seatbelt interaction is reduced and adipose tissue dominates the obese abdomen mechanical response at higher BMIs (>35). The response of the obese abdomen tends to converge regardless of belt angle to an approximately haversine force-deformation response with a peak value between 6000-9000 N.

6. According to the Obese Abdomen FE model predicted response, there is no significant difference in kidney, liver or spleen peak pressure as a result of belt loading as BMI increases thus negating the cushion effect hypothesis

   a. Correlation between BMI and organ pressure show as slight (r =-0.20) cushion effect for the kidneys, no relationship for the spleen (r=0.09), and a slight positive relationship (r=0.31) between liver pressure and BMI, however the model has not been validated for internal organ pressure.

This research provides the first human obese abdomen FE model, and improved whole body obese models that can address the mechanisms of injury to obese occupants. The wheelchair-seated occupant model also provides the first validated surrogate wheelchair model and the first attempt to examine obesity in wheelchair-seated occupants. The use of the models along with the DOE study allowed from multiple variables to be controlled for while examining obesity in a realistic vehicular environment. This data would have been difficult and expensive to obtain by using cadaver tests. The use of models also allowed for the proposed mechanisms of injury to be isolated and studied independent of confounding factors which is not possible using cadaver testing. The models developed in this study provide insight into how obese individuals respond in frontal impacts. The conclusions from this research could provide valuable information for future designs of occupant restraint systems.

BIBLIOGRAPHY

1.   World Health Organization, *Global Database on Body Mass Index*. 2009.

2.   National Center for Health Statistics, *Health, United States*. 2006.

3.   Rehabilitation Research and Training Center on Disability Statistics and Demographics, *Annual Compendium of Disability Statistics Compendium: 2009 Rehabilitation Research and Training Center on Disability Demographics and Statistics*, Hunter and College, Editors. 2009.

4.   Center for Disease Control. *Obesity in US Adults: 2007*. 2007 [cited.

5.   Zarzaur, B.L. and Marshall, S.W., *Motor Vehicle Crashes Obesity and Seat Belt Use: A Deadly Combination?* The Journal of Trauma Injury, Infection, and Critical Care, 2008. **64**: p. 412-419.

6.   *Motor Vehicle Traffic Crash Fatality and Injury Estimates for 2000*. 2001, National Highway Traffic Safety Administration: Washington DC.

7.   National   Highway and Traffic Safety Administration, *FMVSS 208*, U.D.o. Transportation, Editor.

8.   Songer, T., Fitzgerald, S.G., and Rotko, A.K. *The injury risk to wheelchair occupants using motor vehicle transportation*. in *48th annual proceedings of the association for the advancement of automotive medicine*. 2004.

9.   Schneider, L.W., Klinich, K.D., Moore, J.L., and MacWilliams, J.B., *Using in-depth investigations to identify transportation safety issues for wheelchair-seated occupants of motor vehicles*. Medical Engineering and Physics, 2010. **32**: p. 237-247.

10.   American National Standards Organization (ANSI), *ANSI/RESNA WC-19: Wheelchairs used as seats in motor vehicles*. 2000, American National Standards Institute/Rehabilitation Engineering Society of North America (ANSI/RESNA) Wheelchair Standards: Arlington, Va.

11. *SAE Recommended Practice J2249 wheelchair tiedown and occupant restraint systems for use in motor vehicles*, in *2002 SAE Handbook*. 1999, Society of Automotive Engineers: Warrendale, Pa. p. 229-244.

12. ISO, *10542-3: Technical systems and aids for disabled or handicapped persons-wheelchair tiedown and occupant-restraint systems- Part 3: Docking type tiedown systems*. 2005, International Organization for Standardization: Geneva, Switzerland.

13. ISO, *10542-2: Technical systems and aids for disabled or handicapped persons - Wheelchair tiedown and occupant-restraint systems - Part 2: Four-point strap-type tiedown systems.* 2001, International Organization for Standardization: Geneva, Switzerland.

14. ISO, *10542-1 Technical systems and aids for disabled or handicapped persons-Wheelchair tiedown and occupant-restraint systems, Part 1: Requirements for all systems*. 2001, International Organization for Standardization: Geneva, Switzerland.

15. Boulanger, B.R., Milzman, D., Mitchell, K., and Rodriguez, A., *Body habitus as a predictor of injury pattern after blunt trauma.* The Journal of Trauma Injury, Infection, and Critical Care, 1992. **33**: p. 228-232.

16. Moran, S.G., McGwin, G., Metzger, J.S., Windham, S.T., Reiff, D.A., and Rue, L.W., *Injury Rates among Restrained Drivers in Motor Vehicle Collisions: The Role of Body Habitus.* The Journal of Trauma Injury, Infection, and Critical Care, 2002. **52**: p. 1116-1120.

17. Reiff, D.A., Davis, R.P., MacLennon, P.A., McGwin, G., Clements, R., and Rue, L.W., *The Association between Body Mass Index and Diaphragm Injury among Motor Vehicle Collision Occupants.* The Journal of Trauma Injury, Infection, and Critical Care, 2004. **57**: p. 1324-1328.

18. Cormier, J.M., *The influence of body mass index on thoracic injuries in frontal impacts.* Accident Analysis and Prevention, 2008. **40**: p. 610-615.

19. Viano, D.C., Parenteau, C.S., and Edwards, M.L., *Crash Injury Risks for Obese Occupants Using a Matched-Pair Analysis.* Traffic Injury Prevention, 2008. **9**: p. 59-64.

20. Arbabi, S., Wahl, W.L., Hemmila, M.R., Kohoyda-Inglis, C., Taheri, P.A., and Wang, S.C., *The Cushion Effect.* The Journal of Trauma Injury, Infection, and Critical Care, 2003. **54**: p. 1090-1093.

21. Wang, S.C., Bednarski, B., Patel, S., Yan, A., Kohoyda-Inglis, C., Kennedy, T., Link, E., Rowe, S., Sochor, M., and Arbabi, S. *Increased Depth of Subcutaneous Fat is Protective against Abdominal Injuries in Motor Vehicle Collisions*. in *47th Proceedings of the Association for the Advancement of Automotive Medicine*. 2003.

22. Ryb, G.E. and Dischinger, P.C., *Injury Severity and Outcome of Overweight and Obese Patients After Vehicular Trauma: A Crash Injury Research and Engineering Network (CIREN) Study.* The Journal of Trauma Injury, Infection, and Critical Care, 2008. **64**: p. 406-411.

23. Zhu, S., Kim, J.-E., Ma, X., Shih, A., Laud, P.W., Pintar, F., Shen, W., Heymsfield, S.B., and Allison, D.B., *BMI and risk of serious upper body injury following motor vehicle crashes: concordance of real-world and computer-simulated observations.* PLOS Medicine, 2010. **7**(3): p. 1-13.

24. Choban, P., Weireter, L., and Maynes, C., *Obesity and increased mortality.* Journal of Trauma, 1991. **31**: p. 1253-1257.

25. Zhu, S., Layde, P.M., Guse, C.E., Laud, P.W., Pintar, F., Nirula, R., and Hargarten, S., *Obesity and Risk for Death Due to Motor Vehicle Crashes.* American Journal of Public Health, 2006. **96**: p. 734-739.

26. Sivak, M., Schoettle, B., and Rupp, J., *Survival in Fatal Road Crashes: Body Mass Index, Gender, and Safety Belt Use.* Traffic Injury Prevention, 2010. **11**: p. 66-68.

27. Cooper, W. and Salzberg, P., *Safety restraint usage in fatal motor vehicle crashes.* Accident Analysis and Prevention, 1993. **25**: p. 67-75.

28. Reinfurt, D., St Cyr, C., and Hunter, W., *Usage patterns and misuse rates of automatic seat belts by system type.* Accident Analysis and Prevention, 1991. **23**: p. 521-530.

29. Faidy, J., *The coupling phenomenon in the case of a frontal car crash.* Stapp Car Crash Journal, 1995. **39**: p. 71-78.

30. Rouhana, S., *Biomechanics of Abdominal Trauma*, in *Accidental Injury Biomechanics and Prevention*, A. Nahum and J. Melvin, Editors. 2002, Springer: New York, NY. p. 405-453.

31. Lee, J.B. and Yang, K.H., *Development of a Finite Element Model of the Human Abdomen.* Stapp Car Crash Journal, 2001. **45**: p. 79-100.

32. Ruan, J.S., El-Jawahri, R., Barbat, S., and Prasad, P., *Biomechanical Analysis of Human Abdominal Impact Responses and Injuries though Finite Element Simulations of a Full Human Body Model.* Stapp Car Crash Journal, 2005. **49**: p. 343-366.

33. Siegel, J., Mason-Gonzales, S., Dischinger, P.C., Cushing, B., Read, K., Robinson, R., Smialek, J., and al., e., *Safety belt restraints and compartment intrusions in frontal and lateral motor vehicle crashes, mechanisms of injury, complications, and acute care costs.* Journal of Trauma, 1993. **5**(34): p. 736-759.

34.   Melvin, J., Stalnaker, R., Roberts, V., and Trollope, M., *Impact injury mechanisms in abdominal organs.* 17th Stapp Car Crash Conference Proceedings, 1973(SAE # 730968): p. 115-126.

35.   Walfisch, G., Fayon, A., Tarriere, C., and al., e. *Designing of a dummy's abdomen for detecting injuries in side impact collisions.* in *IRCOBI*. 1980.

36.   Lau, V. and Viano, D.C., *How and when blunt injury occurs implications to frontal and side impact protection.* 32nd Stapp Car Crash Conference Proceedings, 1988(SAE # 881714): p. 123-142.

37.   Rouhana, S., Ridella, S., and Viano, D.C., *The effect of limiting impact force on abdominal injury: a preliminary study.* 3oth Stapp Car Crash Conference Proceedings, 1986(SAE # 861879): p. 65-79.

38.   Baudrit, P., Hamon, J., Song, E., Robin, S., and Coz, J.-Y., *Comparative studies of dummy and human body models behavior in frontal and lateral impact conditions.* Stapp Car Crash Journal, 1999. **43**(SAE 99SC05).

39.   Happee, R., Hoofman, M., Kroonenberg, A., Morsink, P., and Wismans, J., *A mathematical human body model for frontal and rearward seated automotive impact loading.* Stapp Car Crash Journal, 1998(SAE 983150).

40.   Hoof, J., Lange, R., and Wismans, J., *Improving pedestrian safety using numerical human models.* Stapp Car Crash Journal, 2003(SAE 2003-22-0018).

41.   Huang, C., King, A.I., and Cavanagh, P., *Finite element modeling of gross motion of human cadavers in side impact.* Stapp Car Crash Journal, 1994(SAE 942207).

42.   Kimpara, H., Iwamoto, M., and Miki, K., *Development of a small female FEM model.* JSAE 20025242, 2002.

43.   Lange, R., Rooij, L., Mooi, H., and Wismans, J., *Objective biofidelity rating of a numerical human occupant model in frontal to lateral impact.* Stapp Car Crash Journal, 2005. **49**.

44.   Lizee, E., Robin, S., Song, E., Bertholon, N., Coz, J.-Y., Besnault, B., and Lavaste, F., *Development of a 3D finite element model of the human body.* Stapp Car Crash Journal, 1998. **42**(SAE 983152).

45.   Ruan, J.S., El-Jawahri, R., Chai, L., Barbat, S., and Prasad, P., *Prediction and Analysis of Human Thoracic Impact Responses and Injuries in Cadaver Impacts Using a Full Human Body Finite Element Model.* Stapp Car Crash Journal, 2003. **47**: p. 299-321.

46.   TNO, *MADYMO Utilities Manual Release 6.3.2.* 2006.

47. McConville, J., Churchill, T., Kaleps, I., Clauser, C., and Cuzzi, J., *Anthropometric Relationships of Body and Body Segment Moments of Inertia*. 1980, Aerospace Medical Research Laboratory, Wright-Patterson Air Force Base: Ohio.

48. Grunhofer, H. and Kroh, G., *A Review of Anthropometric Data on German Air Force and United States Air Force Flying Personnel 1967-1968*. 1975, Advisory Group for Aerospace Research and Development, 7 Rue Ancelle 92200: Neuilly Sur Seine, France.

49. Dsouza, R. and Bertocci, G., *Development and validation of a computer crash simulation model of an occupied adult manual wheelchair subject to a frontal impact.* Medical Engineering and Physics, 2010. **32**(3): p. 272-279.

50. Ha, D. and Bertocci, G. *An investigation of manual wheelchair seat pan and seat back loading associated with various wheelchair design parameters using computer crash simulation*. in *Proceedings of the Annual RESNA Conference*. 2003. Atlanta, GA.

51. Gefen, A. and Haberman, E., *Viscoelastic properties of ovine adipose tissue covering the gluteus muscles.* Journal of Biomechanical Engineering, 2007. **129**(6): p. 924-930.

52. Salipur, Z. and Bertocci, G., *Development and validation of rear impact computer simulation model of an adult manual transit wheelchair with a seated occupant.* Medical Engineering and Physics, 2010. **32**(1): p. 66-75.

53. Foster, C.D., Hardy, W.N., Yang, K.H., and King, A.I., *High-Speed Seatbelt Pretensioner Loading of the Abdomen.* Stapp Car Crash Journal, 2006. **50**: p. 27-51.

54. Lamielle, S., Vezin, P., Verriest, J., Petit, P., Trosseille, X., and Vallancien, G., *3D Deformation and Dynamics of the Human Cadaver Abdomen under Seatbelt Loading.* Stapp Car Crash Journal, 2008. **52**: p. 267-294.

55. Comley, K. and Fleck, N., *The High Strain Rate Response of Adipose Tissue*, in *Mechanical Properties of Cellular Materials*, H. Zhao and N. Fleck, Editors. 2009, Springer. p. 27-33.

56. Todd, B.A. and Thacker, J.G., *Three-dimensional computer model of the human buttocks, in vivo.* Journal of Rehabilitation Research and Development, 1994. **31**(2): p. 111-119.

57. Wu, J.Z., Cutlip, R.G., Andrew, M.E., and Dong, R.G., *Simultaneous determination of the nonlinear-elastic properties of skin and subcutaneous tissue in unconfined compression tests.* Skin Research and Technology, 2007. **13**: p. 34-42.

58. SAE, *Civilian American and European Surface Anthropometry Resource Project - CAESAR*. 2010.

59. Comley, K. and Fleck, N., *The mechanical response of porcine adipose tissue.* Journal of Biomechanical Engineering, 2010(Submitted).

60.   Schneider, L.W. and Manary, M.A., *Wheelchairs, Wheelchair Tiedowns, and Occupant Restraints for Improved Safety and Crash Protection Chapter 17 of Driver Rehabilitation: Principles and Practices*, ed. J. Pellerito. 2006: Moseby Press.

61.   Buchholz, A. and Bugaresti, J., *A review of body mass index and waist circumference as markers of obesity and coronary heart disease risk in persons with chronic spinal cord injury.* Spinal Cord, 2005. **43**: p. 513-518.

62.   Kent, R.W., Forman, J.L., and Bostrom, O., *Is there really a "cushion effect"?: A biomechanical investigation of crash injury mechanisms in the obese.* Obesity, 2010. **18**: p. 749-753.

63.   Mock, C.N., Grossman, D.C., Kaufman, R.P., Mack, C.D., and Rivara, F.P., *The relationship between body weight and risk of death and serious injury in motor vehicle crashes.* Accident Analysis and Prevention, 2002. **34**: p. 221-228.

64.   Hu, J., *Neck injury mechanism in rollover crashes - a systematic approach for improving rollover neck protection*, in *Biomedical Engineering*. 2007, Wayne State University: Detroit, Michigan.

65.   Kim, Y.S., Choi, H.H., Cho, Y.N., Park, Y.J., Lee, J.B., Yang, K.H., and King, A.I., *Numerical Investigations of Interactions between the Knee-Thigh-Hip Complex with Vehicle Interior Structures.* Stapp Car Crash Journal, 2005. **49**: p. 85-115.

66.   Atkinson, P., Benney, J., Sambatur, K., Gudipaty, K., Maripudi, V., and Hill, T., *A parametric study of vehicle interior geometry, delta-v, and instrument panel stiffness on knee injury and upper body kinetic energy.* Stapp Car Crash Journal, 1999(99SC13).

67.   Hayashi, S., Choi, H.Y., Levine, R.S., Yang, K.H., and King, A.I., *Experimental and analytical study of knee fracture mechanisms in a frontal knee impact.* Stapp Car Crash Journal, 1996(962423).

68.   Foret-Bruno, J.-Y., Trosseille, X., Page, Y., Huere, J.-F., Coz, J.-Y., Bendjellal, F., Diboine, A., Phalempin, T., Villeforceix, D., Baudrit, P., Guillemot, H., and Coltat, J.-C., *Comparison of thoracic injury risk in frontal car crashes for occupant restrained without belt load limiters and those restrained with 6 kN and 4 kN belt load limiters.* Stapp Car Crash Journal, 2001. **45**: p. Paper No. 2001-22-0009.

69.   Administration., N.H.a.S., *New Car Assessment Program.* 2010.

70.   Pipkorn, B., Mellander, H., and Haland, Y. *Car driver protection at frontal impacts up to 80 km/h.* in *EVS Conference*. 2005.

71.   Rupp, J., Miller, C.S., Reed, M.P., Madura, N.H., Ritchie, N.L., and Schneider, L.W. *Characterization of knee impacts in frontal crashes*. in *Proceedings of the 20th International Technical Conference on Experimental Safety Vehicles*. 2007.

72. Mertz, H.J., Prasad, P., and Irwin, N.L., *Injury risk curves for children and adults in frontal and rear collisions.* Proceedings of the 41st Stapp Car Crash Conference, 1997: p. 13-30.

73. Mertz, H.J. and Gadd, C.W., *Thoracic tolerance to whole body deceleration.* Proceedings of the 15th Stapp Car Crash Conference, 1971(SAE 710852): p. 135-55.

74. Kuppa, S., Wang, J., Haffner, M., and Eppinger, R.H. *Lower extremity injuries and associated injury criteria*. in *Proceedings of the 17th International Technical Conference on the Enhanced Safety Vehicles*. 2001. Washington D.C.

75. Morgan, R.M., Eppinger, R.H., and Marcus, J.H. *Human cadaver patella-femur-pelvis injury due to dynamic frontal impact to the patella*. in *Proceedings of the 12th International Technical Conference on Experimental Safety Vehicles*. 1989. Washington D.C.

76. SAE, *Instrumentation for impact test - part 1: electronic instrumentation.*, in *Paper No. J211*. 1995, Society of Automotive Engineers: Warendale, Pa.

77. Bertocci, G., Digges, K., and Hobson, D., *Computer simulation and sled test validation of a powerbase wheelchair and occupant subjected to frontal crash conditions.* IEEE Transactions on Rehabilitation Engineering, 1999. **7**(2): p. 234-244.

78. Bertocci, G., Digges, K., and Hobson, D., *Development of a wheelchair occupant injury risk assessment method and its application in the investigation of wheelchair securement point influence on frontal crash safety.* IEEE Transactions on Rehabilitation Engineering, 2000. **8**(1): p. 126-139.

79. Bertocci, G., Szobota, S., Ha, D., and van Roosmalen, L., *Development of Frontal Impact crashworthy wheelchair seating design criteria using computer simulation.* Journal of Rehabilitation Research and Development, 2000. **37**(5): p. 565-572.

80. Ha, D., Bertocci, G., and Jategaonkar, R., *Development and validation of a frontal impact 6-year-old occupant and wheelchair computer model.* Assistive Technology, 2007. **19**(4): p. 223-238.

81. Pipkorn, B. and Eriksson, M. *A method to evaluate the validity of mathematical models*. in *4th European MADYMO Users Meeting*. 2003. Brussels, Belgium.